Title

Investigation of Mosquitocidal Activity of Paraclostridium bifermentans serovar malaysia and Bacillus thuringiensis subspecies israelensis

Author

Andrews, Stefani Michele

Publication Date

2022

Peer reviewed|Thesis/dissertation

UNIVERSITY OF CALIFORNIA
RIVERSIDE

Investigation of Mosquitocidal Activity of *Paraclostridium bifermentans* serovar *malaysia* and *Bacillus thuringiensis* subsp. *israelensis*

A Dissertation submitted in partial satisfaction
of the requirements for the degree of

Doctor of Philosophy

in

Environmental Toxicology

by

Stefani Michele Andrews

December 2022

Dissertation Committee:
Dr. Sarjeet S. Gill, Chairperson
Dr. Michael E. Adams
Dr. Adler R. Dillman

The Dissertation of Stefani Michele Andrews is approved:

Committee Chairperson

University of California, Riverside

ACKNOWLEDGEMENTS

It is hard to accurately describe my gratitude toward everyone who has supported me through this journey and contributed to this dissertation. I would first and foremost like to thank Dr. Sarjeet Gill for his guidance and support through this process. His patience with me was instrumental in my development during my graduate career. I would like to acknowledge Dr. Michael Adams and Dr. Adler Dillman for their support, guidance, and experimental input. Additionally, I'd like to thank Dr. John Trumble and Dr. Howard Judelson, and Dr. David Eastmond for serving on my qualifying committee.

I want to thank Dr. Estefania Contreras, Dr. Harpal Dhillon, and Dr. Swati Chawla for teaching me molecular techniques that have been invaluable during my graduate years. I would also like to thank Dr. Haonan Zhang and Dr. Jianwu Chen for their help in troubleshooting problems over the years. Dr. Sajleen Singh Phagura (Good talk!), Dr. Monique Williams, and Dr. Rachel Rattner have been invaluable for their constant support, peptalks when experiments were not working, and overall helpfulness in all aspects of my life. I would also like to thank Michael Presser, and Alison Presser for giving me a home away from home and allowing me to have emotional support fur babies. Dawn Loyola and Fidel Rivas have been helpful in so many ways, especially for always answering questions promptly and easing my academic career. Thank you to Anthony DeLuca for being a constant support in my life over the past years.

Finally, to my parents, without their support I would not be the person I am today. I thank them for always believing in me even when I lacked confidence in myself. This would not have been possible without them.

DEDICATION

This Dissertation is dedicated to my parents

Howard and Christine Andrews

for their endless support, encouragement, and love.

ABSTRACT OF THE DISSERTATION

Investigation of Mosquitocidal Activity of *Paraclostridium bifermentans* serovar *malaysia* and *Bacillus thuringiensis* subsp. *israelensis*
by

Stefani Michele Andrews

Doctor of Philosophy, Graduate Program in Environmental Toxicology
University of California, Riverside, December 2022
Dr. Sarjeet S. Gill, Chairperson

Aedes aegypti, *Anopheles stephensi*, and *Culex quinquefasciatus* serve as vectors for some of the world's most debilitating diseases; these diseases include dengue fever, malaria, and West Nile fever respectively. One method currently employed to combat these diseases, and the deaths they cause, is to control the mosquito populations that allow them to persist. Multiple methods have been used to control mosquito populations, two of these methods including chemical control through pesticides and biological control through bacterial toxins. *Bacillus thuringiensis israelensis* and *Lysinibacillus sphaericus* have been used to control *Aedes* and *Culex* populations respectively, but no current biological control method primarily targets *Anopheles* mosquitoes. Additionally, some mosquito populations have started to develop resistance against *Lysinibacillus sphaericus* toxins, while resistance has also been seen against single toxins produced by *Bacillus thuringiensis israelensis.*

A new bacteria called *Paraclostridium bifermentans malaysia* (*Pbm*) was discovered in an anopheline environment and produces toxins that target *Anopheles* mosquitoes. The bacterium contains a large 109kb plasmid which encodes two loci that

are toxic to mosquito species, the Cry operon and the Ptox locus. The Cry operon is toxic to *Aedes* mosquitoes while the Ptox locus is toxic to *Anopheles* mosquitoes.

The general mechanism of Cry toxins includes binding to receptors in the midgut of their target organism followed by pore formation and subsequent osmotic imbalance, eventually leading to death. We report steps forward in elucidating the mechanism of action of the Cry operon complex where mutations in loop regions of domain II in Cry17 cause a loss of toxicity of the full Cry operon. This loss of toxicity is not seen when domain II loop regions are mutated in Cry16. We also report a lack of binding between purified Cry16 proteins and *Aedes* brush border membrane fractions. Competition assays between purified Cry16 and Cry11Aa shows that Cry16 itself does not bind but suggests Cry16 may facilitate binding of Cry11Aa to *Aedes* brush border membrane fractions.

The Ptox locus, also found in *Pbm*, is toxic to *Anopheles* mosquitoes. The Ptox locus is similar to botulinum neurotoxin loci; it contains a neurotoxin, NTNH, and three OrfXs. We report an estimated size of the Ptox complex which is consistent with reports of botulinum neurotoxin progenitor complexes. We also report different methods that aid in the purification of the Ptox complex.

Bacillus thuringiensis israelensis is currently used as a biological control method that targets *Aedes* and *Anopheles* mosquitoes. We report an attempt to edit the genome of this bacteria to introduce toxicity to *Anopheles* mosquitoes using CRISPR/Cas9. Here all CRISPR elements were functional, but more screening is required to find a positively edited colony.

Table of Contents

Page

List of Figures

Page

List of Tables

Page

Chapter 1

General Introduction

1. Mosquito- vectored disease burden

Malaria, dengue fever, and West Nile fever are some of the world's most debilitating diseases. These diseases are transmitted by *Anopheles*, *Aedes* and *Culex* mosquitoes respectively. The major mosquito vectors that will be discussed in this dissertation are *Aedes aegypti*, *Anopheles gambiae*, and to a lesser extent *Culex quinquefaciaus.* Vector-borne diseases are responsible for large numbers of deaths worldwide. In Asian and South American countries, dengue fever is a major cause of mortality (Murray et al., 2013), while malaria is a major cause of death in sub-Saharan Africa. In 2012 an estimated 627,000 deaths occurred due to malaria worldwide ("WHO | Fact sheet," n.d.).West Nile Virus fever can be found in many places including Africa, North America, West Asia, the Middle East and Europe ("West Nile virus," n.d.).

Insecticides were used to combat of these diseases, however they began to resurface in the 1970s (Ja, 2001). There are several factors that can contribute to the reemergence of these diseases, including vector and pathogen resistance to insecticides or drugs, or genetic changes in both the vector and the vectored pathogens (Lederberg, 1992). To overcome resistance bacterial insecticides have been used to combat these populations of mosquitoes, namely, *Bacillus thuringiensis* subsp. *israelensis (Bti)* and *Lysinibacillus sphaericus (Ls)*. These bacteria primarily target *Aedes* and *Culex* mosquitoes respectively. There are no current bacterial insecticides that primarily target the malaria vector mosquito, *Anopheles*. Moreover, to date, no resistance has been seen

against *Bti* however, resistance has been seen against *Ls* (Rao et al., 1995). Thus, investigating a new bacterium, that targets anophelines, would be beneficial for combating mosquito populations.

2. Vectors and diseases distribution

Aedes aegypti is present in the sub-tropics and tropics with the majority of their populations residing in northern Brazil, India, southeast Asia, Spain, Greece, Australia, and the temperate area of North America (Figure 1-1A) (Kraemer et al., 2015). *Ae. aegypti* typically have a flight range of less than 250 meters, and can be separated from other populations by freeways, or other urban features (Brady and Hay, 2020). *Aedes* mosquitoes are an effective vector species, due to a multitude of reasons. Female mosquitoes do not have a preference for where they lay their eggs. Their eggs can survive up to four months in a desiccated state, which allows the offspring to live through dry periods. Larvae of *Aedes* also undergo a behavior in which they do not pupate until there are enough resources available (Brady and Hay, 2020). Female mosquitoes require a blood meal for egg production. However, because *Aedes* live close to human populations and are not able to get fructose through plant feeding these mosquitoes require a daily blood meal to sustain their metabolism. This increases the number of dengue virus transmissions (Figure 1-1B) (Brady and Hay, 2020). There is an estimated 50 to 100 million dengue fever cases each year (Braack et al., 2018). There are five serotypes of Dengue virus (DENV), and infection by one does not provide immunity to the other serotypes (Mustafa et al., 2015). Some cases of dengue infection can evolve into a more severe disease called dengue hemorrhagic fever or dengue shock syndrome, both of

which can result in death (Center for Disease Control, n.d.; Gubler, 1998). Causes for the severity of infection may be due to secondary DENV infections, the infecting serotype or genotype, or age(Yung et al., 2015). Of all the arboviruses, dengue causes the most illness and death in humans (Braack et al., 2018).

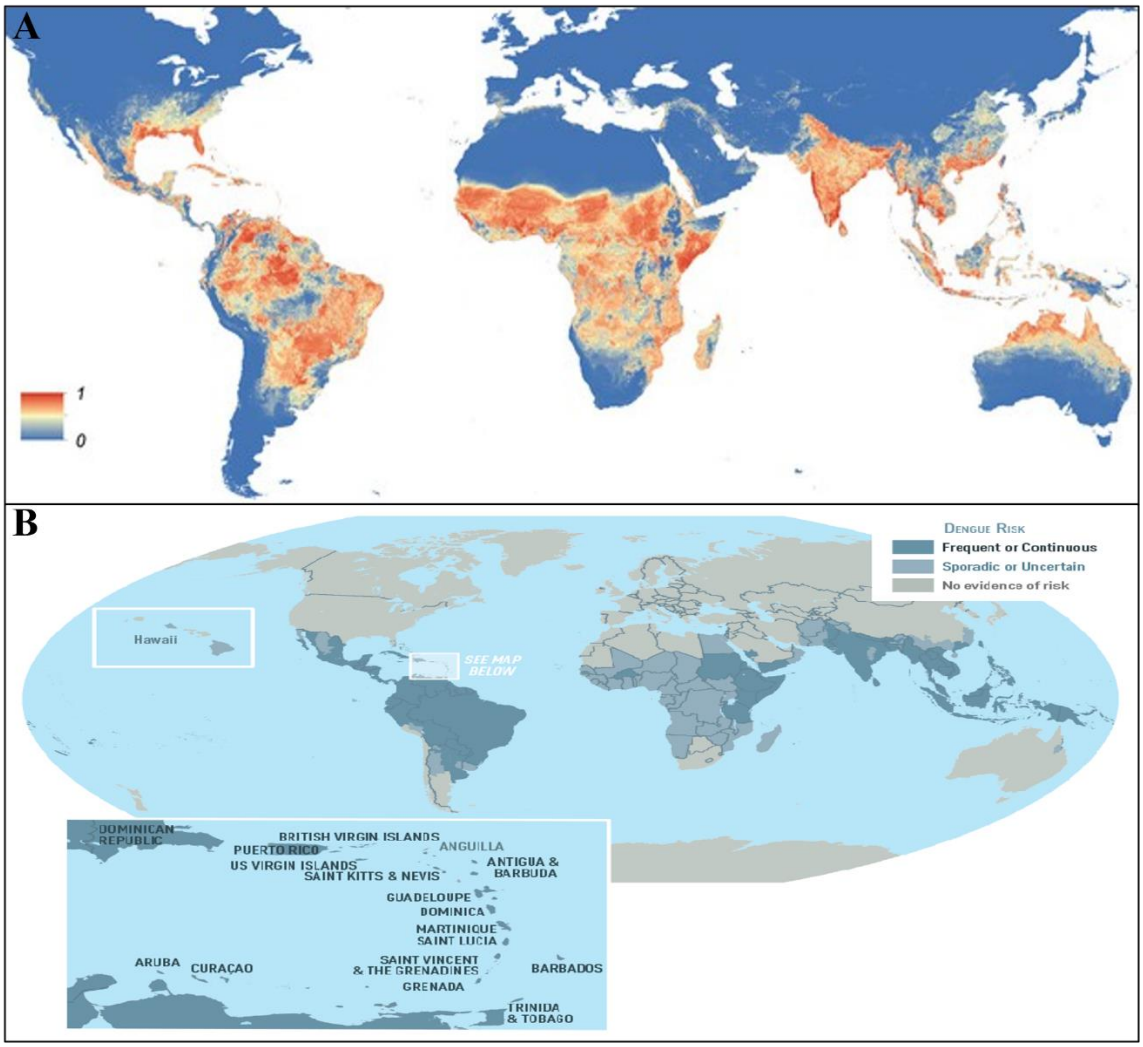

Figure 1-1. Global distribution of *Ae. aegypti* mosquitoes and incidence of dengue fever virus infections.
A) This map shows the predicted global distribution of *Ae. aegypti* mosquitoes. The red color denotes 100% probability of *Ae. aegypti* presence while blue denotes 0% probability. Source: https://doi.org/10.7554/eLife.08347.009. B) This map shows the distribution of dengue virus incidence globally. Dark blue indicated frequent or continued risk of dengue infection, while light blue indicates areas with sporadic or uncertain dengue virus incidence. Source: CDC, https://www.cdc.gov/dengue/areaswithrisk/around-the-world.html

Figure 1-2A shows the global distribution of different *Anopheles* species. *Anopheles* mosquitoes can be found around the world with the exception of Antarctica (CDC-Centers for Disease Control, 2020). Figure 1-2B shows a map of incidence rates of malaria globally in 2018, compiled by the World Health Organization estimates from the World Malaria report (World Health Organization, 2019). The World Malaria Report indicates a decrease in mortality from 2018 to 2019; however, mortality was still within the 400,000 deaths range globally. Mosquitoes threaten people who live in tropical and subtropical regions, which adds up to more than three billion people (Becker et al., 2010).

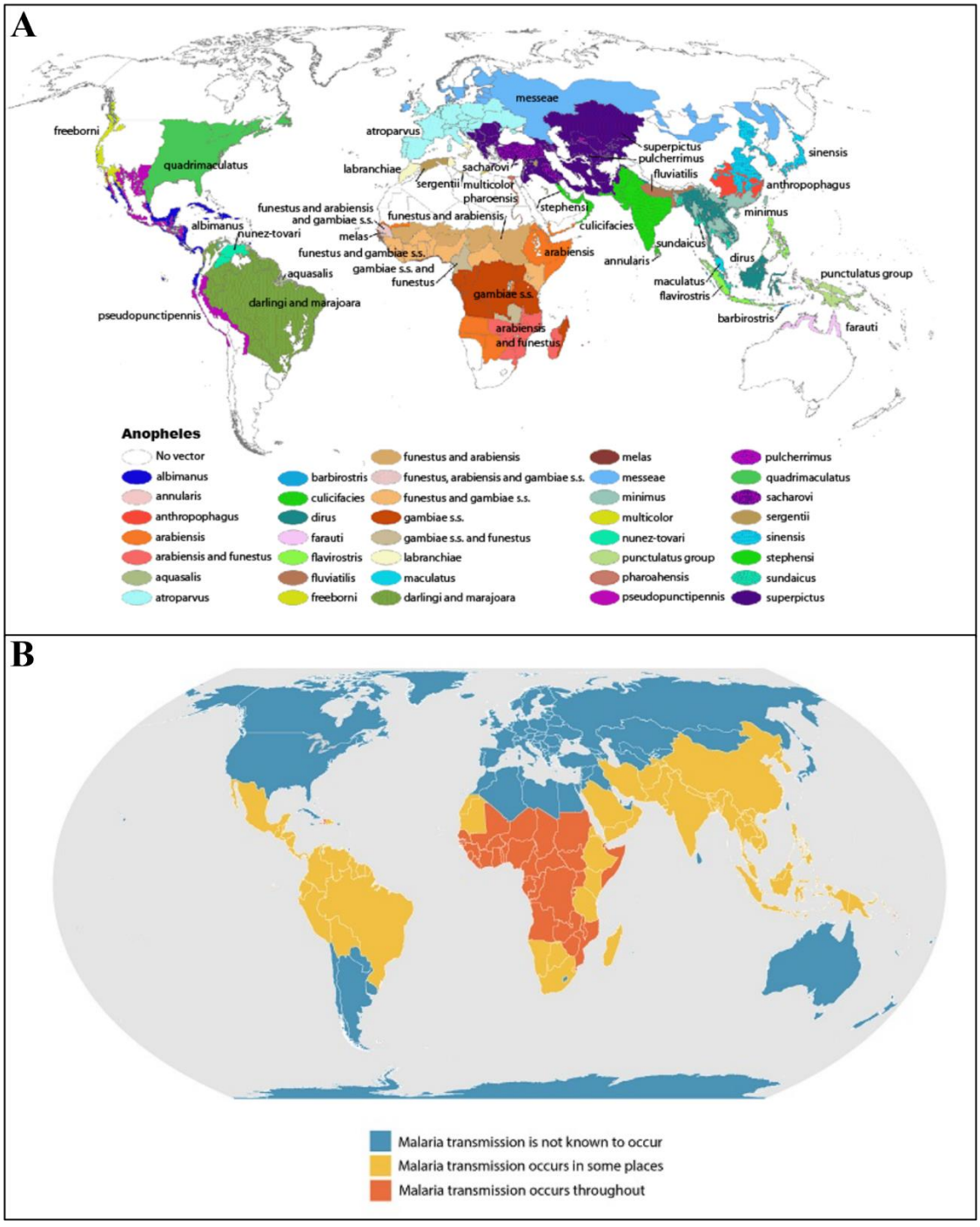
A
messeae
freeborni
atroparvus
superpictus
pulcherrimus
sinensis
quadrimaculatus
labranchiae
sacharovi
fluviatilis
sergentii
multicolor
anthropophagus
pharoensis
funestus and arabiensis and gambiae s.s.
stephensi
minimus
funestus and arabiensis
albimanus
culicifacies
nunez-tovari
melas
sundaicus
funestus and gambiae s.s.
arabiensis
annularis
dirus
gambiae s.s. and funestus
aquasalis
maculatus
punctulatus group
gambiae s.s.
darlingi and marajoara
flavirostris
barbirostris
pseudopunctipennis
arabiensis and funestus
farauti
Anopheles
No vector
albimanus
annularis
anthropophagus
arabiensis
arabiensis and funestus
aquasalis
atroparvus
barbirostris
culicifacies
dirus
farauti
flavirostris
fluviatilis
freeborni
funestus and arabiensis
funestus, arabiensis and gambiae s.s.
funestus and gambiae s.s.
gambiae s.s.
gambiae s.s. and funestus
labranchiae
maculatus
darlingi and marajoara
melas
messeae
minimus
multicolor
nunez-tovari
punctulatus group
pharoahensis
pseudopunctipennis
pulcherrimus
quadrimaculatus
sacharovi
sergentii
sinensis
stephensi
sundaicus
superpictus
B
Malaria transmission is not known to occur
Malaria transmission occurs in some places
Malaria transmission occurs throughout

Figure 1-2. Global distribution of *Anopheles* mosquitoes and incidence of malaria A. Global Anopheles distribution, where each species is indicated in a different color. Source: https://www.cdc.gov/malaria/about/biology/mosquitoes/map.html B. shows incidence of malaria globally in 2020 where orange indicates Malaria transmission throughout the area, yellow denotes some malaria transmission throughout the area, and blue are areas where there malaria is transmission does not occur. source: https://www.cdc.gov/malaria/about/distribution.html

Malaria is caused by a four species of a parasitic protozoans called *Plasmodium*; these species are *P. falciparum*, *P. malariae*, *P. ovale*, , and *P knowlesi*, and *P. vivax* (Cowman et al., 2016; Figtree et al., 2010). Anopheles mosquitoes exclusively transmit these protozoa. About 10% of all *Anopheles* species are able to serve as vectors of human malaria. The most efficient vectors of malaria are *An. gambiae* and *An. arabiensis* and *An. stephensi*. These species of mosquito exhibit anthropophilic behavior as well as seem to be physiologically superior in their ability to coexist with the parasite; these two factors allow them to have a higher vector capacity (Becker et al., 2010).

3. Mosquito habitat, behavior, and lifespan

Mosquitoes can live in a variety of different habitats and have evolved to adapt to these different environments. Eggs are laid by female mosquitoes in stagnant bodies of water, depending on the species, this body of water can be water that has accumulated in a hoof print, tires, or a flooded area among many other options. The offspring then hatches into a larval stage where it develops through four instars and eventually becomes a pupa. This pupa will then emerge as an adult; mosquitoes, like all dipteran, undergo complete metamorphosis. (Becker et al., 2010).

Many factors have contributed to the spread of mosquito populations. An example of an evolutionary advantage is that of *Aedes albopictus*, which has developed photoperiodic sensitivity. A female mosquito will lay different types of eggs depending on whether the day is longer or shorter. Eggs that are laid on shorter days do not hatch until the following season, allowing the offspring to survive the winter months. This adaptation, along with other species whose eggs can resist desiccation and have viable

offspring more than a year later as well as a multitude of artificial breeding sites availability has contributed to the spread of many species of mosquitoes. Some mosquitoes can travel via trade by being laid in plants or tires and thus begin to inhabit a new place (Becker et al., 2010).

4. Effect on disease incidence from climate change

The development of the malarial parasite in a mosquito is referred to as extrinsic incubation. This process depends on environmental temperatures. Temperature affects the development of mosquitoes at different stages including longevity, blood feeding rate and the gonotrophic cycle. An increase in temperature can ultimately increase the probability of transmission by increasing blood meal digestion, which accelerates ovarian development and egg laying. This causes a reduction in gonotrophic cycle and leads to an increased frequency of feeding.

On average it takes about 10 days for an egg to mature to an adult at an optimal temperature of 28°C. The optimal temperature for development of the malaria parasite in *Anopheles* mosquitoes falls between 20 and 30 °C at 60% humidity, however the parasite can develop at temperatures as low as 14.5°C for *P. vivax*, and 16.5°C for *P. falciparum.* The number of days necessary for sporogony of *P. vivax* decreases from 55 days at 16°C to 7 days at 28°C when using the Organoc-Rayevsky method as a guide. *Anopheles* larval stages were shorter at higher temperatures. The gonotrophic cycle of *An. albimanus* decreased by 13 hours when the temperature was increased from 24°C to 27°C. Climate change may also extend the transmission window one to three months. This is because the temperature is shifting, the colder months slow transmission because the vector

cannot survive, however with an increase in temperature globally, the colder months are getting warmer (Dhiman et al., 2008).

Some scientists argue that climate change could shift the disease burden to *Aedes* vectored diseases (Iwamura et al., 2020; Mordecai et al., 2020). Iwamura et al, used models to predict life-cycle completions of mosquitoes for specific locations for a specific amount of time; this modeling was based off empirically derived biophysical responses due to specific environmental conditions. Their data showed the world was 1.5% per decade more suitable to *Aedes* development between 1950 and 2000. They predicted an acceleration of that trend to 3.2-4.4% suitability per decade by 2050. They also predicted that the habitats of *Aedes aegypti* will increase from ~2 to 6km per year by the year 2050. They concluded that the increase in habitat area as well as world suitability will accelerate the mosquitoes global invasion potential (Iwamura et al., 2020). Similarly, Mordecai et al argues climate change could shift disease burden towards arboviruses as the world becomes more suitable for their vector. Vector-borne disease transmission will likely change with climate change. Disease transmission is dependent on many factors including vector population size, survival, biting frequency, pathogen incubation rates and vector competence. Climate change increases the suitability of *Aedes* to survive while also decreasing the potential survival of *Plasmodium* (Mordecai et al., 2020). Climate change will likely change the incidence and burden of vector-borne diseases globally.

5. Current mosquito control methods

There are many control methods that are currently being used to combat these populations of mosquitoes. There are five general methods that are being used, environmental, mechanical, chemical, biological, and genetic. Environmental methods include reducing the number of potential breeding sites, any areas where water can accumulate. Mechanical methods include nets and traps, or ovitraps which exploit the natural behavior of mosquitoes to lay eggs in small containers. These traps along with larvicides or adhesive can prevent the maturation of the eggs that have been laid there. Biological methods include use of fungi, copepods, bacteria or *Wolbachia* (Baldacchino et al., 2015). Some entomopathogenic fungi have been shown to reduce the fecundity, adult survival and blood feeding in some insects, while other fungi manifest a larvicidal and adulticidal activity. Natural mosquito larvae predators, like copepods or fish, are also being employed as a control strategy. Bacterial toxins are also currently being used, *Bti* and *Ls,* as stated earlier, are being used to control larval populations. *Wolbachia* is an endosymbiont that is naturally present in many mosquito species. They have been found to infect the gonads which allows them to be transmitted to the next generation from female adults. Depending on the strain, the presence of *Wolbachia* can cause different phenotypes in mosquitoes and is starting to be investigated as a possible means of control (Baldacchino et al., 2015). Chemical methods include growth regulators, or adulticides. Some insect growth regulators are used as larvicides, but also possess the ability to inhibit egg hatching. Some adulticides include organophosphates, carbamates or pyrethroids, among others. Pyrethroids are mainly used against adult mosquito

populations. Lastly, genetic methods include sterile insect techniques, in which sterile mosquitoes are released into the wild to mate with wild type mosquitoes. RNA interference is also being used to prevent mosquitoes from replicating viral DNA, which ultimately eliminates its ability to pass on the virus to a suitable host (Baldacchino et al., 2015). Although there are many control methods each has their own pitfalls. Some of the most notable problems include off target effects, high costs to produce parts involved, the necessity of community involvement, resistance to chemical control methods and residues left behind. One example of a chemical that leaves behind residues is DDT, which is highly stable in the environment and thought to persist for anywhere between 2 and 150 years ("DDT (General Fact Sheet)," 1999). *Aedes* mosquitoes were largely eliminated from 20 countries following the use of DDT between 1947 and 1962 (Brady and Hay, 2020).

Each of these control methods has their own set of pitfalls. For example, removing breeding sites will control the population, however these methods require community involvement. As stated earlier, some species of mosquitoes were transported via trade routes, where eggs were laid in small amounts of water in tires or transported with plants. Thus, environmental methods must be thorough if they are the only method to be used. Many times with rain, water can pool in unknown areas, and a stagnant pool of water is all that is required for a female to lay eggs (Clements, 1999). Mechanical methods include things like bed nets and traps. Bed nets are not 100% effective against prevention of mosquito bites. The user can become overheated when sleeping under a bed net, or if any part of their body is resting against the net, a mosquito could still bite

(Carlysue et al., 2017). Some mosquitoes bite during the day (Yasuno and Tonn, 1970), in this case a bed net would not be effective.

Chemical pesticides are the most commonly used method to control mosquito populations, although productive against their target insect pest, have also been shown to have off target effects. In some cases, the off-target effects are problematic for the environment and it other cases exposure can cause direct harm to humans. The four main types of insecticides that are neurotoxic are organochlorides, organophosphates, carbamates, and pyrethroids (Oliveira et al., 2017). Organochlorides contain carbon, hydrogen, and chloride while organophosphates contain phosphorus instead of chloride. DDT is one of the most well-known organochlorides, while temephos, malathion are organophosphates. Derivatives from carbamic acid fall under the carbamate class, while pyrethroids are a synthetic version of insecticides modeled after pyrethrins that are produced by chrysanthemums (Oliveira et al., 2017). Carbaryl and bendiocarb are the most used carbamates while deltamethrin is a widely used pyrethroid. DDT and other organochlorides cause hyperexcitation of neurons. This hyperexcitation is due to sodium channels remaining open for longer periods. DDT was introduced in 1940. Organophosphates were introduced in 1950 and are cholinesterase inhibitors which causes an increase in acetylcholine levels. Carbamates started being used in 1960 and also cause an accumulation of acetylcholine by inhibiting acetylcholinesterase in a reversible manner (Silberman and Taylor, 2021). Lastly, pyrethroids were introduced in 1970 and cause paralysis of the central and peripheral nervous system by interacting with

voltage-gated sodium channels (“Bifenthrin - ScienceDirect,” n.d.). Each of these insecticides have their own pitfalls.

Organochlorides can accumulate in fat bodies because the chemicals are lipid soluble. The solubility of these compounds is significant because it can lead to biomagnification in predators. DDT has also been shown to effect egg formation in birds and ultimately leads to a decrease in fertility (Oliveira et al., 2017). Organochlorides have been shown to cause nervous and immune system effects in humans. DDT is highly persistent in both the environment as well as lipids in the human body (Beard, 2006). The pesticide has a slow elimination process from the body, and in third world countries many people still show detectable levels of DDT or its metabolite DDE (Beard, 2006). Although DDT exposure in laboratory animals has been shown to cause cancer, there is not enough information to determine whether this chemical has the same effect on humans. The more problematic side of DDT is its effects on the environment and wildlife. As said earlier, DDE, a metabolite of DDT, causes eggshell thinning and is responsible for a decrease in the reproductive rate in birds. DDT is also highly toxic to aquatic organisms, where its half-life is about 150 years (“DDT (General Fact Sheet),” 1999).

Organophosphates have some advantages over organochlorides, most importantly that they do not bio accumulate in fat tissues, and they biodegrade much faster, between 1 and 12 weeks. Unfortunately, the instability of these chemicals means that reapplication must happen more often. However, this class of insecticides has some pitfalls as well; most notably they are more toxic to vertebrates than their organochlorine counterparts

(Oliveira et al., 2017). There is evidence that exposure to organophosphates may increase risk for developing Parkinson's disease (Oliveira et al., 2017).

Carbamates use a different mode of action than organochloride insecticides. These chemicals, like organophosphates, cause an accumulation of acetylcholine, however the process involved in this accumulation is carboxylation, and carbamate chemicals inhibit acetylcholinesterase. These pesticides can be used against organochloride and organophosphate resistant insects, provided the resistance is not related to an altered acetylcholinesterase (Oliveira et al., 2017). Carbamates have been shown to be highly toxic to fish as well as other aquatic organisms through acetylcholinesterase inhibition. In humans, carbamates have been shown to be associated with many problems, including endocrine disruption, and reproductive disorders. Studies have also shown carbamate can cause problems in vitro; including human immune cell apoptosis and necrosis, as well as natural killer cells and T lymphocytes. There is evidence to suggest that carbamate pesticides may also aid in dioxin toxicity by acting as a ligand for a receptor for hepatic aryl hydrocarbon. Lastly, there is evidence that carbamates may play a role in causing neurobehavioral effects and increasing the risk of non-Hodgkin's lymphoma and dementia (Nicolopoulou-Stamati et al., 2016). Oxidative stress due to carbamates can cause damage to DNA, which can lead to mutations in immune cells and increase risk of cancer. Carbamates down regulate gonadotropin hormone in the hypothalamus gland of the endocrine system. This can lead to increased cortisol secretion, and also increase the risk of cancer as well as infection, autoimmune reactions and allergies (Oliveira et al., 2017).

The last class of pesticides used to control mosquito populations are pyrethroids. Pyrethroids are advantageous as chemical pesticides because they are biodegradable. Their biodegradability aids in their inability to accumulate like the chemical classes listed earlier. Similarly, pyrethroids cause minimal poisoning or deleterious effects on birds and mammals, however aquatic invertebrates and fish are highly susceptible to these chemicals that act on the peripheral and central nervous system (Oliveira et al., 2017). Although pyrethroids seem like the best choice based off a lack of human health toxicity, and a lack of bioaccumulation, this class of chemicals still cause environmental harm.

Aedes and *Anopheles* mosquitoes have shown resistance against both organophosphate and pyrethroid chemicals. Resistance can happen through a handful of mechanisms including, mutations in the target protein, inability of the chemical to absorb through the cuticle, and increased biodegradation by enzymes (Oliveira et al., 2017). A mutation called the kdr, knock down resistance, is a mutation in the voltage-gated sodium channel gene, this mutation renders mosquitoes resistant to both pyrethroids and DDT (Reimer et al., 2008).

There are two bacteria that are currently used as biological control methods. These bacteria will be discussed later in the chapter. The issue of resistance development among mosquito populations against biological control methods is a problem with *L. sphaericus,* one of the bacteria used to combat *Culex* and *Anopheles* mosquito populations, this is discussed in more detail in the *L. sphaericus section*.

The last method of control includes genetically modified mosquitoes. There has been a lot of talk about genetically modified organisms over the years, and this may cause

some unrest in various communities. In 2016, Oxitec was granted permission to release sterile male mosquitoes into the Florida Keys to control mosquito populations. This decision was met with protests from community members (Allen, 2016). Thus, a pitfall of genetic control methods is community apprehension towards genetically modified organisms.

6. *Bacillus thuringiensis*

Bacillus thuringiensis is part of the *Bacillus cerus* group; this group contains three other species, *B. cerus*, *B. anthracis*, and *B. mycoides*. The distinguishing feature of *B. thuringiensis* is its entomopathogenic properties, in that it can kill insects. *Bt* bacteria, of which there are more than 60 serotypes (Nester et al., 2002), produce δ-endotoxins as parasporal inclusions during sporulation. The insecticidal proteins produced are predominantly Cry, Cyt and Vip toxins. These proteins are biodegradable, nontoxic to humans, plants and vertebrates and are highly specific and selective for their target organism (Bravo et al., 2005). Two *B. thuringiensis* strains and the toxins they produce will be discussed in subsequent sections.

7. *Bacillus thuringiensis* subsp. *israelensis*

Bacillus thuringiensis israelensis (*Bti*) is currently being used in the field as a biological control method. The use of *Bti* as a biological control method dates back to the 1990s (Becker, 1997; Guillet et al., 1990). *Bti* was discovered in 1978 by Goldberg and Margalit (Goldberg and Margalit, 1977). This bacterium has a plasmid that encodes six genes involved in toxicity, these genes are cry4Aa, cry4Ba, cry11Aa, cyt1Aa, cry10Aa and cyt2Ba. These 6 toxins target *Anopheles, Aedes* and *Culex* mosquitoes. There has not

been any resistance seen against *Bti* in the field even though it has been used commercially for almost 35 years (CDC, 2020). This lack of resistance is due to different modes of action of the Cry toxins as well as a synergistic effect seen between the cyt and cry toxins. Cry4Aa is most toxic to *Culex* and less toxic to *Anopheles* or *Aedes* while, Cry4Ba is toxic to *Aedes* and *Anopheles* but has low toxicity against *Culex* mosquitoes. Cry11A is more toxic to *Aedes* and *Culex* but less toxic to *Anopheles*. Cry10A shows some synergistic effects with Cyt1A against *Aedes* mosquitoes and with Cry4Ba against *Culex* mosquitoes. Cyt1Aa proteins shows synergistic effects with Cry4Aa, Cry4Ba and Cry11Aa, while Cyt2Ba also shows some synergistic effects with Cry toxins encoded in the plasmid. Cyt1A is thought to play a major role in delaying resistance to *Bti* in the field based on its synergistic traits (Ben-Dov, 2014). Although no resistance against the cocktail of mosquitocidal toxins of *Bti* has been seen, a tolerance to Cry4A and Cry11A single toxins was seen in *Aedes sticticus* populations found in the French Rhône-Alpes region, where *Bti* has been used for decades (Tetreau et al., 2013). The toxicity of *Bti* against *Anopheles* mosquitoes is much lower than *Aedes* and *Culex.*

8. *Bacillus thuringiensis* subsp. *jegathesan*

Bacillus thuringiensis subsp. *jegathesan* was isolated in Malaysia in 1995 (Kawalek et al., 1995). This strain appears to be more toxic than *Bti* against *Culex quinquefasciatus,* and as toxic as *Bti* against *An. stephensi* and *Ae. aegypti* (Kawalek et al., 1995; Seleena et al., 1995; Sun et al., 2013). The toxins found within this strain of *Bt* were found to be distinct from those produced by *Bti* through western blot analysis using polyclonal antibodies made from purified *Bti* toxins (Kawalek et al., 1995). Eight

protoxins were identified in *Bacillus thuringiensis* subsp. *jegathesan* 367 they include Cry11Ba (Delécluse et al., 1995), Cry30Ca, Cry60Aa, and Cry60Ba (Sun et al., 2013), Cry24Aa (Kawalek, 1998), Cyt2Bb (Cheong and Gill, 1997), Cry19Aa (Rosso and Delécluse, 1997), Cry25Aa (Kawalek, 1998). The Cry11Ba toxin is 81kDa and has large regions that are similar to those found in Cry11A. The structures of both Cry11Ba and Cry11Aa were recently solved. One interesting feature of both protein structures involves an extra β-strand between strands β4 and β5 in domain II which has been named β_{pin}. This feature aids in the formation of a modified β-prism and promotes a support of tetramerization through a two-fold axis (Tetreau et al., 2022). Cry11B is reported to be more toxic to *Aedes aegypti, Anopheles stephensi,* and *Culex pipiens* mosquito larvae than Cry11A (Delécluse et al., 1995).

9. *Lysinibacillus sphaericus*

Lysinibacillus sphaericus, previously called *B. sphaericus* was found in 1904 by Neide (Silva Filha et al., 2014). Studies showed the activity of some strains was related to crystalline inclusion production during stage III of sporulation (Silva Filha et al., 2014). Once produced the crystals stay inside the exosporum (Kalfon et al., n.d.). These crystals were later found to contain the binary protoxin, which is the major toxin produced by *Ls* (Baumann et al., 1985). Along with binary toxins (Bin), *Ls* also produces Mtx and Cry48Aa/49Aa toxins which confer its mosquitocidal activity; *Ls* has high activity against *Culex* and *Anopheles* species (Silva Filha et al., 2014). *Ls* strains that produce Bin toxins have the highest activity (Payne and Davidson, 1984), while those

that do not produce Bin protoxins but do contain Mtx toxins show lower toxicity (Myers et al., 1979).

Studies have shown that *Ls* is nontoxic to nontarget organisms including crustaceans, amphibians and fish as well as mammals (Lacey and Mulla, 1990; Mulla et al., 1984; Siegel and Shadduck, 1990). Others have been concerned about the fate of the bacterial spores in the environment and what, if any, problems they will create. Studies in both the lab and the field showed recycling of spores, in that they can thrive in larval cadavers and thus be used in an extended capacity in some sites (Charles and Nicolas, 1986; Nicolas et al., 1987). In areas with treated water or environments that have dried and then been re-flooded recycling of *Ls* spores does not occur (Davidson et al., 1984).

Ls and *Bti* may be released in mixtures as part of control programs. It is often recommended for resistance-management. The mixture allows for a broader spectrum of targets as well as prevents the development of resistance against *Ls* toxins, it also has the potential to cause synergism between bacterial toxins when the two bacteria are ingested together (Silva Filha et al., 2014; Wirth et al., 2004). *Ls* has been used in a control program in Germany since 1985 to work alongside *Bti* to combat *Culex* and *Aedes* mosquitoes (Becker, 1997). *Ls* has also supplemented *Bti* use in Tanzania since 2006 to combat malaria (Fillinger et al., 2008).

Resistance against *Ls* toxins has proven to be a problem over the years. Continuous treatment of mosquito populations, due to their year round proliferation, causes an increase in selection pressure (Silva-Filha et al., 2001). Recycling and persistence of *Ls* toxins in breeding sites causes exposure to insecticidal crystals for prolonged periods (Charles and

Nicolas, 1986). The last factor that has allowed for some resistance development amongst targeted mosquito populations is the mode of action of *Ls* toxins; one primary toxin targeting one class of receptors is important for selection pressure and eventual development of resistance (Ferreira and Silva-Filha, 2013). Resistance has been noted in both laboratory and field settings. In one lab setting, a population of *Cx. pipiens* mosquitoes collected in California became resistant in 12 generations (Wirth et al., 2000) another laboratory population collected in California showed a 37-fold resistance ratio in 80 generations (Rodcharoen and Mulla, 1994). In the field, resistance was seen in a population found in Southern France, this population was subjected to *Ls* for about five years (Sinègre et al., 1994). Other reports of resistance came from India (Rao et al., 1995), Tunisia (Nielsen-Leroux et al., 2002), and Thailand (Mulla et al., 2003) among other areas. The development of resistance against *Ls* produced toxins demonstrates the importance of finding new control methods as well as utilizing multiple methods at once to prevent further resistance development.

10. Cry toxin structure and mechanism of action

Cry toxins contain three domains (Figure 1-3) all of which play a specific role in toxicity. Domain I contains seven α helices and is involved in pore formation, and insertion into the membrane. Whereas, domains II and III are involved in receptor binding. Domain II contains three antiparallel β-sheets with loop regions connecting these sheets. This domain is implicated in species specificity because it is the most diverse among the different toxin protein (Bravo et al., 2005). The α-8 loop in Cry11A and Cry11B has been implicated in toxicity against *Aedes aegypti* mosquitoes. This loop

region which is found in domain II, is important for receptor interactions in the larval midgut (Fernández et al., 2005; Likitvivatanavong et al., 2009). Domain III also contains two antiparallel β- sheets. The loop regions involved in this domain may also play a role in species specificity and thus be involved in receptor binding (Bravo et al., 2005).

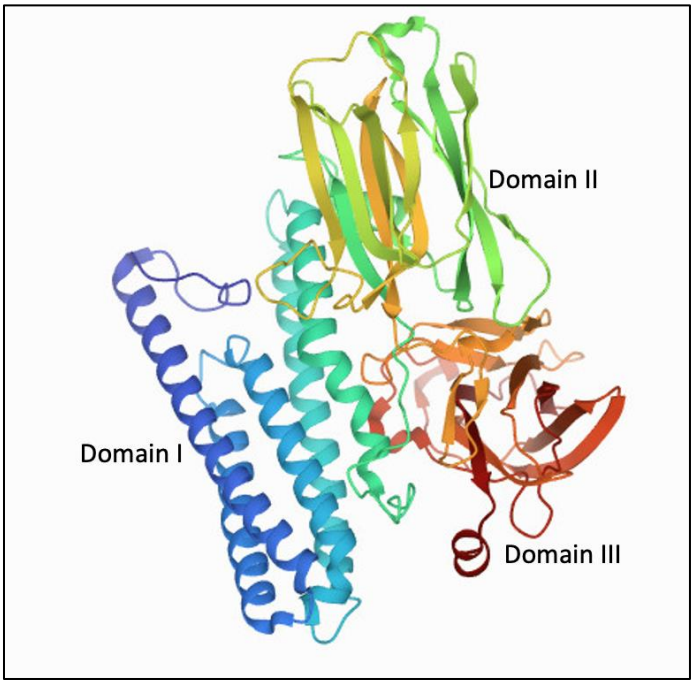

Figure 1-3. Protein structure of Cry Toxin.
Labeled structure of Cry4Ba toxin domains indicating α-helices of domain I (blue) and β-sheets of domains II (green) and III (red). Source: RCSB Protein Data Bank.

Although there are many cry toxins, the mechanism of action of this family of toxins appears to be very similar. Presently there are two proposed mechanisms of action that are recognized within the scientific community. Both proposed mechanisms start with solubilization of the toxin within the midgut of the target organism. This process includes cleavage of disulfide bonds and releasing protoxins. The protoxin is then cleaved and activated by endogenous *Bt* or host proteases. Most activated toxins are 55 to 65 kDa in size and have lost amino acids from both the C- and N-termini. Other Cry

toxins, like Cry4A and Cry11A, result in two peptide fragments when activated (Adang et al., 2014).

The first mechanism is called the sequential binding model and involves the toxin binding to multiple receptors before causing toxicity. The second, is the signaling pathway model which involves binding of the toxin to a receptor which then creates a signaling pathway cascade which in turn causes toxicity. A schematic of these models can be found in Figure 1-4. In the sequential binding model after activation, the toxin binds to cadherin. This binding causes a conformational change and a subsequent cleavage between helices α1 and α2. With the removal of the α1 helix, the rest of the toxin can oligomerize to form the pre-pore structure. This oligomer can then bind to the aminopeptidase (APN) or alkaline phosphatase (ALP) receptors (Gómez et al., 2002). It was shown that the oligomerized form of the toxin has a higher affinity for the APN or ALP receptors than in its monomeric form (Bravo et al., 2004). This binding event causes the insertion of the pre-pore into the membrane. The pore is permeable to small molecules and interferes with the cell physiology by disrupting ionic gradients. This may lead to lysis due to a massive influx of solutes from the midgut lumen (Knowles and Ellar, 1987). The signaling pathway model proposes that cytotoxicity is due to the binding of toxins to cadherin receptors. This binding event then causes signaling pathways to be activated including Mg^{2+}- dependent and adenylyl cyclase/protein kinase A, which lead to necrotic cell death (Zhang et al., 2006, 2005).

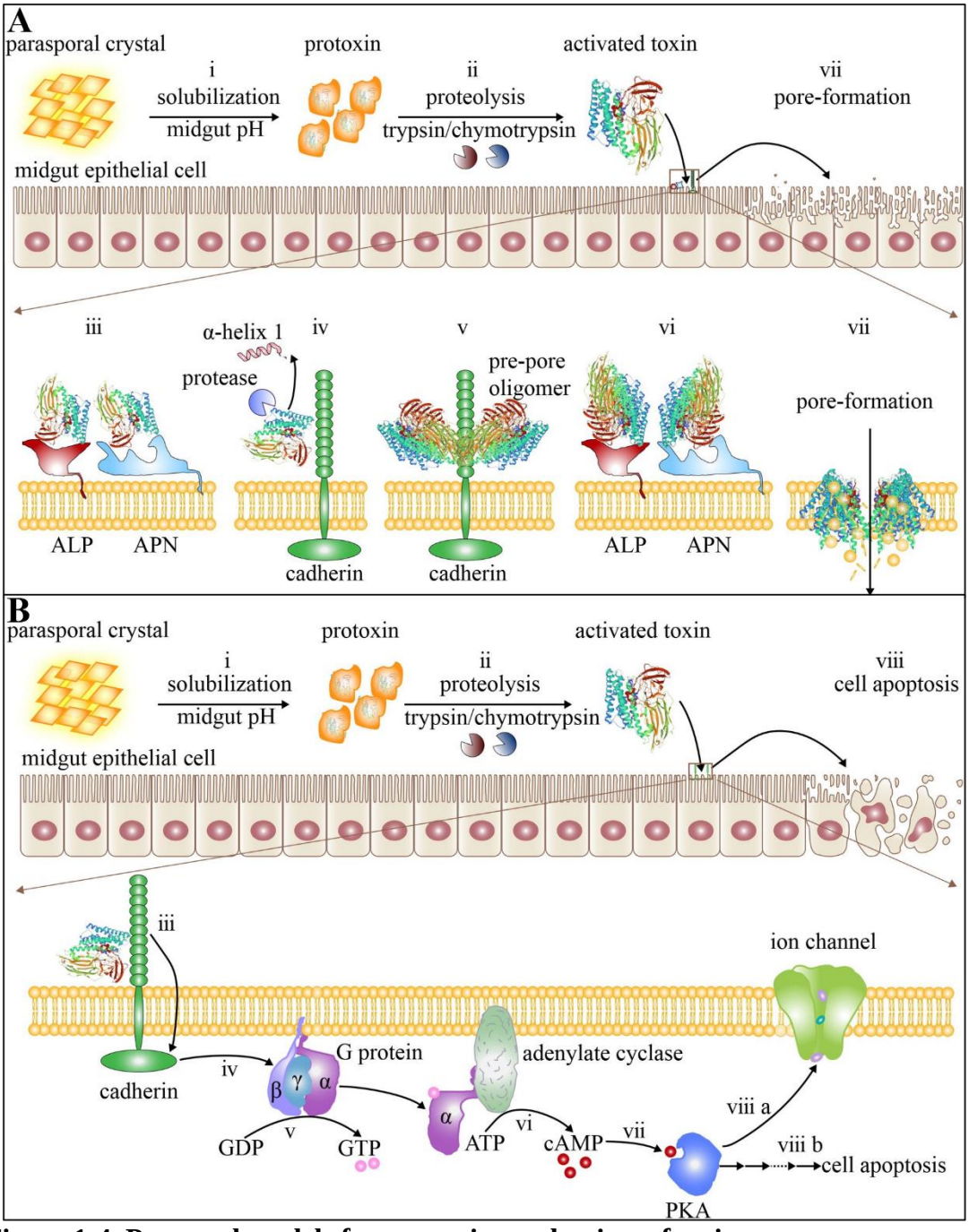

Figure 1-4. Proposed models for cry toxin mechanism of action.
A. Shows a schematic of the proposed sequential binding model that involves binding to various receptors and oligomerization of the toxin to form a pore. B. Shows a schematic of the proposed signaling pathway model which involves activation of a G protein coupled receptor and subsequence cell signaling to trigger apoptosis. Source: https://doi.org/10.3389/fmicb.2021.665101

11. Cytolytic toxins

Cyt toxins were originally found in *Bti* and have been found to synergize with the Cry toxins also found in that bacteria (Adang et al., 2014). Cyt toxins have been seen to synergize with other toxins as well including, the Mtx1 and Bin toxins. The synergism of Cyt1A and Cry4 was able to slow the development of resistance to Cry11A in *Culex quinquefasciatus* as well as overcome resistance to Cry4 alone in the same insect. The proposed mechanism of synergism involves Cyt1A toxin binding to domain II of Cry toxins which causes the formation of a pre-pore oligomer (Adang et al., 2014). López-Diaz et al 2013 found that the synergistic activity between Cyt1A and Cry11A is independent of toxicity, oligomerization and membrane insertion of Cyt1Aa alone (López-Diaz et al., 2013).

12. Binary toxins

Another family of toxins are binary toxins so called because both proteins are essential for toxicity. One well known set of binary toxins are BinA and BinB, both produced in *Ls*. The BinA and BinB proteins are transcribed at the same time from a single operon. Once these toxins reach the larval gut, they undergo solubilization from their crystal inclusions due to the alkaline environment of the gut. These proteins can then undergo proteolysis allowing the toxins to be more toxic. It appears only one Bin protein is involved in binding to receptors in the gut of the mosquito larvae. The mode of action after receptor binding has not been completely elucidated. There is some evidence that pore formation occurs, however others believe the toxins may be endocytosed into the cell and can cause toxicity in that way (Berry, 2012). Another set of toxins that have

been found within *Ls* are Cry48 and Cry49. Cry48 is related to mosquitocidal Cry toxins that have been found in *Bt and* is part of the 3-domain Cry toxin family. However, Cry49 is part of the Bin family of toxins. Neither Cry48 nor Cry49 is toxic alone, but when together, they exhibit high levels of toxicity against *Culex* mosquitoes (Jones et al., 2008). In this case, toxicity is dependent on the amount of Cry48 produced, while with the BinA/BinB binary toxins, a 1:1 ratio is necessary (Berry, 2012).

13. *Clostridium*

The genus *Clostridium* includes about 100 different anaerobic species of bacteria. Some are involved in producing industrial products like acetone, butanol and ethanol which are all produced by *Clostridium acetobutylicum* (Barloy et al., 1996). Other more well-known species of *Clostridium* cause debilitating human diseases like tetanus, botulism, and gas gangrene which are caused by *Clostridium tetani*, *Clostridium botulinum*, and *Clostridium perfringens respectively.* Most bacteria from the genus *Clostridium* are anaerobic and rod shaped, however some can become tolerant of oxygen. These bacteria are gram-positive and spore forming. Spore formation is a characteristic of these bacteria and many are normal permanent members of human skin as well as the gastrointestinal tracts of both humans and animals (Wells and Wilkins, 1996).

14. *Clostridium botulinum*

Clostridium botulinum is an anaerobic, spore forming, gram positive (Gu and Jin, 2013) bacteria that produces a neurotoxin that is responsible for botulism (Solomon and Lilly Jr, 2001). There are eight strains of *C. botulinum* A, B, C1, C2, D, E, F, and G (Tiwari and Nagalli, 2022) and they target and cleave various soluble N-ethylmaleimide

sensitive factor attachment protein receptors (SNARE) proteins, which prevents the release of acetylcholine into the neuromuscular junction and causes paralysis (Gu and Jin, 2013). Botulinum neurotoxin (BoNT) is generally involved in a gene cluster that involves an NTNH gene, and either three HA genes or three orfx genes. The proteins encoded by genes listed form a structure called the progenitor toxin complex (Gu and Jin, 2013). The NTNH protein interacts with the botulinum toxin, and the HA proteins interact with cells in the intestinal epithelial layer and aid in transport of the BoNT to the blood stream (Gu and Jin, 2013).

15. Botulinum progenitor complex and mode of action

As stated in the previous section, the NTNH protein surrounds the BoNT toxin and protects it from being degraded in the gut of the target organism. The HA protein is involved with translocation of the BoNT toxin into the blood stream where it can find its target. The BoNT toxin is comprised of three domains, the light chain which is a protease, and the heavy chain which contains a translocation domain on the N-terminus and a receptor binding domain on the C-terminus (Gu and Jin, 2013). The binding domain binds to receptors on the surface of neurons, once endocytosed, the translocation domain aids in moving the light chain to the acidic cytosol. Once in the cytosol, the light chain will cleave its target SNARE protein. Each strain of BoNT targets a different SNARE protein, the list includes either synaptobrevin, syntaxin or SNAP-25 (Gu and Jin, 2013).

16. *Paraclostridium bifermentans*

Paraclostridium bifermentans is a gram-positive, spore forming anaerobe. It is commonly found in animal feces, soil, water, and sewage. It has been known to cause necrotizing pneumonia and bacteremia with metastatic osteomyelitis. It is also an agent of fermentation, and acts on a variety of different carbohydrates to produce acetate, lactate, ethanol, hydrogen, and carbon dioxide (Wong et al., 2014).

In 1990 a new strain of *Paraclostridium bifermentans* was isolated from mangrove swamp sediment in Malaysia by W.C. Cheong and H.L. Lee. This new strain was identified as *Paraclostridium bifermentans* serovar *malaysia (Pbm*) at the Institute de Pasteur (de Barjac et al., 1990). It was first described by Dr. L. H. Lim and S. Benjamin at the Institute for Medical Research, Kuala Lumpur as having high mosquitocidal activity. Pbm was found to have about 10 times higher toxicity against *An. stephensi* compared to *Bacillus thuringiensis serovar israelensis* (*Bti*). However, it was also found that *Pbm* activity against *Ae. aegypti* and *Cx. pipiens* is 10 times lower than the activity of *Bti* (Isabelle Thiery et al., 1992; I. Thiery et al., 1992). The activity of *Pbm* against mosquitoes reaches its maximum after 8 hours of sporulation and remains toxic until cell lysis occurs. This toxicity was initially thought to be due to inclusion bodies, however this was later found to be false (Charles et al., 1990).

17. CRISPR/Cas9

Gene editing has become a useful tool within the molecular biology community. A new technique involving clustered regularly interspaced short palindromic repeats (CRISPR) has been used to edit the genome of many organisms. CRISPR was originally

found in e.coli in 1987 by Ishino et al. (Ishino et al., 2018). CRISPR-Cas systems are part of the immune system of some archaea and bacteria. Immunity produced through CRISPR-Cas systems involves integrating sequences of foreign DNA, which can include invasive genetic elements like viral DNA or plasmids, into a CRISPR locus. This integration of foreign DNA allows the cell to recognize, remember, and destroy the invasive element if seen again. The type-II-system of CRISPR-Cas9 has been utilized as a gene editing tool. The type-II-system uses a Cas9 protein and a short guide RNA (gRNA) sequence which identifies the complementary sequence for the RNA where the Cas9 protein will cut 3 nucleotides upstream of the protospacer adjacent motif (PAM) region (Tetsch, 2017). The PAM region involves any nucleotide followed by two G nucleotides (Shah et al., 2013). Cells in which CRISPR-Cas9 are being used will then repair the cleaved DNA through two repair methods homologous recombination or nonhomologous end joining (Ran et al., 2013). Depending on the goal of the gene editing, a plasmid can be provided to allow the cell to go through homologous recombination in which a new sequence of DNA can be put into the original sequence. Nonhomologous end joining results in the disruption of sequence whether through frameshift of a small deletion within the DNA which can cause inactivity of a gene (Chatterjee and Walker, 2017).

18. Specific Aims

Aedes, Culex and *Anopheles* mosquitoes serve as vectors that transmits some of the world's most debilitating diseases, including dengue fever, West Nile virus fever and malaria, respectively. Every year these diseases are responsible for hundreds of thousands of deaths worldwide. There are multiple control methods currently employed (Baldacchino et al., 2015), with chemical control being the primary method. No one method is completely effective, however, and resistance to some of these methods has been seen in the field. There are currently two bacteria being used as biological control methods, *Bacillus thuringiensis israelensis* (*Bti*) and *Lysinibacillus sphaericus* (*Ls*). *Bti* exhibits larvicidal effects on *Aedes aegypti* and *Culex quinquefasciatus* while *Ls* has been used to target primarily *Culex* mosquito populations. Both of these bacteria have shown to be quite effective against their mosquito targets; however, neither is highly effective activity against *Anopheles* mosquitoes which indicates a need for alternative methods of control that can target *Anopheles* mosquitoes specifically.

Paraclostridium bifermentans serovar *malaysia* (*Pbm*), a gram positive, anaerobic bacterium, was isolated from mangrove swamp soil in Malaysia (de Barjac et al., 1990). This bacteria exhibit mosquitocidal activity against *Anopheles* and *Aedes* mosquitoes, but not against non-target aquatic organisms or mammals (Yiallouros et al., 1994). To determine which toxin proteins were involved in toxicity, a loss of function mutant was created in our laboratory, its genome was then analyzed and compared to the wild type as well as the non-toxic type strain Parac*lostridium bifermentans (Pb)*. After analysis, it was found that a large 109kb plasmid was present in the toxic strain, and was

absent in the loss of function mutant, and is thus responsible and essential for toxicity. This large plasmid contains two loci, *cry* and *ptox*, that encode potentially toxic proteins. The *cry* operon consists of four proteins, two Cry proteins (Cry16 and Cry17) and two hemolysin-like proteins (Cbm17.1 and Cbm17.2), that form a complex (Qureshi et al., 2014). While the *ptox* locus contains a clostridial-like neurotoxin (pmp1), three orfx genes, a non-toxic non-hemagglutinin gene (NTNH), P47 protein, and a putative metallophosphatase family protein (MPP) (Contreras et al., 2019). The Cry operon is more toxic to *Aedes* mosquitoes, while the *ptox* locus is more toxic to *Anopheles* mosquitoes. We are interested in understanding these two toxin loci further by determining the mechanism of action of the Cry operon and determining when the proteins of the *ptox* locus are expressed, the potential stoichiometry of the proteins within the complex and its size.

Previous work with the Cry operon showed that toxicity was seen only when all four full length proteins in the operon were expressed together. This indicates each protein component may have their own role in the mechanism of action. When tested alone, this operon exhibited toxicity against *Aedes* mosquitoes, but not *Anopheles* mosquitoes. **I hypothesize that Cry 17 is involved in binding to mosquito midguts facilitating the pore formation and subsequent osmotic imbalance. I also hypothesize that the proteins of the *ptox* locus are expressed at the same time, where the NTNH and other proteins function to protect the pmp1 neurotoxin.**

As previously stated, *Bti* and *Ls* are both currently being used in the field to combat mosquito populations. These two bacteria are also most toxic to *Aedes* and *Culex*

mosquitoes thus there is a need to find more ways to target *Anopheles* mosquitoes. **I hypothesize that introducing Cry11B into the *Bti* toxin plasmid (pBtoxis) will increase its toxicity against *Anopheles* mosquitoes.**

Aim 1. Understand the two toxin loci in *Paraclostridium bifermentans*

Pbm is toxic to both *Aedes* mosquitoes and *Anopheles* mosquitoes. Within its 109kb plasmid, there are two loci that are toxic, the cry operon and the ptox locus, described above. The cry operon is toxic to *Aedes* mosquitoes and contains two cry toxins and two aegerolysin proteins under the same promoter. Cry toxins are three domain toxins in which one domain is responsible for pore formation and the other two are important for binding receptors in the midgut of the mosquito. The domains involved in binding to receptors are important for species specific toxicity. Interestingly, toxicity of the Cry operon, against *Aedes aegypti* mosquitoes, requires all four full length proteins. These four proteins also appear to form a complex when expressed together leading to the hypothesis that some part of the complex is important for receptor binding while the others lead to the pore formation and subsequent death of the organism. There are two goals of this aim the first is to determine the critical loop region and amino acids responsible for operon toxicity by mutating the loop regions of the cry toxins and testing for toxicity.

The ptox locus is toxic to *Anopheles* mosquitoes. The second goal is to verify that a complex is formed by the proteins encoded in the ptox locus as well as determine the size, potential stoichiometry, and time of expression of the complex proteins.

Aim 2. Increase the toxicity of *Bti* against *Anopheles* mosquitoes

Bti is most toxic to *Aedes* and *Culex* mosquitoes due to the toxins encoded in its large pBtoxis plasmid. I will increase the toxicity of *Bti* to *Anopheles* mosquitoes using CRISPR/Cas9 technology. A plasmid vector was created (Toymentseva and Altenbuchner, 2019) in which a Cas9 protein is under the control of a xylose inducible promoter. This plasmid was created to perform genome editing in *Bacillus subtilis*, but I will use it to edit the pBtoxis plasmid of *Bti*. The plasmid contains cloning sites for guide RNA as well as a homologous region to be edited into the target when the cell uses homologous recombination to repair the double strand break created by Cas9. I will use this plasmid to attempt to introduce LacZ into the pBtoxis plasmid to perform a proof-of-concept experiment which can be utilized later to introduce Cry11B into pBtoxis and cause *Bti* to be toxic to *Anopheles* mosquitoes.

References

Adang, M.J., Crickmore, N., Jurat-Fuentes, J.L., 2014. Chapter Two - Diversity of Bacillus thuringiensis Crystal Toxins and Mechanism of Action, in: Dhadialla, T.S., Gill, S.S. (Eds.), Advances in Insect Physiology, Insect Midgut and Insecticidal Proteins. Academic Press, pp. 39–87. https://doi.org/10.1016/B978-0-12-800197-4.00002-6

Allen, G., 2016. Florida Keys Approves Trial Of Genetically Modified Mosquitoes To Fight Zika. NPR.

Baldacchino, F., Caputo, B., Chandre, F., Drago, A., Torre, A. della, Montarsi, F., Rizzoli, A., 2015. Control methods against invasive Aedes mosquitoes in Europe: a review. Pest Manag. Sci. 71, 1471–1485. https://doi.org/10.1002/ps.4044

Barloy, F., Delécluse, A., Nicolas, L., Lecadet, M.M., 1996. Cloning and expression of the first anaerobic toxin gene from Clostridium bifermentans subsp. malaysia, encoding a new mosquitocidal protein with homologies to Bacillus thuringiensis delta-endotoxins. J. Bacteriol. 178, 3099–3105.

Baumann, P., Unterman, B.M., Baumann, L., Broadwell, A.H., Abbene, S.J., Bowditch, R.D., 1985. Purification of the larvicidal toxin of Bacillus sphaericus and evidence for high-molecular-weight precursors. J. Bacteriol. 163, 738–747. https://doi.org/10.1128/jb.163.2.738-747.1985

Beard, J., 2006. DDT and human health. Sci. Total Environ. 355, 78–89. https://doi.org/10.1016/j.scitotenv.2005.02.022

Becker, N., 1997. Microbial control of mosquitoes: Management of the upper rhine mosquito population as a model programme. Parasitol. Today 13, 485–487. https://doi.org/10.1016/S0169-4758(97)01154-X

Becker, N., Petrić, D., Zgomba, M., Boase, C., Madon, M., Dahl, C., Kaiser, A., 2010. Mosquitoes and Their Control, 2nd ed. Springer-Verlag, Heidelberg, Germany.

Ben-Dov, E., 2014. Bacillus thuringiensis subsp. israelensis and Its Dipteran-Specific Toxins. Toxins 6, 1222–1243. https://doi.org/10.3390/toxins6041222

Berry, C., 2012. The bacterium, Lysinibacillus sphaericus, as an insect pathogen. J. Invertebr. Pathol. 109, 1–10. https://doi.org/10.1016/j.jip.2011.11.008

Bifenthrin - ScienceDirect [WWW Document], n.d. URL https://www.sciencedirect.com/science/article/pii/B9780123864543011696 (accessed 12.26.21).

Braack, L., Gouveia de Almeida, A.P., Cornel, A.J., Swanepoel, R., de Jager, C., 2018. Mosquito-borne arboviruses of African origin: review of key viruses and vectors. Parasit. Vectors 11, 29. https://doi.org/10.1186/s13071-017-2559-9

Brady, O.J., Hay, S.I., 2020. The Global Expansion of Dengue: How Aedes aegypti Mosquitoes Enabled the First Pandemic Arbovirus. Annu. Rev. Entomol. 65, 191–208. https://doi.org/10.1146/annurev-ento-011019-024918

Bravo, A., Gómez, I., Conde, J., Muñoz-Garay, C., Sánchez, J., Miranda, R., Zhuang, M., Gill, S.S., Soberón, M., 2004. Oligomerization triggers binding of a Bacillus thuringiensis Cry1Ab pore-forming toxin to aminopeptidase N receptor leading to insertion into membrane microdomains. Biochim. Biophys. Acta 1667, 38–46. https://doi.org/10.1016/j.bbamem.2004.08.013

Bravo, A., Soberón, M., Gill, S.S., 2005. 6.6 - Bacillus thuringiensis: Mechanisms and Use, in: Gilbert, L.I. (Ed.), Comprehensive Molecular Insect Science. Elsevier, Amsterdam, pp. 175–205. https://doi.org/10.1016/B0-44-451924-6/00081-8

Carlysue, #038;r=pg', Loading='lazy'/>carylsue, #038;r=pg 2x' Class='avatar Avatar-20 Photo' Height='20' Width='20', 2017. Are Mosquitoes Outsmarting Mosquito Nets? Natl. Geogr. Educ. Blog. URL https://blog.education.nationalgeographic.org/2017/04/03/are-mosquitoes-outsmarting-mosquito-nets/ (accessed 3.15.21).

CDC, 2020. Bti \ CDC [WWW Document]. Cent. Dis. Control Prev. URL https://www.cdc.gov/mosquitoes/mosquito-control/community/bti.html (accessed 6.22.22).

CDC-Centers for Disease Control, 2020. CDC - Malaria - About Malaria - Biology [WWW Document]. URL https://www.cdc.gov/malaria/about/biology/index.html (accessed 6.22.22).

Center for Disease Control, n.d. Pathophysiology of Severe Dengue.

Charles, J.F., Nicolas, L., 1986. Recycling of Bacillus sphaericus 2362 in mosquito larvae: a laboratory study. Ann. Inst. Pasteur Microbiol. 137B, 101–111. https://doi.org/10.1016/s0769-2609(86)80097-7

Charles, J.F., Nicolas, L., Sebald, M., de Barjac, H., 1990. Clostridium bifermentans serovar malaysia: sporulation, biogenesis of inclusion bodies and larvicidal effect on mosquito. Res. Microbiol. 141, 721–733. https://doi.org/10.1016/0923-2508(90)90066-y

Chatterjee, N., Walker, G.C., 2017. Mechanisms of DNA damage, repair and mutagenesis. Environ. Mol. Mutagen. 58, 235–263. https://doi.org/10.1002/em.22087

Cheong, H., Gill, S.S., 1997. Cloning and characterization of a cytolytic and mosquitocidal delta-endotoxin from Bacillus thuringiensis subsp. jegathesan. Appl. Environ. Microbiol. 63, 3254–3260. https://doi.org/10.1128/aem.63.8.3254-3260.1997

Clements, A.N., 1999. The Biology of Mosquitoes. Cabi Publishing.

Contreras, E., Masuyer, G., Qureshi, N., Chawla, S., Dhillon, H.S., Lee, H.L., Chen, J., Stenmark, P., Gill, S.S., 2019. A neurotoxin that specifically targets Anopheles mosquitoes. Nat. Commun. 10, 2869. https://doi.org/10.1038/s41467-019-10732-w

Cowman, A.F., Healer, J., Marapana, D., Marsh, K., 2016. Malaria: Biology and Disease. Cell 167, 610–624. https://doi.org/10.1016/j.cell.2016.07.055

Davidson, E.W., Urbina, M., Payne, J., Mulla, M.S., Darwazeh, H., Dulmage, H.T., Correa, J.A., 1984. Fate of Bacillus sphaericus 1593 and 2362 spores used as larvicides in the aquatic environment. Appl. Environ. Microbiol. 47, 125–129. https://doi.org/10.1128/aem.47.1.125-129.1984

DDT (General Fact Sheet), 1999.

de Barjac, H., Sebald, M., Charles, J.F., Cheong, W.H., Lee, H.L., 1990. [Clostridium bifermentans serovar malaysia, a new anaerobic bacterium pathogen to mosquito and blackfly larvae]. C. R. Acad. Sci. III 310, 383–387.

Delécluse, A., Rosso, M.L., Ragni, A., 1995. Cloning and expression of a novel toxin gene from Bacillus thuringiensis subsp. jegathesan encoding a highly mosquitocidal protein. Appl. Environ. Microbiol. 61, 4230–4235.

Dengue Around the World | Dengue | CDC [WWW Document], 2021. URL https://www.cdc.gov/dengue/areaswithrisk/around-the-world.html (accessed 6.23.22).

Dhiman, R.C., Pahwa, S., Dash, A.P., 2008. Climate change and malaria in India: Interplay between temperatures and mosquitoes 12, 6.

Fernández, L.E., Pérez, C., Segovia, L., Rodríguez, M.H., Gill, S.S., Bravo, A., Soberón, M., 2005. Cry11Aa toxin from Bacillus thuringiensis binds its receptor in Aedes aegypti mosquito larvae through loop alpha-8 of domain II. FEBS Lett. 579, 3508–3514. https://doi.org/10.1016/j.febslet.2005.05.032

Ferreira, L.M., Silva-Filha, M.H.N.L., 2013. Bacterial larvicides for vector control: mode of action of toxins and implications for resistance. Biocontrol Sci. Technol. 23, 1137–1168. https://doi.org/10.1080/09583157.2013.822472

Figtree, M., Lee, R., Bain, L., Kennedy, T., Mackertich, S., Urban, M., Cheng, Q., Hudson, B.J., 2010. Plasmodium knowlesi in human, Indonesian Borneo. Emerg. Infect. Dis. 16, 672–674. https://doi.org/10.3201/eid1604.091624

Fillinger, U., Kannady, K., William, G., Vanek, M.J., Dongus, S., Nyika, D., Geissbühler, Y., Chaki, P.P., Govella, N.J., Mathenge, E.M., Singer, B.H., Mshinda, H., Lindsay, S.W., Tanner, M., Mtasiwa, D., de Castro, M.C., Killeen, G.F., 2008. A tool box for operational mosquito larval control: preliminary results and early lessons from the Urban Malaria Control Programme in Dar es Salaam, Tanzania. Malar. J. 7, 20. https://doi.org/10.1186/1475-2875-7-20

Goldberg, L.J., Margalit, J., 1977. A bacterial spore demonstrating rapid larvicidal activity against Anopheles sergentii, Uranotaenia unguiculata, Culex univitattus, Aedes aegypti and Culex pipiens. Mosq. News 37, 355–358.

Gómez, I., Sánchez, J., Miranda, R., Bravo, A., Soberón, M., 2002. Cadherin-like receptor binding facilitates proteolytic cleavage of helix α-1 in domain I and oligomer pre-pore formation of Bacillus thuringiensis Cry1Ab toxin. FEBS Lett. 513, 242–246. https://doi.org/10.1016/S0014-5793(02)02321-9

Gu, S., Jin, R., 2013. Assembly and Function of the Botulinum Neurotoxin Progenitor Complex. Curr. Top. Microbiol. Immunol. 364, 10.1007/978-3-642-33570–9_2. https://doi.org/10.1007/978-3-642-33570-9_2

Gubler, D.J., 1998. Dengue and Dengue Hemorrhagic Fever. Clin. Microbiol. Rev. 11, 480–496. https://doi.org/10.1128/CMR.11.3.480

Guillet, P., Kurtak, D.C., Philippon, B., Meyer, R., 1990. Use of Bacillus thuringiensis israelensis for Onchocerciasis Control in West Africa, in: de Barjac, H., Sutherland, D.J. (Eds.), Bacterial Control of Mosquitoes & Black Flies: Biochemistry, Genetics & Applications of Bacillus Thuringiensis Israelensis and Bacillus Sphaericus. Springer Netherlands, Dordrecht, pp. 187–201. https://doi.org/10.1007/978-94-011-5967-8_11

Ishino, Y., Krupovic, M., Forterre, P., 2018. History of CRISPR-Cas from Encounter with a Mysterious Repeated Sequence to Genome Editing Technology. J. Bacteriol. 200, e00580-17. https://doi.org/10.1128/JB.00580-17

Iwamura, T., Guzman-Holst, A., Murray, K.A., 2020. Accelerating invasion potential of disease vector Aedes aegypti under climate change. Nat. Commun. 11, 2130. https://doi.org/10.1038/s41467-020-16010-4

Ja, N., 2001. Malaria control: achievements, problems and strategies. Parassitologia 43, 1–89.

Jones, G.W., Wirth, M.C., Monnerat, R.G., Berry, C., 2008. The Cry48Aa-Cry49Aa binary toxin from Bacillus sphaericus exhibits highly restricted target specificity. Environ. Microbiol. 10, 2418–2424. https://doi.org/10.1111/j.1462-2920.2008.01667.x

Kalfon, A., Charles, J.-F., Bourgouin, C., De Barjac, H.Y. 1984, n.d. Sporulation of Bacillus sphaericus 2297: an Electron Microscope Study of Crystal-like Inclusion Biogenesis and Toxicity to Mosquito Larvae. Microbiology 130, 893–900. https://doi.org/10.1099/00221287-130-4-893

Kawalek, M.D., 1998. Cloning and characterization of mosquitocidal genes from Bacillus thuringiensis subsp. jegathesan (Ph.D.). University of California, Riverside, United States -- California.

Kawalek, M.D., Benjamin, S., Lee, H.L., Gill, S.S., 1995. Isolation and Identification of novel toxins from a new mosquitocidal isolate from Malaysia, Bacillus thuringiensis subsp. jegathesan. Appl. Environ. Microbiol. 61, 2965–2969. https://doi.org/10.1128/aem.61.8.2965-2969.1995

Knowles, B.H., Ellar, D.J., 1987. Colloid-osmotic lysis is a general feature of the mechanism of action of Bacillus thuringiensis δ-endotoxins with different insect specificity. Biochim. Biophys. Acta BBA - Gen. Subj. 924, 509–518. https://doi.org/10.1016/0304-4165(87)90167-X

Kraemer, M.U., Sinka, M.E., Duda, K.A., Mylne, A.Q., Shearer, F.M., Barker, C.M., Moore, C.G., Carvalho, R.G., Coelho, G.E., Van Bortel, W., Hendrickx, G., Schaffner, F., Elyazar, I.R., Teng, H.-J., Brady, O.J., Messina, J.P., Pigott, D.M., Scott, T.W., Smith, D.L., Wint, G.W., Golding, N., Hay, S.I., 2015. The global distribution of the arbovirus vectors Aedes aegypti and Ae. albopictus. eLife 4, e08347. https://doi.org/10.7554/eLife.08347

Lacey, L.A., Mulla, M.S., 1990. Safety of Bacillus thuringiensis ssp. israelensis and Bacillus sphaericus to nontarget organisms in the aquatic environment [WWW Document]. URL https://agris.fao.org/agris-search/search.do?recordID=US9105330 (accessed 6.16.22).

Lederberg, J., 1992. The interface of science and medicine, in: The Mount Sinai Journal of Medicine. Presented at the Human cancer : from precurable to curable. Symposium, pp. 380–383.

Likitvivatanavong, S., Aimanova, K., Gill, S.S., 2009. Loop residues of the receptor binding domain of Bacillus thuringiensis Cry11Ba toxin are important for mosquitocidal activity. FEBS Lett. 583, 2021–2030. https://doi.org/10.1016/j.febslet.2009.05.020

Liu, L., Li, Z., Luo, X., Zhang, X., Chou, S.-H., Wang, J., He, J., 2021. Which Is Stronger? A Continuing Battle Between Cry Toxins and Insects. Front. Microbiol. 12.

López-Diaz, J.A., Cantón, P.E., Gill, S.S., Soberón, M., Bravo, A., 2013. Oligomerization is a key step in Cyt1Aa membrane insertion and toxicity but not necessary to synergize Cry11Aa toxicity in Aedes aegypti larvae. Environ. Microbiol. 15, 3030–3039. https://doi.org/10.1111/1462-2920.12263

Mordecai, E.A., Ryan, S.J., Caldwell, J.M., Shah, M.M., LaBeaud, A.D., 2020. Climate change could shift disease burden from malaria to arboviruses in Africa. Lancet Planet. Health 4, e416–e423. https://doi.org/10.1016/S2542-5196(20)30178-9

Mulla, M.S., Darwazeh, H.A., Davidson, E.W., Dulmage, H.T., Singer, S., 1984. Larvicidal activity and field efficacy of Bacillus sphaericus strains against mosquito larvae and their safety to nontarget organisms. Mosq. News USA.

Mulla, M.S., Thavara, U., Tawatsin, A., Chomposri, J., Su, T., 2003. Emergence of resistance and resistance management in field populations of tropical Culex quinquefasciatus to the microbial control agent Bacillus sphaericus. J. Am. Mosq. Control Assoc. 19, 39–46.

Murray, N.E.A., Quam, M.B., Wilder-Smith, A., 2013. Epidemiology of dengue: past, present and future prospects. Clin. Epidemiol. 5, 299–309. https://doi.org/10.2147/CLEP.S34440

Mustafa, M.S., Rasotgi, V., Jain, S., Gupta, V., 2015. Discovery of fifth serotype of dengue virus (DENV-5): A new public health dilemma in dengue control. Med. J. Armed Forces India 71, 67–70. https://doi.org/10.1016/j.mjafi.2014.09.011

Myers, P., Yousten, A.A., Davidson, E.W., 1979. Comparative studies of the mosquito-larval toxin of Bacillus sphaericus SSII-1 and 1593. Can. J. Microbiol. 25, 1227–1231. https://doi.org/10.1139/m79-193

Nester, E.W., Thomashow, L.S., Metz, M., Gordon, M., 2002. 100 Years of Bacillus thuringiensis: A Critical Scientific Assessment: This report is based on a colloquium, “100 Years of Bacillis thuringiensis, a Paradigm for Producing Transgenic Organisms: A Critical Scientific Assessment,” sponsored by the American Academy of Microbiology and held November 16–18, in Ithaca, New York, American Academy of Microbiology Colloquia Reports. American Society for Microbiology, Washington (DC).

Nicolas, L., Darriet, F., Hougard, J.M., 1987. Efficacy of Bacillus sphaericus 2362 against larvae of Anopheles gambiae under laboratory and field conditions in West Africa. Med. Vet. Entomol. 1, 157–162. https://doi.org/10.1111/j.1365-2915.1987.tb00337.x

Nicolopoulou-Stamati, P., Maipas, S., Kotampasi, C., Stamatis, P., Hens, L., 2016. Chemical Pesticides and Human Health: The Urgent Need for a New Concept in Agriculture. Front. Public Health 4, 148. https://doi.org/10.3389/fpubh.2016.00148

Nielsen-Leroux, C., Pasteur, N., Prètre, J., Charles, J.-F., Sheikh, H.B., Chevillon, C., 2002. High resistance to Bacillus sphaericus binary toxin in culex pipiens (Diptera: Culicidae): the complex situation of west Mediterranean countries. J. Med. Entomol. 39, 729–735. https://doi.org/10.1603/0022-2585-39.5.729

Oliveira, S., Caleffe, R., Conte, H., 2017. Chemical control of Aedes aegypti: a review on effects on the environment and human health. Rev. Eletrônica Em Gest. Educ. E Tecnol. Ambient. - REGET 21, 240–247. https://doi.org/10.5902/2236117027692

Payne, J.M., Davidson, E.W., 1984. Insecticidal activity of the crystalline parasporal inclusions and other components of the Bacillus sphaericus 1593 spore complex. J. Invertebr. Pathol. 43, 383–388. https://doi.org/10.1016/0022-2011(84)90084-3

Qureshi, N., Chawla, S., Likitvivatanavong, S., Lee, H.L., Gill, S.S., 2014. The Cry Toxin Operon of Clostridium bifermentans subsp. malaysia Is Highly Toxic to Aedes Larval Mosquitoes. Appl. Environ. Microbiol. 80, 5689–5697. https://doi.org/10.1128/AEM.01139-14

Ran, F.A., Hsu, P.D., Wright, J., Agarwala, V., Scott, D.A., Zhang, F., 2013. Genome engineering using the CRISPR-Cas9 system. Nat. Protoc. 8, 2281–2308. https://doi.org/10.1038/nprot.2013.143

Rao, D.R., Mani, T.R., Rajendran, R., Joseph, A.S., Gajanana, A., Reuben, R., 1995. DEVELOPMENT OF A HIGH LEVEL OF RESISTANCE TO BACILLUS SPHAERICU,SIN A FIELD POPULATION OF CTJLEX QUINQUEFASCIATUS FROM KOCHI, INDIA 5.

Reimer, L., Fondjo, E., Patchoké, S., Diallo, B., Lee, Y., Ng, A., Ndjemai, H.M., Atangana, J., Traore, S.F., Lanzaro, G., Cornel, A.J., 2008. Relationship Between kdr Mutation and Resistance to Pyrethroid and DDT Insecticides in Natural Populations of Anopheles gambiae. J. Med. Entomol. 45, 260–266. https://doi.org/10.1093/jmedent/45.2.260

Rodcharoen, J., Mulla, M.S., 1994. Resistance Development in Culex quinquefasciatus (Diptera: Culicidae) to Bacillus sphaericus. J. Econ. Entomol. 87, 1133–1140. https://doi.org/10.1093/jee/87.5.1133

Rosso, M.L., Delécluse, A., 1997. Contribution of the 65-kilodalton protein encoded by the cloned gene cry19A to the mosquitocidal activity of Bacillus thuringiensis subsp. jegathesan. Appl. Environ. Microbiol. 63, 4449–4455. https://doi.org/10.1128/aem.63.11.4449-4455.1997

Seleena, P., Lee, H.L., Lecadet, M.M., 1995. A new serovar of Bacillus thuringiensis possessing 28a28c flagellar antigenic structure: Bacillus thuringiensis serovar jegathesan, selectively toxic against mosquito larvae. J. Am. Mosq. Control Assoc. 11, 471–473.

Shah, S.A., Erdmann, S., Mojica, F.J.M., Garrett, R.A., 2013. Protospacer recognition motifs. RNA Biol. 10, 891–899. https://doi.org/10.4161/rna.23764

Siegel, J.P., Shadduck, J.A., 1990. Mammalian Safety of Bacillus sphaericus, in: de Barjac, H., Sutherland, D.J. (Eds.), Bacterial Control of Mosquitoes & Black Flies: Biochemistry, Genetics & Applications of Bacillus Thuringiensis Israelensis and Bacillus Sphaericus. Springer Netherlands, Dordrecht, pp. 321–331. https://doi.org/10.1007/978-94-011-5967-8_21

Silberman, J., Taylor, A., 2021. Carbamate Toxicity, in: StatPearls. StatPearls Publishing, Treasure Island (FL).

Silva Filha, M.H.N.L., Berry, C., Regis, L., 2014. Chapter Three - Lysinibacillus sphaericus: Toxins and Mode of Action, Applications for Mosquito Control and Resistance Management, in: Dhadialla, T.S., Gill, S.S. (Eds.), Advances in Insect Physiology, Insect Midgut and Insecticidal Proteins. Academic Press, pp. 89–176. https://doi.org/10.1016/B978-0-12-800197-4.00003-8

Silva-Filha, M.H., Regis, L., Oliveira, C.M., Furtado, A.E., 2001. Impact of a 26-month Bacillus sphaericus trial on the preimaginal density of Culex quinquefasciatus in an urban area of Recife, Brazil. J. Am. Mosq. Control Assoc. 17, 45–50.

Sinègre, G., Babinot, M., Quermel, J.M., Gavon, B., 1994. First field occurrence of Culex pipiens resistance to Bacillus sphaericus in southern France. 8th Eur. Meet. Soc. Vector Ecol.

Solomon, H.M., Lilly Jr, T., 2001. BAM Chapter 17: Clostridium botulinum. FDA.

Sun, Y., Zhao, Q., Xia, L., Ding, X., Hu, Q., Federici, B.A., Park, H.-W., 2013. Identification and Characterization of Three Previously Undescribed Crystal Proteins from Bacillus thuringiensis subsp. jegathesan. Appl. Environ. Microbiol. 79, 3364–3370. https://doi.org/10.1128/AEM.00078-13

Tetreau, G., Sawaya, M.R., De Zitter, E., Andreeva, E.A., Banneville, A.-S., Schibrowsky, N.A., Coquelle, N., Brewster, A.S., Grünbein, M.L., Kovacs, G.N., Hunter, M.S., Kloos, M., Sierra, R.G., Schiro, G., Qiao, P., Stricker, M., Bideshi, D., Young, I.D., Zala, N., Engilberge, S., Gorel, A., Signor, L., Teulon, J.-M., Hilpert, M., Foucar, L., Bielecki, J., Bean, R., de Wijn, R., Sato, T., Kirkwood, H., Letrun, R., Batyuk, A., Snigireva, I., Fenel, D., Schubert, R., Canfield, E.J., Alba, M.M., Laporte, F., Després, L., Bacia, M., Roux, A., Chapelle, C., Riobé, F., Maury, O., Ling, W.L., Boutet, S., Mancuso, A., Gutsche, I., Girard, E., Barends, T.R.M., Pellequer, J.-L., Park, H.-W., Laganowsky, A.D., Rodriguez, J., Burghammer, M., Shoeman, R.L., Doak, R.B., Weik, M., Sauter, N.K., Federici, B., Cascio, D., Schlichting, I., Colletier, J.-P., 2022. De novo determination of mosquitocidal Cry11Aa and Cry11Ba structures from naturally-

occurring nanocrystals. Nat. Commun. 13, 4376. https://doi.org/10.1038/s41467-022-31746-x

Tetreau, G., Stalinski, R., David, J.-P., Després, L., 2013. Monitoring resistance to Bacillus thuringiensis subsp. israelensis in the field by performing bioassays with each Cry toxin separately. Mem. Inst. Oswaldo Cruz 108, 894–900. https://doi.org/10.1590/0074-0276130155

Tetsch, L., 2017. The adaptive bacterial immune system CRISPR-Cas and its therapeutic potential. Med. Monatsschr. Pharm. 40, 17–23.

Thiery, Isabelle, Hamon, S., Cosmao Dumanoir, V., De Barjac, H., 1992. Vertebrate Safety of Clostridium bifermentans Serovar malaysia, a New Larvicidal Agent for Vector Control. J. Econ. Entomol. 85, 1618–1623. https://doi.org/10.1093/jee/85.5.1618

Thiery, I., Hamon, S., Gaven, B., De Barjac, H., 1992. Host range of Clostridium bifermentans serovar. malaysia, a mosquitocidal anaerobic bacterium. J. Am. Mosq. Control Assoc. 8, 272–277.

Tiwari, A., Nagalli, S., 2022. Clostridium Botulinum, in: StatPearls. StatPearls Publishing, Treasure Island (FL).

Toymentseva, A.A., Altenbuchner, J., 2019. New CRISPR-Cas9 vectors for genetic modifications of Bacillus species. FEMS Microbiol. Lett. 366. https://doi.org/10.1093/femsle/fny284

Wells, C.L., Wilkins, T.D., 1996. Clostridia: Sporeforming Anaerobic Bacilli, in: Baron, S. (Ed.), Medical Microbiology. University of Texas Medical Branch at Galveston, Galveston (TX).

West Nile virus [WWW Document], n.d. URL https://www.who.int/news-room/fact-sheets/detail/west-nile-virus (accessed 3.16.21).

WHO | Fact sheet: WHO/UNICEF report “Achieving the malaria MDG target” [WWW Document], n.d. . WHO. URL http://www.who.int/malaria/media/malaria-mdg-target/en/ (accessed 3.16.21).

Wirth, M.C., Georghiou, G.P., Malik, J.I., Abro, G.H., 2000. Laboratory Selection for Resistance to Bacillus sphaericus in Culex quinquefasciatus (Diptera: Culicidae) from California, USA. J. Med. Entomol. 37, 534–540. https://doi.org/10.1603/0022-2585-37.4.534

Wirth, M.C., Jiannino, J.A., Federici, B.A., Walton, W.E., 2004. Synergy between toxins of Bacillus thuringiensis subsp. israelensis and Bacillus sphaericus. J. Med. Entomol. 41, 935–941. https://doi.org/10.1603/0022-2585-41.5.935

Wong, Y.M., Juan, J.C., Gan, H.M., Austin, C.M., 2014. Draft Genome Sequence of Clostridium bifermentans Strain WYM, a Promising Biohydrogen Producer Isolated from Landfill Leachate Sludge. Genome Announc. 2. https://doi.org/10.1128/genomeA.00077-14

World Health Organization, 2019. World malaria report 2019 [WWW Document]. URL https://www.who.int/publications/i/item/9789241565721 (accessed 3.15.21).

Yasuno, M., Tonn, R.J., 1970. A study of biting habits of Aedes aegypti in Bangkok, Thailand. Bull. World Health Organ. 43, 319–325.

Yiallouros, M., Storch, V., Thiery, I., Becker, N., 1994. Efficacy of Clostridium bifermentans serovar Malaysia on target and nontarget organisms. J. Am. Mosq. Control Assoc. 10, 51–55.

Yung, C.-F., Lee, K.-S., Thein, T.-L., Tan, L.-K., Gan, V.C., Wong, J.G.X., Lye, D.C., Ng, L.-C., Leo, Y.-S., 2015. Dengue Serotype-Specific Differences in Clinical Manifestation, Laboratory Parameters and Risk of Severe Disease in Adults, Singapore. Am. J. Trop. Med. Hyg. 92, 999–1005. https://doi.org/10.4269/ajtmh.14-0628

Zhang, X., Candas, M., Griko, N.B., Rose-Young, L., Bulla, L.A., 2005. Cytotoxicity of Bacillus thuringiensis Cry1Ab toxin depends on specific binding of the toxin to the cadherin receptor BT-R1 expressed in insect cells. Cell Death Differ. 12, 1407–1416. https://doi.org/10.1038/sj.cdd.4401675

Zhang, X., Candas, M., Griko, N.B., Taussig, R., Bulla, L.A., 2006. A mechanism of cell death involving an adenylyl cyclase/PKA signaling pathway is induced by the Cry1Ab toxin of Bacillus thuringiensis. Proc. Natl. Acad. Sci. U. S. A. 103, 9897–9902. https://doi.org/10.1073/pnas.0604017103

Chapter 2

Determining the Mechanism of Action of the Cry Operon Found in *Paraclostridium bifermentans* serovar *malaysia*

Abstract

Aedes mosquitos can serve as vectors for diseases like yellow fever, dengue fever and zika, among others. These diseases cause hundreds of thousands of infections a year, some of which lead to death. Currently two bacteria are used as mosquito biological control methods. *Bacillus thuringiensis israelensis* (*Bti*) is currently used against *Aedes* mosquitoes in the field. Although there has not been any resistance against the cocktail of toxins produced in this bacterium, resistance has been seen against single toxins produced by *Bti* and thus new methods should be developed to replace this control method should the need arise. *Paraclostridium bifermentans* serovar *malaysia* (*Pbm*) contains a toxin operon that has been found to be toxic to *Aedes* mosquitoes. Here we look to determine what proteins are required for toxicity, specific loop regions involved in toxicity and the potential mechanism of action of each of the gene found within the Cry operon. All full-length proteins are required for toxicity, and only the putative loop 1 region of Cry17 affects toxicity of the full expressed operon. This putative loop 1 region and a lack of binding by Cry16 points to Cry17 being involved in binding of the Cry operon protein complex in *Aedes* mosquitos.

Introduction

Mosquitoes are responsible for hundreds of thousands of deaths and even more infections due to their ability to vector diseases. (CDC, 2020; “Chikungunya fact sheet,” 2020; “Dengue Fever | NIH,” 2016; “Global Health - Newsroom - Yellow Fever,” 2019). One major mosquito vector is *Aedes aegypti* which serves as a vector for diseases like dengue fever, yellow fever, chikungunya, and zika (Souza-Neto et al., 2019). One method for attempting to slow the infection rates of these diseases is through control of mosquito populations.

Biological control of mosquito populations currently utilizes *Bacillus thuringiensis* subsp. *israelensis (Bti)* and *Lysinibacillus sphaericus (Ls).* Each bacteria produces species-specific insecticidal toxins that target different species of mosquitoes. *Bti* contains a large plasmid that encodes genes for 4 cry toxins and two cyt toxins (Ben-Dov, 2014), while *Ls* produces binary toxins and mtx toxins (Silva Filha et al., 2014). No resistance has been seen against the full cocktail of *Bti* toxins, however, resistance has been seen in the laboratory against single toxins produced by this bacteria (Georghiou and Wirth, 1997). Resistance has been seen against the toxins produced by *Ls* in the field (Sinègre et al., 1994; Wirth et al., 2000).

A new bacteria was found to show mosquitocidal activity, this bacteria is *Paraclostridium bifermentans* serovar m*alaysia* (*Pbm*) and was isolated from a mangrove swamp soil in Malaysia in 1990 (de Barjac et al., 1990; Lee and Seleena, 1990a). This species has shown high toxicity to *Anopheles* mosquitoes and less toxicity to *Aedes* mosquitoes (Lee and Seleena, 1990b; Thiery et al., 1992). It has also been shown that *P.*

bifermentans subsp. *malaysia* it not toxic to mammals, goldfish or other nontarget organisms (Thiery et al., 1992; Yiallouros et al., 1994). Similarly to *Bti* and *Ls*, the toxicity of *Pbm* occurs during sporulation and decreases with cell lysis (Charles et al., 1990). In contrast, *Pbm* does not produce parasporal inclusions like those associated with the toxicity of *Bti* (Charles et al., 1990).

Previous research found four major proteins involved in the toxic activity of *Pbm*. Cbm71, a 71,128 Da protein, was found along with 3 other proteins, Cbm72, a 71,727 Da protein, Cbm17.1, which is a 17,189 Da protein, and Cbm17.2, a 17,451 Da protein (Barloy et al., 1998, 1996). Cbm71 and Cbm72 showed some sequence similarity to *B. thuringiensis* delta-endotoxins however, the were not found to be immunologically related to the Cry toxins found in *Bti*, and was thought to be part of a novel class of proteins that exhibits toxicity against mosquitoes (Barloy et al., 1996). Later both proteins were renamed Cry16 and Cry17 respectively. Cbm17.1 and Cbm17.2 show 44.6% similarity to hemolysin proteins found in *Aspergillis fumigatus*. These proteins were not found to exhibit mosquitocidal activity alone (Barloy et al., 1998). These genes were later determined to be part an operon, where all the genes are encoded under the same promoter in a large 109kb plasmid. In some strains of *B. thuringiensis*, Cry toxins and hemolysin proteins are known to act synergistically to create high levels of toxicity (Juárez-Pérez and Delécluse, 2001). The presence of Cry like proteins and potentially hemolytic proteins suggests a similar synergistic effect involved in the toxic activity of *Pbm*. An effort was made to determine the role each protein had in toxicity by expressing each gene either alone or in different combinations under their own promoters in a

crystal-minus *Bt* strain (Barloy et al., 1998, 1996). Cry16 was the only protein successfully expressed under these conditions. The recombinant strains of *E. coli* and *Bt* that expressed Cry16 did not show toxicity. When Cry17 was transformed into both *E. coli* and *Bt*, toxin production was not seen. However, Cry17 was detected via western blot when Cry16 was co-expressed. When both Cry16 and Cry17 were co-expressed in a recombinant *Bt* strain, the resulting analysis showed a lack of mosquitocidal activity. Thus, they concluded that the mosquitocidal activity must be due to another factor found in *Pbm* (Juárez-Pérez and Delécluse, 2001). Later, it was determined the toxins produced by the Cry operon target *Aedes aegypti* mosquitoes; and toxicity of the Cry operon requires all toxins to form a complex (Qureshi et al., 2014).

The Cry operon is toxic to *Aedes* mosquitoes (Qureshi et al., 2014) while the Ptox locus, also found within *Pbm*, is toxic to *Anopheles* mosquitoes (Contreras et al., 2019). Since the discovery of the Cry operon, much work has been done to better understand its toxicity. Gibson Assembly™ was utilized to insert the Cry operon into the pHT315 shuttle vector under the control of a Cyt1A promoter. This vector was then transformed into *Bt*, 4Q7 cells. Many different constructs were created to test the toxicity of each protein alone as well as in different combinations. Each construct was expressed in *Bt* grown in sporulation media. These cultures were then used in a bioassay against *Aedes* mosquitoes to determine toxicity. A list of constructs as well as their toxicity data is shown in Figure 2-1 (Qureshi et al., 2014).

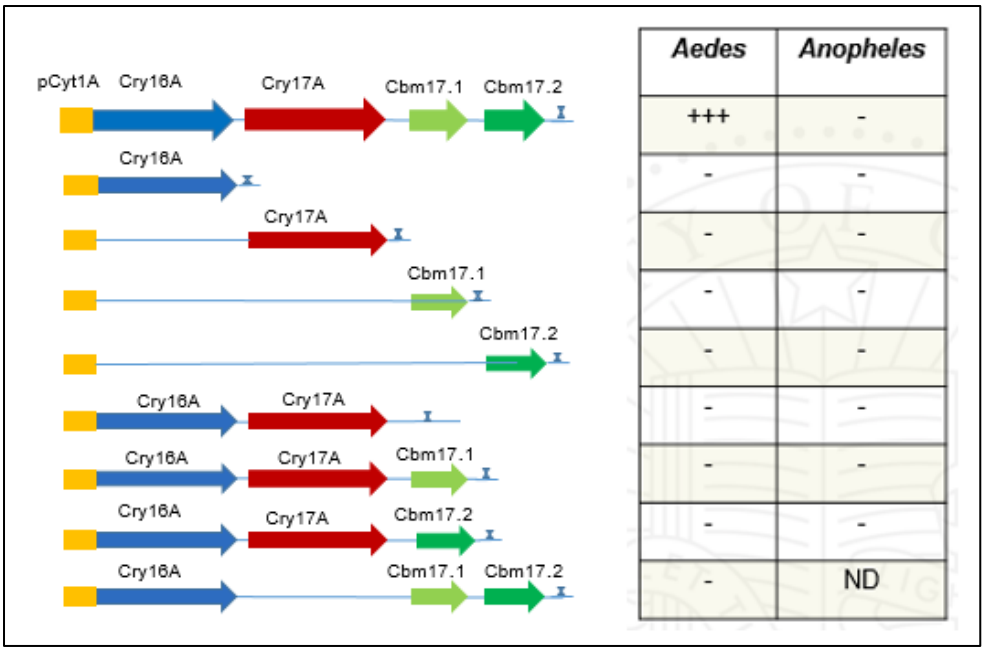

Aedes	Anopheles
+++	-
-	-
-	-
-	-
-	-
-	-
-	-
-	-
-	ND

Figure 2-1. Cry operon toxin constructs and toxicity data.
Constructs created, where each different colored arrow represents a different gene, and the associated toxicity data against *Aedes* and *Anopheles* mosquitoes. (Qureshi et al., 2014).

Work in our lab was done to identify genes responsible for mosquitocidal activity. A genomic approach comparing 3 different strains of *P. bifermentans* (*Pb*); the type strain, *Paraclostridium bifermentans* serovar *malaysia* (*Pbm)* and *Paraclostridium bifermentans* serovar *Paraiba* (*Pbp*), which also exhibits mosquitocidal activity, were used to determine genes of interest. *P. bifermentans* the type strain does not exhibit mosquitocidal activity, therefore the goal was to sequence the genomes of each strain to determine which genes may be involved in toxicity. The genomes of *Pb*, *Pbp*, and *Pbm* were all sequenced, and showed some variation in size. *Pb* was about 3.6 Mb whereas the genome of *Pbm* and *Pbp* were both about 3.9 Mb. *Pb* lacks between six and eight scaffolds that are present in *Pbm*, which may account for the difference in genome size. The mutagenesis of *Pbm* with gamma irradiation helped to determine where the toxicity

of the bacteria was present. This loss of function mutant was sequenced, and this data was compared to other sequences. It was determined that *Pbm* contains eight plasmids, two of which are shared with Pb, and five of which are also found in *Pbp*. A summary of this information is shown in Table 2-1.

Table 2-1. Plasmid data from different *Pb* strains.

Bacterial Strain				Plasmid	Size			
	1.84 Kb	1.96 Kb	3.6 Kb	4.0 Kb	7.2 Kb	14.8 Kb	35.8 Kb	109 Kb
Pb	-	+	-	-	-	+	-	-
Pbp	+	-	-	+	+	+	-	+
Pbm	+	+	+	+	+	+	+	+
Pbm-	-	+	+	-	-	+	+	-

The size of plasmids found in *Pb*, *Pbm* and P*bp* determined by Next Generation Sequencing as well as the plasmids found in the *Pbm* mutant labeled *Pbm-* (Contreras et al., 2019).

After comparison of the sequence data for both the loss of function mutant and the wildtype strain it was found that the largest, a 109kb, was not present in the loss of function mutant. This 109Kb plasmid contains the Cry operon which contains the c*ry16Aa, cry17Aa,* and two putative hemolysin genes, *cbm17.1* and *cbm17.2*, all of which had previously been implicated as important genes for toxicity. Another toxin locus was identified called the Ptox locus which includes the paraclostridial mosquitocidal protein1 (*pmp1*), *ntnh*, *orfx1*, *orfx2*, *orfx3*, *mpp* and a *p47* gene. From this information a plasmid map of the large plasmid was constructed using DNAPlotter (Artemis).

The map (Figure 2-2) shows the Cry operon, transposons, insertion sequences, uncharacterized putative genes, as well as genes that encode replication proteins, a type IV secretion system and cell wall associated hydrolases. The Cry operon and ptox locus are indicated in the figure.

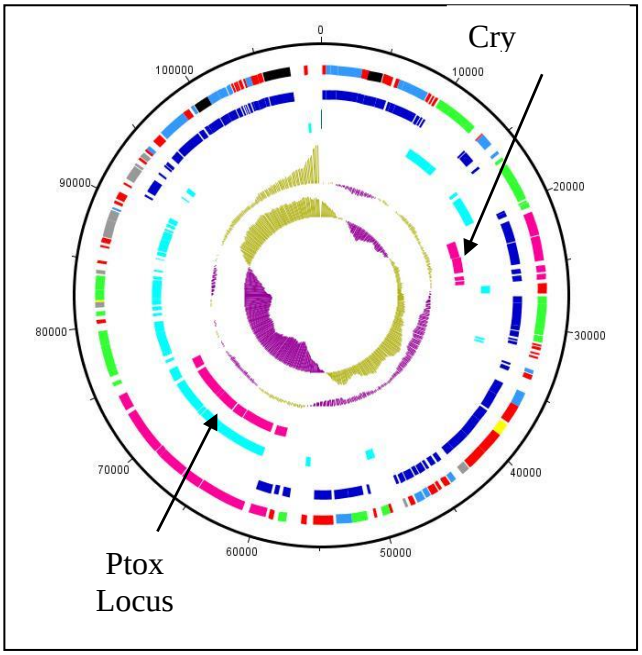

Figure 2-2. Plasmid map of the large 109kb plasmid found only in *Pbm*.
The outside circle represents the base number from the predicted origin. The inner circle represents the GC bias, the lines facing the center of the circle represent negative values while the lines reaching away from the center represent positive values. The second circle from the center represents G+C content. The third circle from the center represents the toxin containing operons which are indicated by arrows. The smaller of the two is the Cry operon, and the larger is the CMP loci. The fourth circle from the center represents the predicted genes on the forward strand. The fifth circle from the center represents predicted genes on the reverse strand. The outer ring indicates different genes which include regulatory genes, toxin genes, conserved hypothetical, unknown, transposon related, surface associated, cell wall associated and miscellaneous metabolic genes. (Contreras et al., 2019)

Since the discovery of the Cry operon, much work has been done to better understand its toxicity. Gibson Assembly™ was utilized to insert the Cry operon into the pHT315 shuttle vector under the control of a Cyt1A promoter. This vector was then transformed into *Bt*, 4Q7 cells. Many different constructs were created to test the toxicity of each gene alone as well as in different combinations. Each construct was expressed in *Bt* grown in sporulation media. These cultures were then used in a bioassay against Aedes

mosquitoes to determine toxicity. A list of constructs as well as their toxicity data is shown in Figure 2-1 (Qureshi et al., 2014).

Cry toxins contain three domains (Bravo et al., 2005). All three domains are thought to be involved in toxicity. For single cry toxins, domains II and III are thought to be responsible for binding to receptors in the target organism. Domains II and III are highly specific and are responsible for the insecticide activity or lack of depending on the organism. Domain I is responsible for creating a pore in the gut membrane which subsequently leads to osmotic imbalance and eventual death of the organism (Liu et al., 2021). Loop regions found between β- sheet structures are responsible for binding to receptors in the midgut of target organisms. The α8 loop region and three other loop regions that project out of the protein structure bind to receptors like cadherin, alkaline phosphatase and aminopeptidase (Adang et al., 2014). This chapter explores steps to determine the mechanism of action of the Cry operon by looking for specific molecular involvement as well as the overall role in toxicity of each protein involved.

Materials and Methods

Genomic DNA isolation

One ml of overnight culture was pelleted, the pellet was resuspended in 1ml of 0.1x SSC created from a 20X stock (Saline-Sodium Citrate pH 7.2, 3M NaCl, 0.3M sodium citrate). The resuspended bacterial pellet was then spun for 10 min at 4°C and 6,000g. The pellet was resuspended in 500µl of TE buffer (Tris-EDTA pH 8) and then incubated with RNase A, Lysozyme and Proteinase K for 1 h at 37°C. After 1 h, 20% SDS was added and incubated for another h at 37°C. 500µl if 1:1 phenol chloroform was

added. The sample was spun for 5 min at 9000 g and the top aqueous layer was collected. The last step was repeated two more times. The collected aqueous layer was used to precipitate DNA by adding 0.1 volumes of 3M NaAC and 2.5 volumes of 100% ethanol. The precipitated DNA was spun at 13,200 g for 10 min. The pellet was washed with 500µl of 70 % ethanol. The ethanol was allowed to evaporate, and the pellet was resuspended using water.

Cloning

Klenow digestion

pCryO plasmid created previously (Qureshi et al., 2014) was used to create two Cry operon constructs were made using restriction digestion and ligation. The first construct was cut with ApaI, which leaves a four base pair overhang, the ends were then made blunt using the enzyme Klenow, which cleaves off 3' overhangs. These blunt ends were ligated together using T4 DNA ligase. The loss of 4pb caused a frameshift in the reading frame leading to an early stop codon; the resulting construct was named pCryO-A and produced a truncated Cry17 protein. The second construct was cut with ApaI, the ends were made blunt using Klenow and the resulting DNA was cut again using MscI; this sequential digest resulted in a 636bp deletion. The blunt ends were then ligated together using T4 DNA ligase, the resulting construct was named pCryO-AM.

Cry17 loop switch

To determine which loop region was important for receptor binding in the Cry operon a loop switch experiment was designed. The goal of this experiment was to

replace the 1st and 2nd loop region of domain II of Cry17 with a known loop region of another Cry toxin (Cry4B) to change species specificity of the Cry operon as a whole.

A portion of the Cry operon was cut out using MscI and HindIII restriction enzymes and cloned into pUC57 using the EcoRV and HindIII sites. Two fragments were synthesized containing either the loop 1 or loop 2 region of Domain II of Cry4B flanked by BglII and SpeI restriction sites respectively. This fragment containing the loop regions was subcloned into the smaller portion of the Cry operon in pUC57 using BglII and SpeI restriction sites. The Cry operon fragment with the new loop sequences was then cloned back into the full-length Cry operon construct using ApaI and HindIII restriction sites. This created two constructs one with loop 1 and one with loop 2 from Cry4B. To create the construct that had both loop 1 and loop 2 an annealing PCR was performed. PCR was used to isolate each loop alone, then the PCR product was annealed using an outside set of primers (VV37/VV41) to combine the two PCR products together, a schematic of the cloning design can be found in Figure 2-3, and a schematic of the overlapping PCR can be found in Figure 2-4. This PCR fragment was then cloned back into the full-length Cry operon construct. The construct with substituted loop 1 is called pwL1 while the construct with substituted loop 2 is called pwL2. These constructs were then transformed into Bt 4Q7 cells to be used for a bioassay of toxicity against both *Aedes* and *Anopheles* mosquitoes (Table 2-2).

Table 2-2. Primers for loop switch overlap PCR to create single loop constructs.

Primer	Sequence	Use
VV13R	GATTAGAGGGGGAGCTAGT	Colony PCR using new loop 2 in Cry17
VV14R	GTAAATCTTGATATATAGTATTTC	Colony PCR using new loop 1 in Cry17
VV19F	GCCCCTCGTGACTTATATATTAGTCC	Sequence before BglII
VV20R	GTTATGATTAGCAGCGT	Sequence from SpeI side
VV36F	GCAACAAAATTACAAACTCTG	Outside, loop 1 Cry17
VV37F	GACAAGAACAGTTTTTTCAG	inside VV36 loop 1 Cry17
VV38R	GCTAACGCCACATTATCAAT	Reverse loop 1
VV39F	GAAGGTGATCTATTTGGCTATAC	loop 2 Cry17
VV40R	GTGCTCCAATATAATCATG	loop 2 Cry17
VV41R	GCAGCGTAATATATACGT	loop 2 Cry17

Primers were used to isolate single loops from the original synthesized fragment. These single loops were cloned into their own constructs to later be used in a bioassay. F or R in the primer name indicates the sequence is a forward or reverse primer

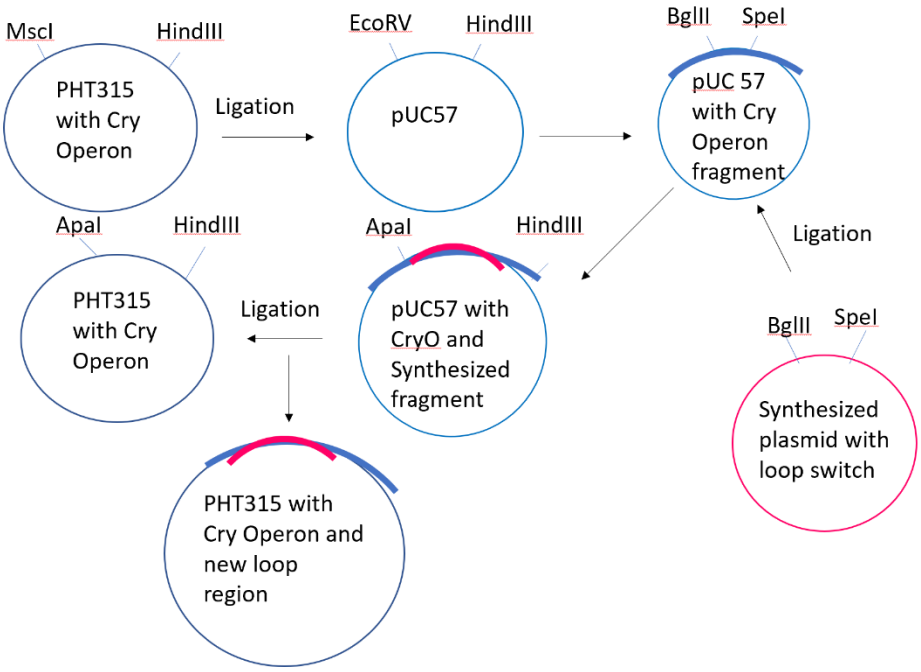

Figure 2-3. Schematic of loop switch experimental design.
This figure is a visual representation of the cloning design used to insert the new loop 1 and loop 2 regions into *cry17* of the original Cry operon. The lines represent where each plasmid was cut to move the fragment to its next vector. MscI and HindIII were used to move a fragment from the original pHT315 Cry operon construct and into the ApaI/HindIII site in pUC57. The synthesized plasmid was cut with BglII and SpeI, this fragment was then cloned into pUC57 containing the MscI/HindIII fragment. pUC57 with the synthesized fragment and the original pHT315 construct were cut with ApaI and HindIII to insert the new loop containing fragment into the pHT315 Cry operon construct.

Alanine substitutions in Cry17 putative loop regions

Primers were designed to introduce mutations into each of the three putative loop regions of Cry17. Three or four important amino acids were determined in each putative loop region by creating a 3D model based on the structure of a positively charged mutant Cry3Aa endotoxin (7EAR) on Expasy and analyzing the loop regions. Two different types of mutations were designed. The first set of mutations involved replacing each of the 3 or 4 putative loop region amino acids with an alanine all at the same time. The

second set of mutations involved mutating a single amino acid per construct. All constructs were made to determine which loop and which amino acid was critical for toxicity.

The mutations were introduced into the *cry17* gene using overlapping PCR (Figure 2-4) and primers that contained different mutations (Table 2-3). A PCR was performed to create two fragments of Cry17 that contain a 20-21 base pair overlap in their sequence. These two fragments were checked in a 1% agarose gel and then PCR or gel purified. The two fragments were then annealed together before adding the end primers and extending each of the fragments. These overlapped fragments were checked again on a 1% agarose gel, gel purified and then ligated into pCR4-Topo cloning vector. Each construct was sequenced using Sanger sequencing, and once determined to have the correct mutation was cloned back into the pUC57 plasmid containing the Cry17 fragment, the experimental design of the loop switch experiments was utilized to make these constructs using BglII and SpeI (Figure 2-3). This section was then cloned into the full Cry operon construct using ApaI and HindIII. The resulting plasmids were named Cry17-L1, Cry17-L2, Cry17-L3, Cry17-L1-A1, Cry17-L1-A2, and Cry17-L1-A3, indicating which Cry toxin was mutated, which loop region, and which individual amino acid if applicable. After validating the plasmid had the insert and was sequenced for correctness, the plasmid was then transformed into 4Q7 cells. These cells were used in a colony PCR to verify the full Cry operon plasmid was present. The correct colonies were then used in a bioassay against mosquito larvae

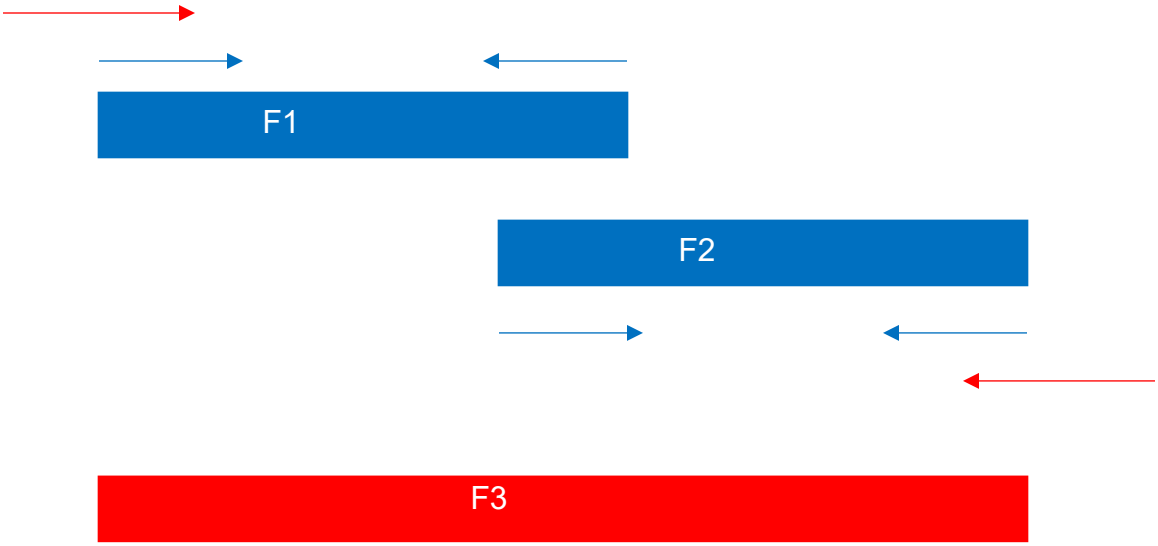

Figure 2-4. Overlapping PCR schematic.
F1 indicates fragment 1 where the reverse primer includes DNA mutations to create an alanine substitution in the translated DNA sequence. F1 has two sets of primers specific to the fragment desired. F2 indicates fragment 2 where the forward primer includes DNA mutations to create the alanine substitution in the translated DNA sequence. Fragment 3 is obtained by using F1 and F2 as the DNA template for a PCR using external primers on the outside of the original fragments. F3 is a DNA fragment that is cloned into pCR4-Topo vector for verification.

Table 2-3. Primers used for alanine substitution of Cry17 loop regions.

Primer	Sequence	Use
E97F	GCAGAAGGAGATCTTGTTTTAACTGG	outside BglII site
E98R	AAATTTACTAGTATTATTGAATGCTGTTAATAGAGG	outside SpeI site
E99F	GAGATCTTGCTGCAGCTGGTTTTAG	loop 1 - DLAAAGF
F01R	CTAAAACCAGCTGCAGCAAGATCTC	loop 1 - DLAAAGF
F02F	GTTTTTATTGCTGCTGCGGCGTTAGCTATT	loop 2 AAAALA
F03R	AATAGCTAACGCCGCAGCAGCAATAAAAAC	loop 2 AAAALA
F12F	GCATCACTATGGTGCTGCCGCTGCTGATTCTTATTTATTC CAATG	loop 3 AAAA
F13R	CATTGGAATAAATAAGAATCAGCAGCGGCAGCACCATA GTGATGC	loop 3 AAAA
F16F	GAGATCT TGCTTTAACTGGTTTTAG	L1 DLALTGF
F17R	CTAAAACCAGTTAAAGCAAGATCTC	L1 DLALTGF
F18F	GA GATCT TGTTGCAACTGGTTTTAG	L1 DLVATGF
F19R	CTAAAACCAGTTGCAACAAGATCTC	L1 DLVATGF
F20F	GAGATCT TGTTTTAGCTGGTTTTAG	L1 DLVLAGF
F21R	CTAAAACCAGCTAAAACAAGATCTC	L1 DLVLAGF

F or R in the primer name denotes a forward or reverse primer. Rows with L1 in the use were used for single amino acid substitutions.

Alanine substitutions in Cry16 putative loop regions

The putative domain II loop regions of Cry16 were also evaluated to see if they were important in toxicity. A 3D model using a positively charged mutant Cry3Aa endotoxin (7EAR) was created on Expasy. This model was used to determine the loop regions from domain II that may be involved in receptor binding. DNA primers were designed to perform an alanine substitution in which the 3 or 4 putative amino acids in the loop region responsible for receptor binding were replaced with alanine amino acids.

Similar to the Cry17 loop switch experiment, a fragment of the Cry operon was subcloned into a pCR 2.1-Topo vector using KpnI and BglII restriction enzymes. Concurrently the loop mutation fragments were created using High Fidelity Taq polymerase and used to perform an overlapping PCR (Figure 2-4). The primers used to introduce the alanine substitution can be found in Table 2-4. Ultimately the overlapping PCR product was ligated into pCR4-Topo vector. The PCR products were verified for correctness by Sanger sequencing. Correct loop constructs were then cloned into the pCR 2.1-Topo vector that contains the partial fragment of the Cry operon using NsiI and AleI restriction enzymes. These constructs were verified by DNA sequencing. Correct constructs were cut using KpnI and BglII to clone the new loop regions into the full Cry operon (Figure 2-5). The resulting constructs were named Cry16-L1, Cry16-L2, and Cry16-L3 to indicate the specific Cry toxin mutated, and which loop region had changed.

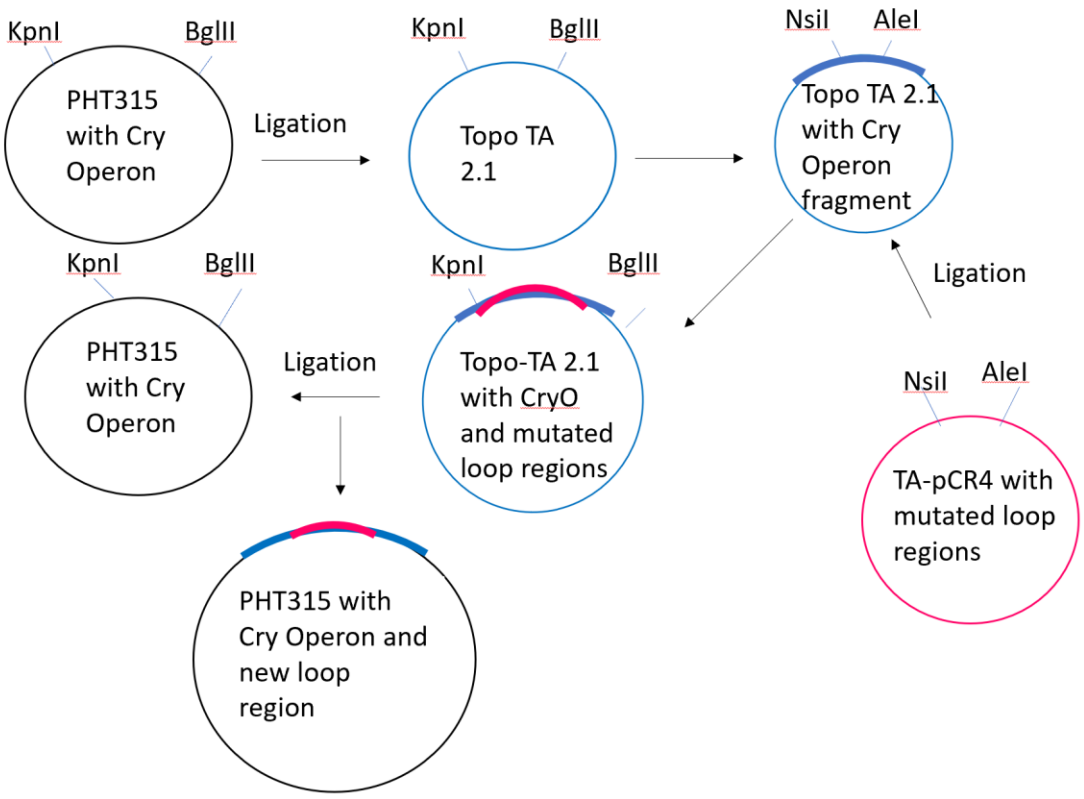

Figure 2-5. Cry16 alanine loop substitution cloning schematic.
This figure gives a visual representation of the cloning design to introduce the alanine substituted loop regions of Cry16 into the Cry operon in pHT315. The original Cry operon construct was cut with KpnI and BglII, this fragment was cloned into those restriction sites in the pCR 2.1-Topo vector. This pCR 2.1-Topovector was then cut with NsiI and AleI concurrently with the pCR4-Topo vector that housed the overlap PCR product with the substituted loop regions. The fragment containing the substituted loop regions was cloned into the pCR 2.1-Topovector. The last step involved cutting the original Cry operon vector and the pCR 2.1-Topovector with KpnI and BglII again to clone the new fragment into the full construct housed in pHT315.

Table 2-4. Primers used for alanine substitution of loop regions in Cry16 and their use.

Primer	Sequence	Use
E89F	GATGGTATGATTTATGGAGATGCAT GG	NsiI site overall fwd
E90R	CTTTATAACAGATATTTCACTATAGTGTTCAGAGCT	AleI site overall rev
E91F	TATACTAATAAAGCTGCAGCTAAATTTTTAAATGGT	loop 1 AAA
E92R	ACCATTTAAAAATTTAGCTGCAGCTTTATTAGTATA	loop 1 AAA
E93F	CATTTTTTAATACAGCAGCTGCTAACCCTACATCTGTT AA	loop 2 NTAAANP
E94R	TTAACAGATGTAGGGTTAGCAGCTGCTGTATTAAAAA ATG	loop 2 NTAAANP
F14F	GGCTAATAACGACAAAATAGCAGCTGCTGCAGATACT CCTCATAG	loop 3 IAAAAD
F15R	CTATGAGGAGTATCTGCAGCAGCTGCTATTTTGTCGTT ATTAGCC	loop 3 IAAAAD

Primers used for alanine substitution in loop regions of Cry16. F and R in the primer name indicates a primer is a forward or reverse sequence. The specific use of each primer is also listed in this table.

Change of promoters

The original construct was created with a Cyt1A promoter. Another pHT315 plasmid was created with a Cry3A promoter. A PCR was performed to isolate the Cry operon from genomic DNA using primers with restriction sites AscI and XhoI upstream and downstream of the primers respectively. The PCR product was transformed originally into pCR 2.1-Topo vector, for verification using Sanger sequencing, and subsequently cloned into pHT315 with the Cry3A promoter using T4 DNA ligase and the AscI/XhoI restriction sites. The resulting construct was called p3ACryO and was transformed into *Bt* (4Q7) cells. This was used in a bioassay, but toxicity was not restored.

pStop cloning

The pStop1622 plasmid (MoBiTec Molecular Technology), has a xylose inducible promoter. A PCR using primers that contained flanking SacI and KpnI restriction sites were used to clone the full 6kb Cry operon. The original PCR product was ligated into pCR 2.1-Topo vector sent for Sanger sequencing for verification and then cloned into pStop1622 using the SacI and KpnI cut sites and T4 DNA ligase. The resulting plasmid was called pStop-CryO and was transformed into *Bacillus megaterium* to check both toxicity and Cry operon expression.

Bacterial transformations

***Escherichia coli* transformation**

Plasmids containing the target gene to be expressed were transformed into BL21 *E. coli* bacteria. DNA, 200 ng, was transformed into *E. coli* bacteria. The bacterial cells were kept on ice for 30 min then heat shocked at 42°C for 30 sec. The cells were then incubated on ice for 2 min then left shaking for 1 h with SOC media at 37°C. After the outgrowth step, the cells were plated on LB agar plates containing the correct antibiotic to allow for selection of cells that contained the plasmid and grown at 37°C overnight.

***Bt* (4Q7) electrocompetent cell production**

A single 4Q7 colony was inoculated in 10mL of BHIG (Brain Heart Infusion + 0.5% glycerol) in a 250mL flask. The cells were incubated at 30°C overnight with moderate shaking. 5ml of overnight culture was diluted into 95ml of BHIG in a 1L flask. The dilutions were incubated for 1 h with vigorous shaking at 30°C. The cells were pelleted by centrifugation (17,000 g, 10 min, 4°C), in 2 separate 50mL falcon tubes.

From this step forward cells were kept cold to ensure competency. EB (0.625M sucrose, 1mM $MgCl_2$), kept on ice, was used to resuspend the pellet, and fill the falcon tube to 50ml. The centrifugation step was repeated, and the pellet was resuspended in 5ml of cold EB again. Once resuspended 0.8ml aliquots of cells were stored at -80°C until use.

***Bacillus thuringiensis* transformation**

Electrocompetent 4Q7 (*Bt*) cells were thawed on ice. The cells were then incubated with DNA for 10 min. After 10 min a single pulse at 2.5kV, 25µF, 1000 Ω was applied using the Bio-Rad Gene Pulser™ coupled with the Bio-Rad Pulse Controller and Bio-Rad Capacitance Extender. The cells were then diluted in 1.6ml of BHIG (Brain Heart Infusion media with 0.5% glycerol autoclaved) and incubated for 2 h at 30°C with moderate shaking. The cells were then plated on Nutrient Agar plates with the necessary antibiotic for selection and incubated overnight at 30°C.

***Bacillus megaterium* Transformation**

Prior to the *Bacillus megaterium* transformation solutions were prepared: 2X SMM (40mM maleic acid, 80mM NaOH, 40mM $MgCl_2$ x6H_2O, 1M sucrose, filter sterilized), solution A (51.5 g sucrose,3.25 g MOPS, 300 mg NaOH, in 250 ml of water, with pH adjusted to 7.3 using NaOH, and finally sterilized by filtration), solution B (2g agar, 100mg casamino acids, 5g yeast extract in 142.5 ml of water and autoclaved), 8xCR5 salts (1.25 g K_2SO_4, 50 g $MgCl_2 \times 6$ H2O, 250 mg KH_2PO_4, 11 g $CaCl_2$, solubilized in 625ml of water and autoclaved) 12% proline, and 20% glucose. To transform *Bacillus megaterium*, 50 µl of protoplasts (MoBiTec Molecular Technology) were combined with 500ng of pStop-CryO plasmid DNA. Then 150µl of Peg-P (20g

PEG-6000 with 1X SMM filled to 50ml and autoclaved) was added, mixed gently, and incubated at room temperature for 2 min. Next 500µl of SMMP (2X AB3 [7g Antibiotic Medium No.3 (Difco) in 200ml water, autoclaved] and 2X SMM combined in a 1:1 ratio) was added and mixed carefully. The cells were harvested by centrifugation at 1,300 x g for 10 min at room temperature and the supernatant was discarded. Then another 500 µl of SMMP were added and the mixture was incubated at 30°C for 90 min with gentle shaking (100rpm max). During this incubation 2.5ml aliquots of CR5-top agar were prepared by adding 1.25 ml solution A, 288 µl CR5 salts, 125 µl 12% proline, and 125 µl 20% glucose together. After the cells had incubated for 90 minutes, solution B was boiled, and 713 µl were added to the CR5-top agar mixture in sterile tubes. After incubation the cells were added to the sterile tubes containing the CR5-top agar and mixed. Finally, the cells and agar were poured onto LB plates containing tetracycline. The plates were incubated overnight at 30°C.

Expression

***Bacillus megaterium* expression and analysis**

To analyze protein expression in *B. megaterium* a single colony was inoculated in LB media and grown overnight for 14 h at 37°C with agitation at 100 rpm. The overnight culture was diluted 1:100 and grown to an OD_{600} of .3-.4 at 37°C under vigorous shaking. A sample was taken before induction, and then the culture was induced using 0.5% (w/v) of (D)-xylose. The culture was then incubated at 37°C with vigorous shaking and a 1ml

sample was collected after 1, 3, 4 and 5 h. The aliquots were pelleted at 17,000 g for 10 min at 4°C and then frozen at -20°C.

To analyze the intracellular proteins, the pellet was resuspended in 30µl of lysis buffer (100 mM Na3PO4, 5 mg/ml lysozyme pH 6.5 (adjust with H3PO4), 1 µl of a 1 M MgSO4 solution and, 2 µl TurboNuclease (250 U/µl, cat.# GENUC10700-01, final concentration of 500 U/ml) per ml lysis buffer shortly before use). The mixture was incubated for 30 min at 37°C shaking. The lysate was then spun down for 30 min at 18,000 g and 4°C. Then 27µl of the supernatant was mixed with 13µl of SDS sample buffer to load. To analyze the insoluble proteins, the pellet was resuspended in 30µl of 8M urea and centrifuged again at 17,000 g, 4°C for 30 min. Then 27µl of the resulting supernatant was mixed with 13µl of SDS sample buffer. Both samples were boiled at 95°C for 5 min and then loaded in an SDS-PAGE.

Cry16 expression

For Cry16 expression, BL21 bacteria containing RSFDuet vector with the *cry16* gene were grown overnight in 10ml of LB with kanamycin at 37°C shaking. The overnight culture was diluted 1:20 into 200ml of LB broth with no antibiotic. The dilution was grown until $O.D._{600}$ of .5-.6. Then 200ml of 1M IPTG was added to the culture to induce expression and the culture was grown for another 3 h. After 3 h the cells were centrifuged at 5,000 g for 30 min at 4°C. The cells were stored at -20 C for at least 1 h. To prepare cells for His-tag purification they were thawed on ice. Once thawed, 10ml NPI-10 (50mM NaH_2PO_4, 30mM NaCl, 10mM imidazole, pH 8.0) was used to resuspend the pellet. The resuspended cells were transferred to a 50ml falcon tube, for sonication.

The cells were sonicated at 30% on ice for 1 min on, then allowed to rest for 1 min; this procedure was repeated 3 times. After sonication the cells were pelleted down at 13,000 g, 4 C for 30 min. The lysate was collected and used for protein purification.

Purification

Cry16 purification using His-tag

Ni-NTA beads, 2ml, were placed in a gravity column. The beads were equilibrated using 10ml of NPI-10 (50mM NaH_2PO_4, 30mM NaCl, 10mM imidazole, pH 8.0) and allowed to drain by gravity. The lysate was then transferred to the column and incubated, rocking for 1 h at 4°C, then the flow through was collected. The beads were then washed twice with 10ml of NPI-20 (50mM NaH_2PO_4, 30mM NaCl, 20mM imidazole, pH 8.0). The beads were incubated 20 min for each wash and left rocking at 4°C; these wash eluants were collected. To elute 0.5ml of NPI-250 (50mM NaH_2PO_4, 30mM NaCl, 250mM imidazole, pH 8.0) was added to the column. The solution was allowed to incubate 1 min before elution. The purification was verified using SDS-PAGE stained with Coomassie.

Cry11 expression and purification

One large crystal producing colony was inoculated in 3ml of sporulation media with erythromycin and grown overnight at 30°C, shaking at 250rpm. Then 500µl of overnight culture was added to 500ml of sterilized sporulation media and was incubated for 4-5 days at 30°C shaking at 250rpm. The bacterial culture was poured into 250ml bottles and centrifuged using Sorval 5B at 6,990 g for 10 min at 5-30°C. The supernatant was discarded after centrifugation. Then the pellet was washed three times, two times

with 1M NaCl, and the last time with deionized water. Deionized water was added to a total of 30ml, and the cells were resuspended. NaBr solutions (38%, 42%, 45%, 49%, 52%, 56%) were used for purification, in a plastic test tube 5ml of each solution, densest at the bottom, were added. Each solution was pipetted on top of the other being careful not to disturb the layer underneath. Then 5ml of washed bacteria pellet was added to the top and then the tube was topped off with deionized water to the brim of the test tube. The tubes were placed in the ultracentrifuge the centrifuge was vacuumed to 40 microns and tubes were centrifuged at 9,300 g for 1.5hrs at 4°C, the white layer of toxin was collected in 50ml tube and centrifuged again at 9,300 g for 10 min at 4°C.

Cry17 purification

Cry17 was expressed using the same steps as Cry16 expression in 2.4 L of culture. The protein was also purified using Ni/NTA beads and NPI-10, NPI-20 and NPI-250 solutions. Since this did not provide sufficient purification; an anion exchange column was used to further purify the protein. The Ni/NTA elutions of Cry17 were dialyzed with 25mM Tris with .25mM TCEP and 10% glycerol overnight at 4°C. The dialyzed protein was loaded on an anion exchange column to attempt to purify the protein further. Buffers (25mM Tris with .25mM TCEP and 10% glycerol) with varying salt concentrations were created (50mM, 100mM, 200mM, 300mM, 500mM and 1M NaCl). Each solution was used for 10ml and then switched to the next higher concentration of salt. The 1M salt solution was allowed to run until peak conductivity. The resulting fractions were analyzed using an SDS-PAGE stained with Coomassie.

Cry11A solubilization and activation

To solubilize Cry11A the toxin was pelleted at 9,300 g for 10 min. The pellet was then resuspended in 1ml of 50mM Na_2Co_3, pH10. The toxin was left for 4 h shaking at 37°C. To activate Cry11A of stock(1mg/ml) trypsin was added in a concentration of 1µg tryps/ 20µg of toxin. Once added the tube was inverted and incubated at 37°C for 16 h. This solubilized and activated Cry11A toxin was used in binding and competition assays with *Aedes* brush border membrane fractions.

Brush border membrane fraction (BBMF) preparation

The protocol by (Nielsen-Leroux et al., 2002) was used to prepare brush border membrane fractions from *Aedes* larvae. Fourth instar larvae were frozen and then thawed and resuspended in buffer A (0.3M mannitol, 5mM EGTA, 20mM Tris-Cl pH7.4). The larvae were then homogenized in an equal volume of $MgCl_2$ (24mM), then incubated on ice for 20 min. The homogenate was centrifuged at 3,000 x g for 15 min at 4°C. The supernatant was kept on ice while the pellet was resuspended in buffer A, incubated on ice for 20 min then centrifuged at 3,000 g for 15 min at 2°C. The two supernatant samples were pooled and centrifuged at 14,000 x g for 1 h at 4°C. The subsequent pellet was resuspended in Buffer A and kept at -80°C long term or -20°C for a shorter period of time.

Biotin Labeling

Using GE Healthcare - Amersham™ ECL™ Protein Biotinylation Module, toxins were biotin labeled to be used for a binding assay. Bicarbonate buffer was prepared to a working concentration of 40mM. The biotinylating reagent was equilibrated to room

temperature before use. The protein was diluted or concentrated to 1mg/ml in the diluted bicarbonate buffer. Then 40µl of biotinylation reagent was added for each mg of protein and incubated at room temperature for 1 h with constant agitation. A Sephadex G25 column was utilized to purify the biotin labeled protein. Briefly, the column was equilibrated with 5ml of PBS containing 1% bovine serum albumin pH7.5, followed by 20ml of PBS. Then the protein was applied to the column. The protein was incubated with the column for 1 minute and then the labeled toxin was eluted using PBS in five, 1ml fractions.

Binding and competition assays

For the binding assay, BBMF (20µg) were incubated with biotin labeled protein (10nM) in 100µl of binding buffer (1% BSA, 1% Tween-20, PBS pH7.4). They were incubated for 1 h at room temperature then centrifuged for 10 min at 14,000 g. The pellet was washed twice with 100µl of binding buffer and subsequently resuspended in 1X PBS, pH7.4 and 30µl were loaded in an SDS-PAGE, the proteins were then transferred in a western blot and the biotin was detected using a streptavidin antibody (described later).

For the competition assay, BBMF (20µg) was incubated with 20 µg of unlabeled toxin and 20ng of biotin labeled toxin in100µl of binding buffer (1% BSA, 1% Tween-20, PBS pH7.4). They were incubated for 1 h at room temperature then centrifuged for 10 min at 14,000 g. The pellet was washed twice with 100µl of binding buffer and subsequently resuspended in 1X PBS, pH7.4 and 30µl were loaded in an SDS-PAGE, the proteins were then transferred in a western blot and the biotin was detected using a streptavidin antibody.

SDS-PAGE

All SDS-PAGE were prepared with 10% acrylamide, and 30µl of a sample was loaded into each well. The gel was run at 90V until the dye front reached the bottom of the gel. The proteins of the SDS-PAGE were then either transferred to a PVDF membrane through western blot run overnight at 21V at 4°C or stained using Coomassie stain.

Streptavidin to detect Biotin labeled protein

After the transfer of biotin labeled proteins, the membrane was blocked with a 5% blocking buffer (Skim Milk) in PBST at room temperature for 1 h. The membrane was washed for 10 min with 1X PBS pH7.4. The membrane was then washed for 20 min in PBST (1x PBS, pH 7.4 with 1% Tween-20). Two more washes followed at 15 min each in PBST. Next, the membrane was incubated with streptavidin conjugated peroxidase (1:4000) for 1 h at room temperature. After incubation the membrane was washed quickly 3 times with water, twice with PBST for 15 min and one final time with PBS for 10 min. The membrane was developed using SuperSignal™ West Dura by Thermo Scientific, which is an enhanced chemiluminescence horseradish peroxidase substrate that will react with a secondary antibody that was conjugated to horseradish peroxidase. using the ImageQuant LAS 4000 mini by GE.

Protein detection in western blot

After the western transfer of proteins to the PVDF membrane, each membrane is blocked with 5% skim milk in PBST for 1 h at room temperature. The membrane was then quickly washed 3 times with water and then incubated for 5 min with water shaking;

the same steps were done using PBST. Then the membrane was incubated with a primary antibody (1:2000) in 1% skim milk in PBST for 1h at room temperature. After incubation with a primary antibody the membrane was washed quickly 3 times with water, and then incubated for 5 min shaking with water, those same steps are repeated using PBST. Next the membrane was incubated with a secondary antibody in PBST (anti-rabbit at 1:5000 dilution). The membrane was then washed following the same water and PBST protocol. The membrane was developed using SuperSignal™ West Dura by Thermo Scientific, which aids in the detection of horseradish peroxidase conjugated secondary antibodies, using the ImageQuant LAS 4000 mini by GE.

Protein Quantification of Cry operon complex expression

Different amounts of BSA protein were loaded into a 10% SDS-PAGE. These protein standards were analyzed using ImageJ software. The values determined by image J and the amounts of protein loaded into the gel were plotted in a graph. A best fit line was determined for the graph. This equation was then used to determine the amount of protein produced in each construct used in a bioassay. Then 100µl, and 200µl of overnight culture were pelleted for one minute, the pellet was resuspended in 30µl of 1X PBS pH 7.4. SDS loading dye was added to a total volume of 30µl for each sample and was then boiled at 95°C for 5 min. Then 22.5µl of sample was run in a 10% SDS-PAGE and stained with Coomassie stain. The destained gel was imaged and used for analysis with ImageJ. The intensity of each band found with ImageJ was used to determine the protein amount in each band using the equation found for the BSA proteins standards.

Mosquito Rearing

Three strains of *Aedes aegypti* mosquitoes were used, Gill lab, Orlando wildtype, and Liverpool wildtype. These strains were propagated in a room kept between 60 and 70% humidity. Eggs were hatched in water supplemented with fish food pellets (TetraMin, Tropical Tablets) as food for the larvae. Once the larvae reached pupation, they are moved to a larger cage where they can emerge as adults. The females of these cages are allowed to blood feed on anesthetized mice and mate with male mosquitoes contained in the same cage. The room in which these insects are kept follows a timed light:dark cycle of 14:10 h.

Bioassay

Bioassays were performed by taking 20, 3rd instar Orlando wildtype larvae and placing them in 200ml of water. Alternatively, when *Anopheles* larvae were used for the bioassay, 20 3rd instar larvae were placed in 100ml of water. The larvae were then dosed with different culture amounts and then left at room temperature. After 24 and 48 h, mortality was observed. IBM SPSS Statistics 28 software was used to find the LC50 dose and ImageJ was used to determine protein concentration from whole culture. Alternatively, to determine the amount of bacteria used in bioassays, colony counts were used. Briefly, serial dilutions were plated onto Nutrient agar plates supplemented with erythromycin. The next day the number of colonies on the plate were counted and used to determine the number of colony forming units per milliliter (CFU/ml).

Results

To identify the critical genes within the Cry operon, deletion constructs were made (Figure 2-6). The first construct (pCryO-A) resulted in a truncated Cry17 protein; the blunting of the ends resulted in a four base pair deletion, shifting the reading frame and resulting in an early stop codon. The second construct (pCryO-AM), which was cut by two restriction enzymes resulted in a 636 base pair deletion within the *cry17* gene. Only the full operon with the full proteins caused toxicity to mosquito larvae. Interestingly, both the full operon and the construct that contained the partial deletion in the *cry17* gene created a complex that was seen by running a native gel with the cultured bacteria. This operon is more toxic to *Aedes aegypti* than *Anopheles gambiae* (Qureshi et al., 2014).

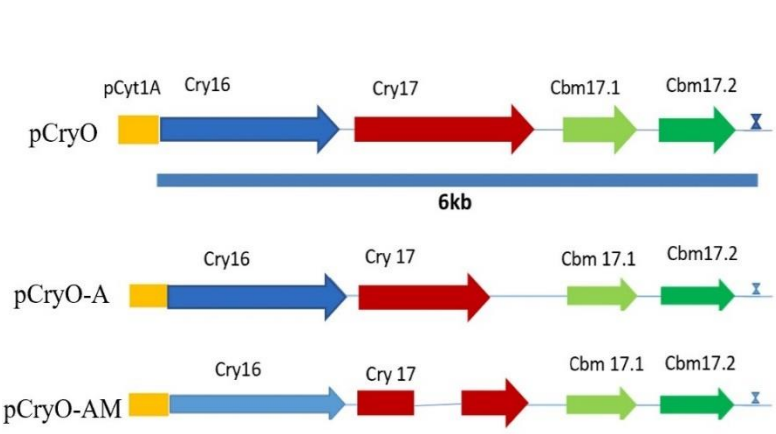

Toxicity

Aedes	*Complex Formation*
+++	+
-	+
-	+

Figure 2-6. Truncated and deletion Cry17 constructs.
Two new constructs that were made, one with a truncated Cry17 and one with a 636 bp deletion within Cry17, the table on the right indicates the toxicity of each construct and if it forms a complex in a native-page gel

.

It was interesting that the complex lost toxicity when a portion of the Cry17 protein was deleted. This portion may be important for receptor binding in the midgut of *Aedes* mosquitoes. The loop regions of domain II are believed to be involved in receptor

binding as well as species specificity. The original project was to introduce toxicity to *Anopheles* mosquitoes by using the Cry operon and changing the loop regions of domain II in Cry17 to those found in a toxin that is toxic to *Anopheles*. To do this the amino acid sequence of Cry4B, which is known to be toxic to *Anopheles* mosquitoes, was aligned to the amino acid sequence of Cry17A resulting in Figure 2-7.

```
EMBOSS_001      322 KRVDFWTNTIYQDLRFLSANKIGFSYTNS--SAMQESGIYGSSGFGSNLT    369
                    :  :::.||...| :.:..:..|::..|.  ....:|.||..:.|..|:.
EMBOSS_001      316 R--NYFRNTYIND-QIIEGDLFGYTTNNERYKLFTDSKIYKVTVFIDNVA    362

EMBOSS_001      370 HQIQLNSNVYKTSITDTSSPSNRVTKMDFYKIDGT-LASYNSNITPTPEG    418
                    ..|      .|....||.:     .:.||.|.|.| :..|..
EMBOSS_001      363 LAI------VKLIFHDTDN-----KEWDFSKTDITDINKYRK--------    393

EMBOSS_001      419 LRTTFFGFSTNENTPNQPTVNDYTHILSYIKTDVIDYNSNRVSFAWTHKI    468
                     ...:....:|.....:|     :|.|..:.....:||.:.: |.|.|:.
EMBOSS_001      394 -EEVYLNLLSNNEIQKEP-----SHYLYKMHHYGDNYNDSYL-FQWIHQS    436
```

Figure 2-7. Alignment of Cry4B and Cry17 amino acid sequence.
The highlighted regions in the 1st, 3rd and 5th rows indicates the putative loops 1, 2 and 3 respectively in Cry4B, the highlighted regions in rows 2,4 and 6 indicate the predicted corresponding putative loop 1, 2 and 3 regions in Cry17 respectively.

The loop regions were determined based off the putative loop regions determined by Abdullah et al., 2003. Next, a cloning strategy was created (Figure 2-5), by taking the original construct, which included all four proteins, cutting a fragment from this original construct and inserting it into the pUC57 vector plasmid. Concurrently a fragment which included the new putative loop 1 and loop 2 regions of Cry4B with in the Cry17 domain II was synthesized. This synthesized fragment was inserted into the pUC57 plasmid containing part of Cry17. A smaller portion of this plasmid was then reinserted into the original construct, creating a Cry operon that contained *cry16*, c*ry17*, c*bm17.1* and *cbm17.2*, however, loops 1 and 2 of domain II in Cry17 had been changed to resemble the domain II loop regions of Cry4B these constructs were called pwL1 and pwL2 respectively. This plasmid was then transformed into *E. coli* and subsequently into 4Q7

(*Bacillus thuringiensis*) cells after verification of the mutation. These *Bt* cells were then cultured for 18 h, and a bioassay was performed on early 4th instar *Anopheles* gambiae, and *Aedes aegypti* larvae. Each bioassay contained 20 larvae in 100mL of H_2O (*Anopheles*) or 20 larvae in 200mL H_2O (*Aedes*), and 1mL of overnight culture was used for the dose in each bioassay. No toxicity was seen against any of these mosquito larvae.

Upon analysis of the bioassay data, it was seen that there was no toxicity against either species of mosquito, *Aedes* or *Anopheles*. Interestingly the original positive control, pCryO, was no longer as toxic as previously seen. To try to restore toxicity the Cry operon was first cloned behind a different promoter in pHT315, the Cry3A promoter which expresses during the vegetative growth stage (p3ACryO). This new promoter did not rescue toxicity. The Cry operon was then cloned into a new vector called pStop (pStopCryO). This vector can be expressed in *Bacillus megaterium* protoplasts and is controlled by a xylose inducible promoter. The hope for this construct was to force the expression of the Cry operon, rather than have the proteins consistently expressed as they were in the pHT315 shuttle vector, and in doing so, the proteins would prove to be toxic once again. After expression in *B. megaterium* it appears the proteins may be degrading (Figure 2-8) and did not rescue toxicity.

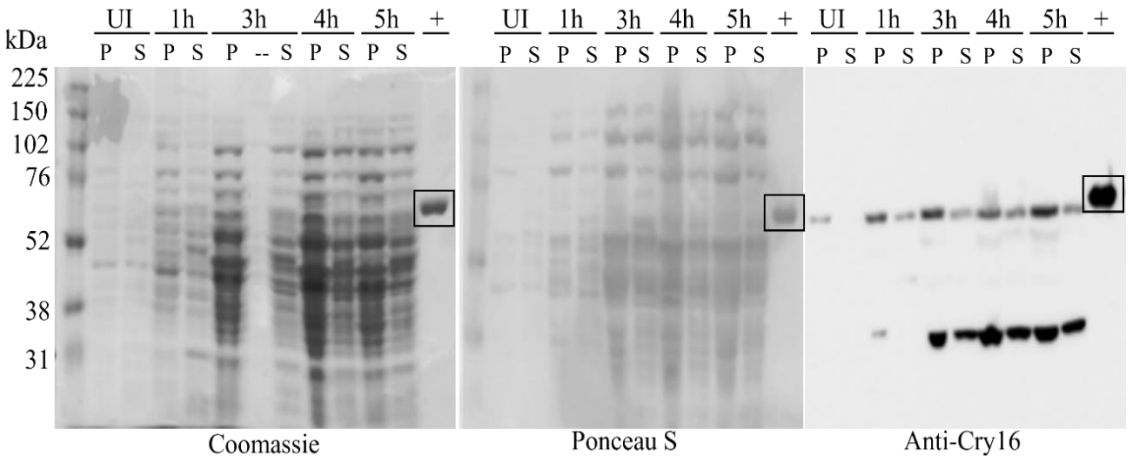

Figure 2-8. Cry operon western blot and Ponseau S stained membrane.
The membrane (left) and blot (right) both contain proteins expressed by *B.megaterium*, expressing the Cry operon. Ui is the uninduced culture while 1-5 indicates the number of hours after induction. Each sample has two lanes, the lane on the left is protein found in the bacterial pellet, while the right lane is protein found in the supernatant. The western blot was probed with Cry16 antibody and the control, indicated by the +, was purified Cry16 protein.

Another bioassay was performed against three different strains of *Aedes* mosquito, Orlando wildtype, Gill lab and Liverpool wildtype, all collected from different areas. This bioassay showed that the Cry operon construct expressed in *Bt* (pCryO) was most toxic to the Orlando strain (Table 2-5), and thus, this strain was used for subsequent bioassays. The bioassays that were discussed earlier were performed on the Gill lab strain. Subsequent bioassays showed none of the loop switch constructs, pwL1 or pwL2, were toxic while the original Cry operon was toxic.

Table 2-5. Mortality of Cry operon against different *Aedes* strains.

Aedes strain	24h mortality	48h mortality	72h mortality
Orlando	5%	100%	100%
Liverpool	50%	50%	50%
Gill Lab wildtype	0%	40%	40%

The table shows the percent mortality from a bioassay with 3rd instar *Aedes* larvae collected at different times. One ml of overnight culture was used to dose mosquito larvae.

To determine the optimal amount of time to produce the highest toxicity, a bioassay was performed on 3rd instar Orlando wildtype *Aedes* larvae, where 1ml of culture was used to dose the larvae. These cultures were grown for 12, 18, 24 and 48 h; the bioassay data can be found in Table 2-6. This validates previous data where high levels of toxicity were seen in whole *Pbm* culture between 12 and 24 h (Qureshi et al., 2014).

Table 2-6. Percent mortality of mosquito larvae when fed cultures grown for different amounts of time.

Time Cultured (h)	24 h mortality	48 h mortality
12	90%	95%
18	90%	95%
24	60%	67.5%
48	62.5%	77.5%

This table shows the percent mortality from three replicate bioassay experiments using 20 3rd instar larvae and 1ml of culture grown for a specific number of hours either 12, 18, 24 or 48. Mortality was noted after 24 and 48 h.

To be sure the Cry operon was expressed the cultures were run in both a native-PAGE as well as an SDS-PAGE and proteins were transferred to a PVDF membrane. Figure 2-9 shows the 8% native-PAGE and 10% SDS-PAGE stained with Coomassie. The bands in this gel indicate that the ~70kDa proteins from the Cry operon are expressed and the Cry operon does form a complex and is found in the pellet, meaning the proteins are not excreted from the cells.

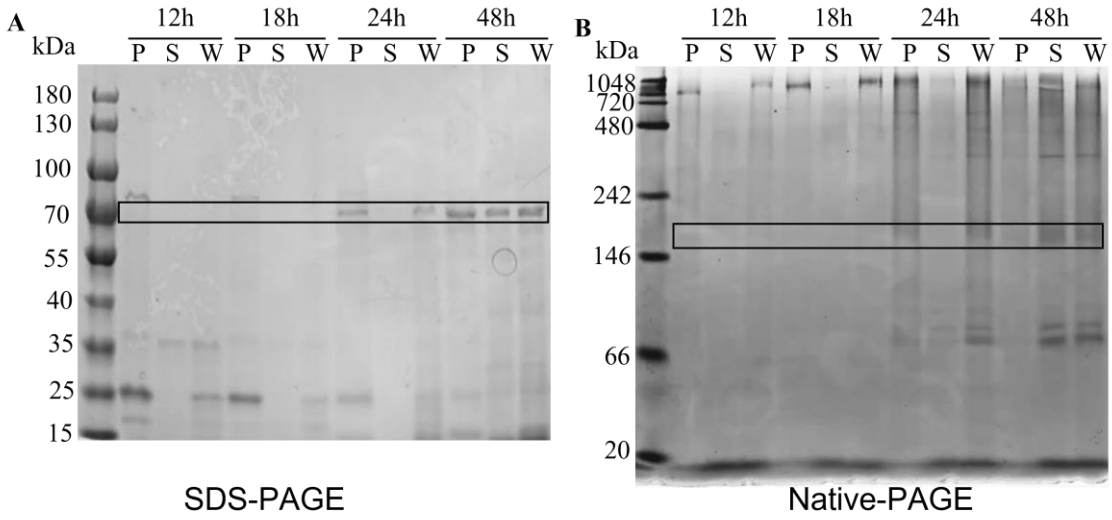

Figure 2-9. Cry operon culture in SDS and Native-PAGE Coomassie stained. The gel on the left contains samples run in a 10% SDS-PAGE, and the gel on the right contains the same samples run in an 8% native-PAGE. S and N indicate either SDS ladder or Native ladder respectively. Three samples per culture were loaded on the gel, lanes labeled 1-3 are 12 h culture, 4-6 are 18 h culture, 7-9 are 24 h cultures and 11-13 are 48 h culture. The first lane of each grouping is pelleted culture that has been resuspended, the second lane is supernatant and last lane is whole culture. The gels have been stained with Coomassie stain to visualize proteins.

Pelleted samples for each culture were run in a 10% SDS-PAGE and transferred to a PVDF membrane in a western blot. The Cry16 and Cbm17.1 antibodies were used to detect protein in each sample (Figure 2-10), this indicates that the bands from the SDS and native gels in Figure 2-9 are in fact proteins from the Cry operon.

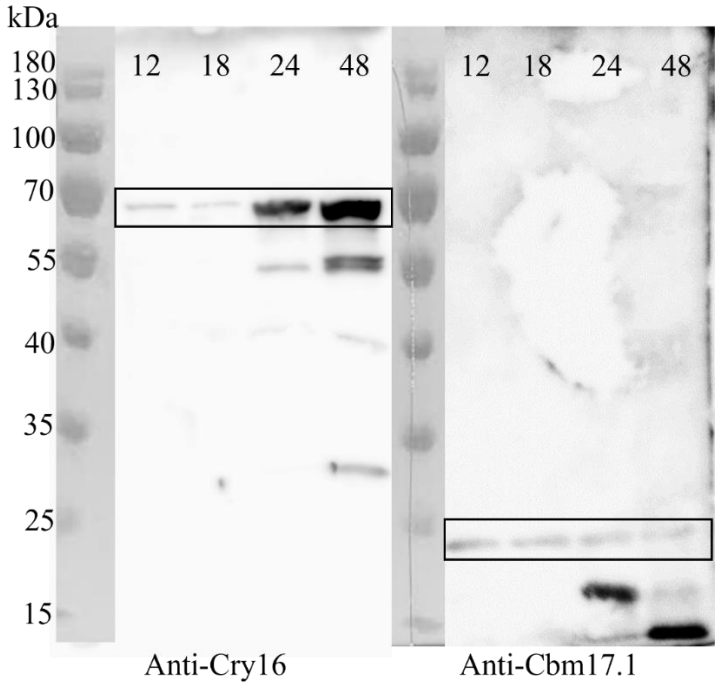

Figure 2-10. Antibody probed PVDF membrane with Cry operon culture samples. The lanes from left to right are 12hr, 18hr, 24hr and 48 h culture samples. The left membrane was probed using the Cry16 antibody, and the right membrane was probed with Cbm17.1 antibody indicating that both proteins were expressed in all cultures.

After determining the optimal growth time for maximum toxicity, a loop substitution experiments were performed. There had the same cloning design as the original loop switch project. The loop regions were determined by 3D protein modeling using a Cry3A mutant as a model using the Swiss Model software through Expasy (https://swissmodel.expasy.org/). This software created the potential 3D model of both Cry16 and Cry17 (Figure 2-11) and allowed for the determination of the putative loop regions of domain II that would likely bind to receptors. These loop regions contained three or four amino acids, and for the first part of this experiments, the entire putative loop region was replaced with the corresponding number of alanine amino acids.

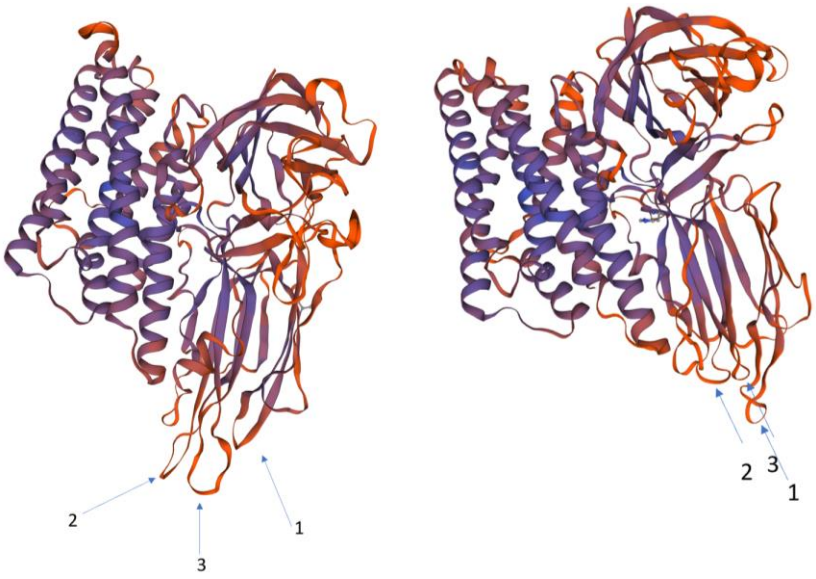

Figure 2-11. Putative 3-D model of Cry16 and Cry17.
The figure shows the putative loop regions of Cry16 (Left) and Cry17 (Right) based on the structure of a mutated Cry3A using https://swissmodel.expasy.org/ software.

Six new constructs were created, three with Cry16 loop substitutions, and three with Cry17 loop substitutions. The putative Cry16 loop regions were ^{301}SGN^{304} for loop 1, ^{357}QNN^{359} for loop 2, and ^{422}QINI^{425} for loop 3. These putative loop regions were mutated to ^{301}AAA^{304}, ^{357}AAA^{359}, and ^{422}AAAA^{425} respectively these constructs are named Cry16-L1, Cry16-L2 and Cry16-L3 respectively. The Cry17 putative loop substitutions were ^{311}VLT^{313} for loop 1, ^{359}DNV^{361} for loop 2, and ^{422}DNYN^{425} for loop 3 to ^{311}AAA^{313}, ^{359}AAA^{361}, and ^{422}AAAA^{425} respectively and are named Cry17-L1, Cry17-L2 and Cry17-L3. These mutations were made using primers and an overlapping PCR. The cloning design for Cry16 can be found in Figure 2-5, while the cloning design for Cry17 can be found in Figure 2-3. The final substituted constructs were cloned into pHT315 that contained the Cry operon. These constructs were then transformed into 4Q7

cells and used in a bioassay against 3rd instar Orlando wildtype *Aedes* larvae (Figure 2-12). All but one construct maintained their toxicity similar to the full Cry operon.

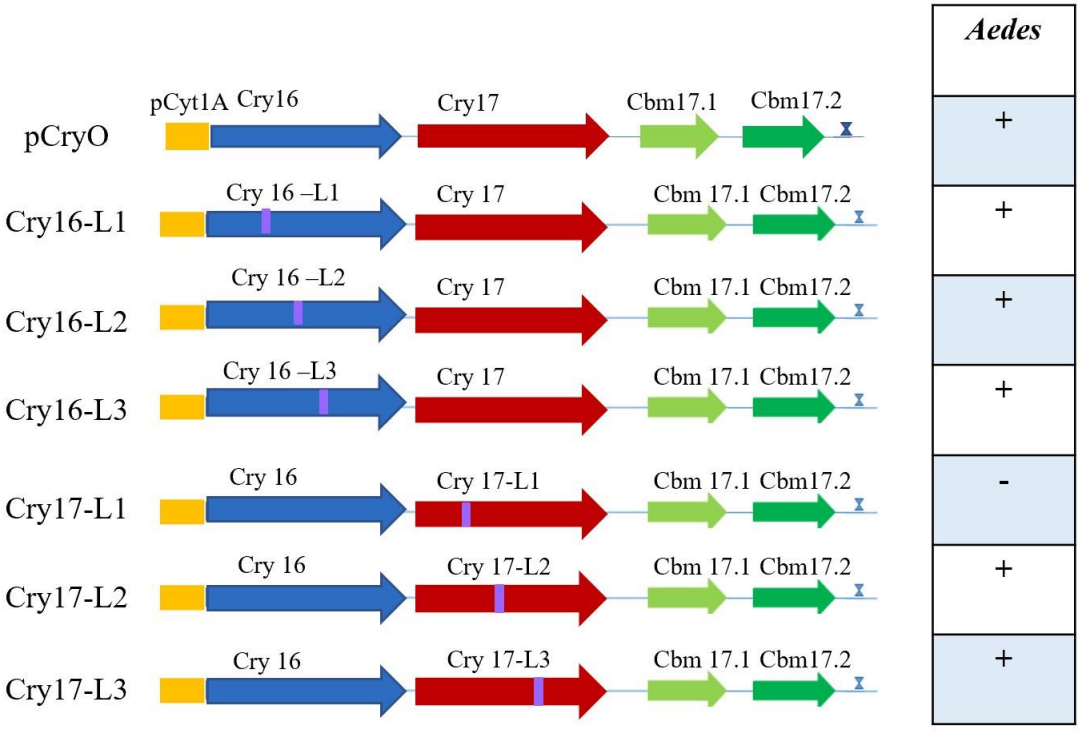

Figure 2-12. New Cry operon substitution constructs and their toxicity.
The figure above shows the six constructs made with alanine substitutions within either the *cry16* or *cry17* gene in the Cry operon L1, L2 and L3 indicate which loop region of domain II in each *cry* gene is mutated. The table to the right indicates toxicity of each construct against 3rd instar *Aedes* larvae.

Three other constructs were created to determine if all three amino acids were important for the function of loop 1 in Cry17. Each amino acid, within the putative loop 1 region of Cry17, was substituted individually to make ^{311}ALT^{313}, ^{311}VAT^{313}, and ^{311}VLA^{313} and are called Cry17-L1-A1, Cry17-L1-A2, and Cry17-L1-A3. The full constructs were transformed into 4Q7 cells and used in a bioassay; the results can be seen in Figure 2-13.

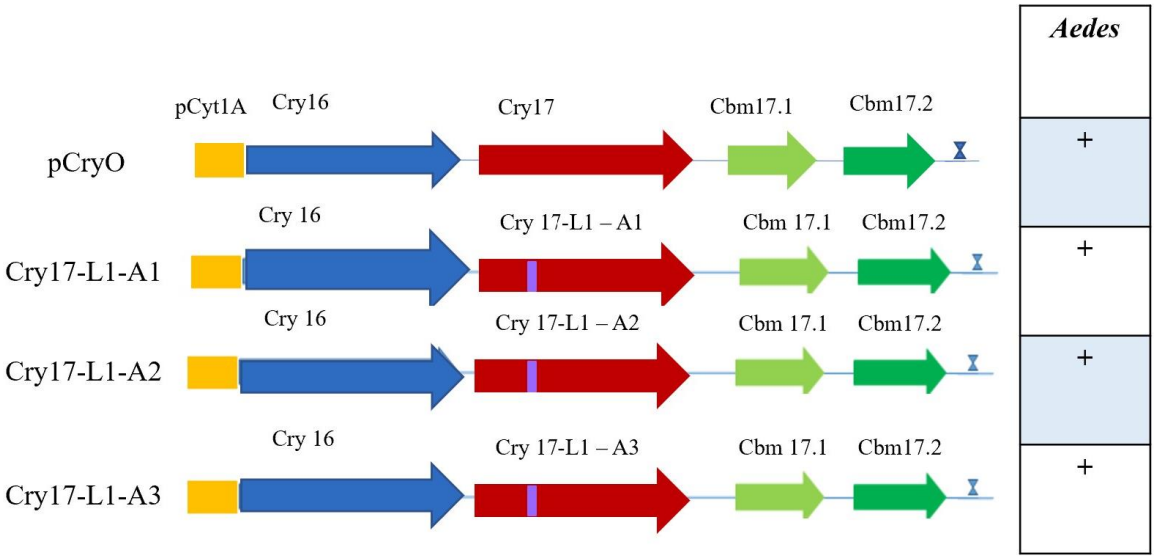

Figure 2-13. Putative loop 1 single amino acid substitution.
The figure to the left shows each construct where a single amino acid within the putative loop 1 region of Cry17 has been substituted with an alanine amino acid, A1, A2 and A3 indicates which amino acid of the putative loop1 region is mutated. The table on the right shows the toxicity of the construct against 3rd instar *Aedes* mosquitoes.

Another bioassay was conducted to determine the dose that would cause 50% of the larvae to die (LC50). The bioassay mortality data was analyzed using the Probit program in the SPSS software. The LC50 data as well as the corresponding colony forming units (CFU) per milliliter of each culture as well as the CFU calculated at LC50 or at the highest dose, for those constructs that do not cause toxicity can be found in table 2-7.

Table 2-7. Bioassay LC50 data.

Construct	LC50 (µl of culture)	CFU/ml	Total CFU at LC50	Total CFU at highest dose (no toxicity)
pCryO	595.683	$3.67X10^7$	$2.18X10^7$	-
Cry16-L1	499.694	$9.9X10^6$	$4.95X10^6$	-
Cry16-L2	732.497	$1.1X10^7$	$8.06X10^6$	-
Cry16-L3	645.229	$1.14X10^7$	$7.35X10^6$	-
Cry17-L1	No Toxicity	$2.56X10^7$	-	$3.07X10^7$
Cry17-L2	638.069	$9.0X10^6$	$5.74X10^6$	-
Cry17-L3	305.05	$1.14X10^7$	$3.47X10^6$	-
Cry17-L1-A1	343.785	$1.19X10^7$	$4.09X10^6$	-
Cry17-L1-A2	553.047	$2.20X10^7$	$1.21X10^7$	-
Cry17-L1-A3	394.437	$1.55X10^7$	$6.11X10^6$	-
pwL1	No Toxicity	$2.40X10^7$	-	$2.89X10^7$
pwL2	No Toxicity	$2.37X10^7$	-	$2.84X10^7$
pHT315	No Toxicity	$5.57X10^7$	-	$6.68X10^7$

This table contains each construct, the calculated LC50 dose, the colony forming units of each liquid culture, and the amount of colony forming units calculated in the LC50 dose or the highest dose that does not show toxicity.

The overall toxicity data as well as the LC50 data shown in Table 2-7 indicate that all the mutated constructs except for the Cry17 full loop 1 mutation (Cry17-L1) are toxic similar to the original full cry operon construct. The mutation of loop 1 of Cry17 caused a complete loss of toxicity against Orlando wildtype mosquitoes.

To determine the protein levels of the toxin in each of the constructs, bacterial cultures were used in another bioassay were analyzed in an SDS page protein gel (Figure 2-14). The LC50 for these cultures was noted with all other LC50 data from previous bioassay experiments. The average of the LC50 data can be found in Table 2-9. Concurrently an SDS page protein gel was run with known amounts of bovine serum albumin (BSA) protein. The BSA protein gel (Figure 2-14) was used as a protein standard and analyzed using ImageJ. The band intensity data, determined by ImageJ software, and the corresponding protein amount can be found in Table 2-8. A plot (Figure 2-15) of this data was used to determine a best fit line and equation.

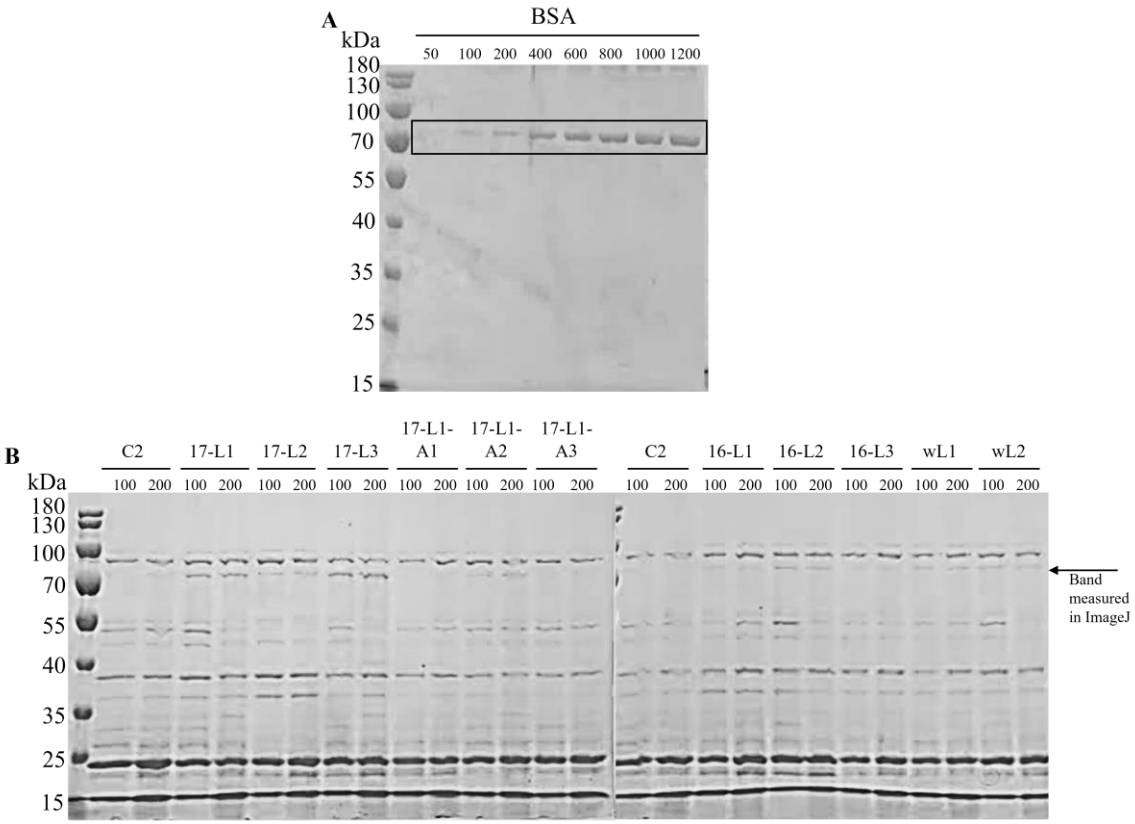

Figure 2-14. SDS-PAGE of BSA protein standards and Cry operon construct samples.

Panel A contains the BSA standards that were used to determine an equation relating the intensity of the band seen in the gel with the amount of protein loaded into the gel. The amounts of BSA are loaded in an increasing order from 50 to 2000ng, the exact amounts can be found in Table 2-8. The gels in panel B contain overnight culture from the loop substitution constructs. Each sample was loaded twice using either 100µl or 200µl of overnight culture pelleted and resuspended in PBS to load into the gel. The band at the level indicated by the arrow was measured using ImageJ to find the protein concentration.

Table 2-8. ImageJ intensity measurements for BSA.

Lane	BSA amount (ng)	ImageJ intensity
1	50	354.506
2	100	1251.31
3	200	2128.18
4	400	4560.47
5	600	6079.69
6	800	8200.35
7	1000	9643.13
8	1200	10629.5

This table indicates the lane, amount loaded, and ImageJ calculated intensity of each protein band in the SDS-PAGE. A scatterplot of this data and a best fit line that was determined and can be found in Figure 2-15.

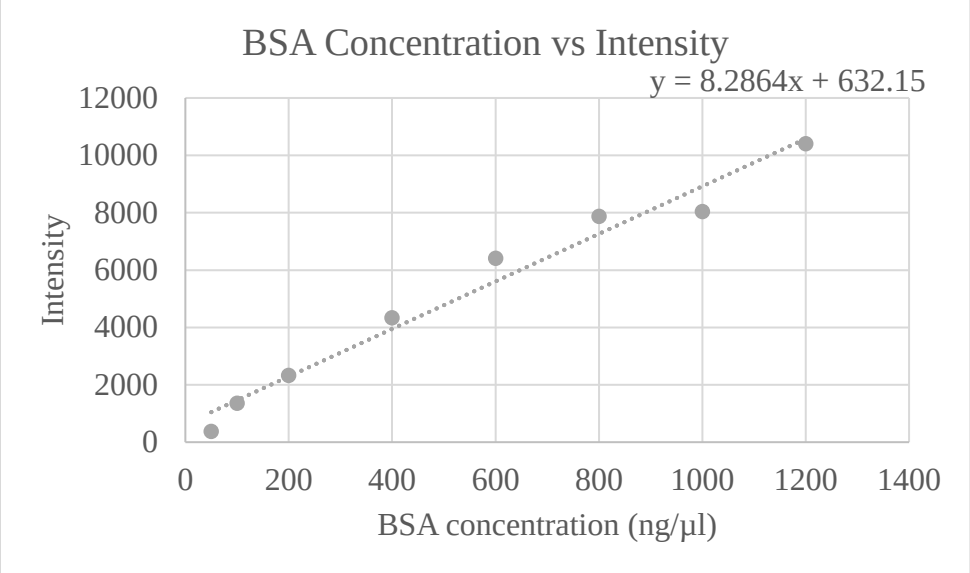

Figure 2-15. Scatterplot BSA concentration vs intensity.
This graph shows the BSA concentration plotted with the intensity determined using ImageJ software. A best fit line was determined using Microsoft Excel. This equation was used to determine protein amount of Cry Operon mutation construct samples used in bioassays as well as determine the amount of protein in an LC50 dose.

ImageJ software was used to determine the protein amount produced in each Cry Operon mutation construct as well as the original construct. The gel that was used to determine the protein amount can be found in Figure 2-14. A western blot was performed using a

Cry16 antibody to verify the correct band to measure on ImageJ, this image can be found in Figure 2-16.

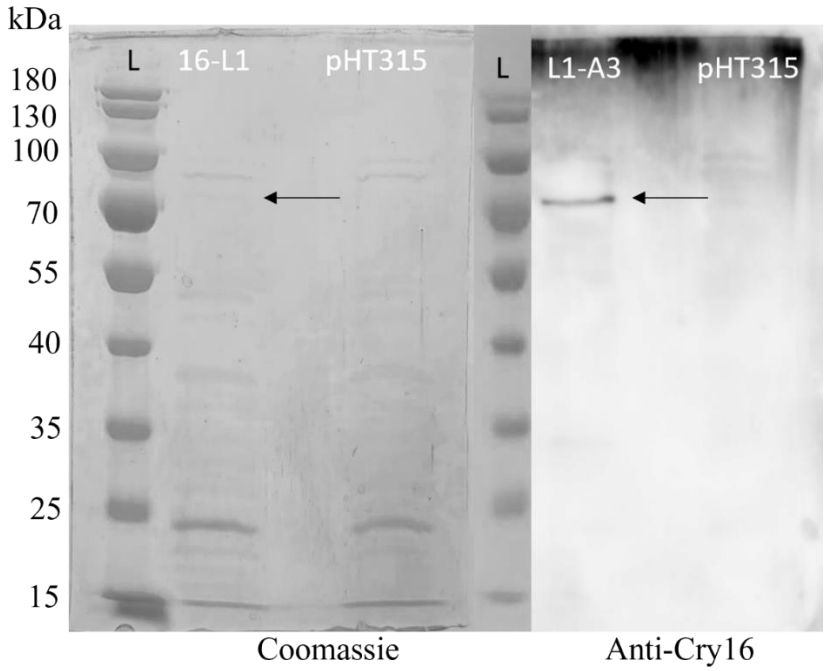

Figure 2-16. Cry16 band verification via western blot.
The SDS-PAGE on the left contains one Cry operon mutated sample and pHT315 sample for comparison, the western blot membrane on the right is probed using Cry16 antibody to determine the correct band to be measured using ImageJ software. The arrow indicates the correct band to be quantified.

The western blot developed using Cry16 antibody showed which band should be quantified for protein amount. This band was used to determine the protein concentration used at an LC50 value. LC50 data was determined using the Probit function in SPSS software. Table 2-9 shows the average LC50 value over 4 replicates as well as the protein concentration determined from the SDS-PAGE in Figure 2-14.

Table 2-9. LC50 and protein concentration.

Construct	LC50 Average (µl)	LC50 (ug)	Total Protein (ug) at highest dose with no toxicity
pCryO	455.52183	.352	-
Cry17-L2	466.1425	.902	-
Cry17-L3	405.85725	.766	-
Cry17-L1-A1	450.974	.412	-
Cry17-L1-A2	479.86125	.203	-
Cry17-L1-A3	483.23525	.355	-
Cry16-L1	490.56175	.213	-
Cry16-L2	444.87867	.158	-
Cry16-L3	383.96475	.132	-
Cry17-L1	N/A	-	2.626
pwL1	N/A	-	.251
pwL2	N/A	-	.228
pHt315	N/A	-	0

This table contains average LC50 data over all bioassays as well as protein concentration determined using the best fit line from Figure 2-15 and intensity data determined by ImageJ software.

This data suggests some mutation constructs may be more toxic (Cry16-L1, Cry16-L2, Cry16-L3, 17-L1-A1), while others may be less toxic (Cry17-L2, Cry17-L3), more replicates of the experiments should be done to confirm this data.

Some work has also been done with Cry16 alone to determine if Cry16 binds to mosquito midguts similar to the normal mechanism of cry toxins. Cry16 was expressed with a histidine tag and was purified using a Ni/NTA column. The purified Cry16 was then labeled with biotin and ultimately incubated with *Aedes* brush border membrane fractions prepared from 4th instar mosquito larvae. These binding assays were then run in a SDS page protein gel and probed using streptavidin in a western blot to see if binding occurred. A binding assay using purified Cry11A that was biotin labeled was used as a control. These two proteins were also used in a competition assay, Cry11A labeled with Cry11A unlabeled toxin, Cry11A labeled with Cry16 unlabeled toxin and Cry16 labeled

with Cry11A unlabeled toxin. The western blot probed with streptavidin can be seen in Figure 2-17. The bands in this blot are smaller than expected if Cry16 was binding, this indicates that Cry16 does not bind, but Cry11A does bind to BBMF. The intensity of lane 4 shows Cry16 may help with facilitating the binding of Cry11A, however more experiments are necessary to determine if this is the case.

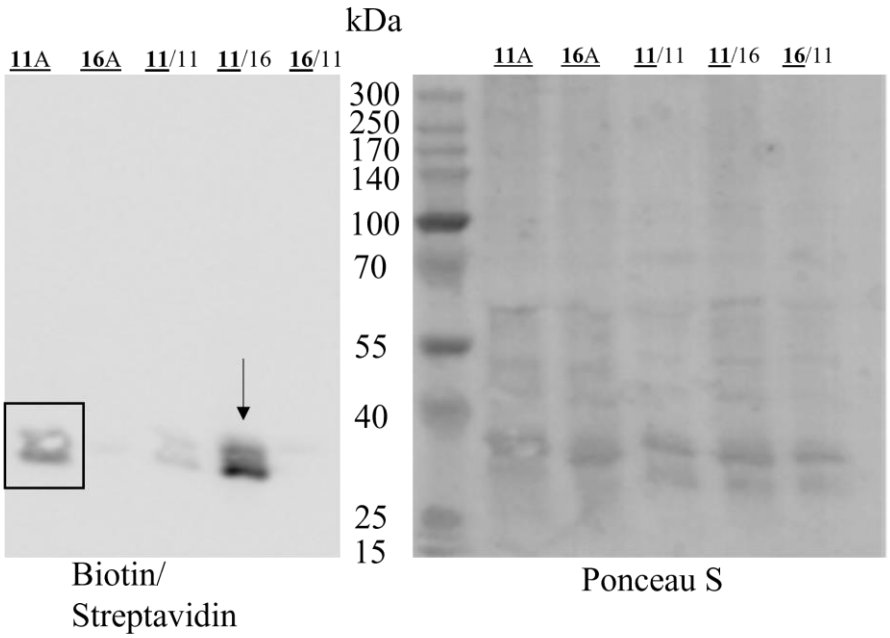

Figure 2-17. Binding and competition assay using Cry11A and Cry16.
Both images are western blot membranes, the membrane on the left is developed using an extended duration substrate, and the membane on the right has been stained with Ponceau S. The proteins are labeled with biotin, and the membrane is visualized using streptavidin. The lanes contain binding assays or competition assays, the underlined number indicates which toxin is labeled with biotin. The first two lanes are Cry11A and Cry16A binding asays respectively. The next three lanes are labeled Cry11A competed with unlabeled Cry11A, labeled Cry11A competed with unlabeled Cry16A, and labeled Cry16A competed with unlabeled Cry11A. The box in the left pannel indicates the Cry11A binding assay. The intensity of the band indicated by the arrow should be noted, and may indicate that Cry16A helps to facilitate binding of Cry11A.

Cry17 was cloned into the pQE30 vector to provide the protein with an N-terminal histidine tag to allow for purification using a Ni/NTA column. Previously,

Cry17 had not been expressed stably or seen in an SDS protein gel. Some bands can be seen, and one of these bands is Cry17 as it can be detected using a Cry17 antibody as well as a histidine antibody. The amount of protein produced from Cry17 expression is substantially less than Cry16, and after purification there were other contaminants. An anion exchange column was used to further purify Cry17, while there was better isolation of the protein, there were still contaminants present (Figure 2-18). Binding assays were not performed with Cry17 because pure protein was never attained.

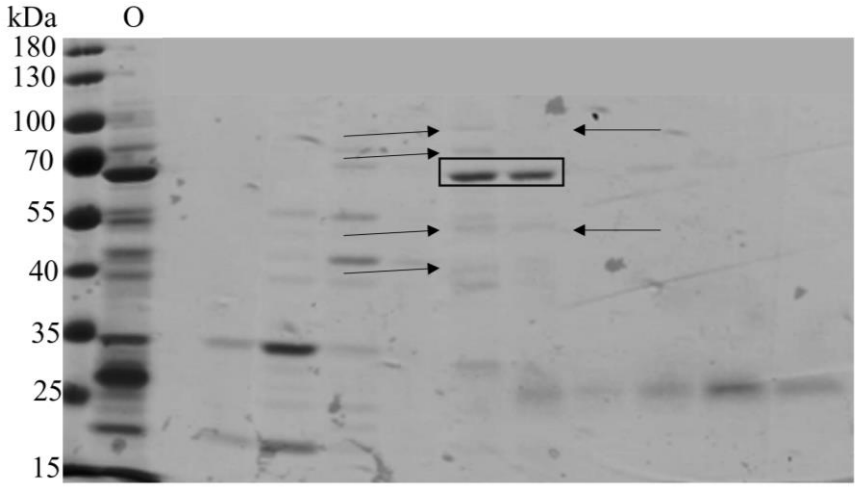

Figure 2-18. SDS-PAGE of Cry17 purified using an anion exchange column. This is an SDS-PAGE loaded with samples purified by anion-exchange chromatography. The lane indicated with O is the original sample loaded into the column. This sample was purified using a Ni-NTA column. The two bands indicated by the box in the middle of the gel are the correct size of Cry17, however as the arrows indicate, there are other proteins still present in those samples, thus Cry17 was not purified through anion-exchange chromatography.

Discussion

During this project a loss of toxicity problem occurred. The original full length Cry operon construct lost toxicity. The loss of toxicity occurred both when replating original bacteria and when a fresh transformation was done into *Bt* 4Q7 cells. In an attempt to remedy this loss of toxicity the full Cry operon was cloned behind two

separate promoters Cry3A and Cyt1A, both promoters found in Cry and Cyt producing bacteria. Neither of these promoters changed the toxicity of the Cry operon against *Aedes* mosquitoes when expressed in 4Q7 cells using sporulation media. In another attempt to rescue toxicity the Cry operon was cloned into a pStop vector which contained a xylose inducible promoter. pStop is expressed in *Bacillus megaterium* however, toxicity was not rescued through this means either. The most likely cause of the loss of toxicity is a combination mismanagement of lab strains and a lack of experience choosing larvae at the correct age. In lab there is a Gill lab wildtype stain as well as a resistant strain that was used in another experiment that had been selected against Cry11A to elucidate resistance genes. If the resistant strain was mated with the Gill lab wildtype it could reduce toxicity to the wildtype strain, but cross-resistance is unlikely. The original bioassay data was collected from Gill lab wildtype mosquitoes at 3rd instar. Recently, a bioassay was performed using all *Aedes* strains kept in lab these include Gill Lab, Liverpool and Orlando. Of these three strains, the Orlando wildtype mosquitoes were the most susceptible to the Cry operon producing bacteria, because of this data, Orlando mosquitoes were used for the subsequent bioassay experiments.

Once toxicity was seen again, six new constructs were created to determine if the domain II loop regions from Cry16 or Cry17 were important for toxicity of the protein complex. In each of these constructs 3 or 4 amino acids within the loop regions were substituted for alanine amino acids. This alanine substitution causes the amino acids within the loop to be physiochemically inert because the side chains of the amino acids have been reduced to a single methyl group (Gray et al., 2017). This substitution showed

that only the putative loop1 region of Cry17 was important for toxicity of the full Cry operon as all other constructs with alanine substitutions maintained their toxicity. The experiment was taken one step farther by isolating single amino acids within the putative loop 1 region of Cry17 and substituting them with alanine. In this experiment, none of the single amino acid substitutions caused a loss of toxicity, thus all three amino acids of putative loop 1 in Cry17 are likely involved in toxicity and potentially receptor binding. This data helps to support previous binding data where Cry16 did not bind to brush border membrane fractions, and thus Cry17 may be the membrane binding toxin.

When first investigating the mechanism of action of the Cry operon we hypothesized that the two cry toxin proteins encoded in the operon may act similarly to binary toxins. There are some notable binary cry toxins that have been investigated, they are Cry34Ab1/Cry35Ab1 (Masson et al., 2004) from *Bacillus thuringiensis* and Cry48Aa/Cry49Aa (Jones et al., 2008) from *Bacillus sphaericus.* Cry34Ab1/Cry35Ab1 is toxic against Western Corn Rootworm and was found to be pore forming and has the ability to permeabilize liposomes to form ion channels (Masson et al., 2004). It was shown that a 3:1 molar mixture of Cry34Ab1 to Cry35Ab1 was necessary to induce channel activity. Cry34Ab1 can create a pore on its own, however Cry35Ab1 did not have that ability. Cry35Ab1 did however have the ability to destabilize the membrane (Masson et al., 2004). Similarly, Cry48Aa and Cry49Aa found in *Bacillus sphaericus* also act as a binary toxin. Although Cry48A is part of a family that includes BinA and BinB it also shares this family with Cry36 and Cry35; Cry48A shows 30% identity to Cry4Aa (Jones et al., 2008). These two toxins are considered a binary toxin because

alone they do not cause toxicity in their target organism. When administered in a 1:1 ratio, this binary toxin shows high level toxicity against *Culex quinquefasciatus* (Jones et al., 2008). Although Cry16 did not bind to brush border membrane fractions, there was a higher intensity of the Cry11A band in the competition assay. This may mean that Cry16 can help facilitate binding of other toxins, in particular Cry17. Currently there are Cyt toxins that have been shown to have synergizing effects with Cry toxins. The most notable are found in *Bti* where Cyt1A has been shown to synergize with Cry4 (Adang et al., 2014) and cause higher toxicity than Cry4 alone. Cyt1A has also been shown to synergize with Cry11A and was shown to function like a receptor molecule against *Ae. aegypti* (Pérez et al., 2005).

Although our original hypothesis was that Cry16 and Cry17 may work similarly to a binary toxin where one is involved in binding and the other is involved in pore formation another hypothesis has come about involving the two aegerolysin-like proteins that are also encoded in the Cry operon. The full complex is required for toxicity, and the aegerolysin-like proteins may play a more critical role than originally thought. The aegerolysin family consists of β-structured proteins and can be found in both eukaryotes as well as bacteria. These proteins are known for their ability to interact with specific membrane lipids and lipid domains. Fungal aegerolysin proteins have been shown to interact with sphingomyelin and cholesterol domains. A fungal aegerolysin was shown to interact with another protein that has a membrane-attack-complex/perforin (MACPF) domain; these proteins together can then act as a pore-forming complex on membranes that contain specific lipid domains (Panevska et al., 2019). Cbm17.1 and cbm17.2 were

identified as aegerolysin-like proteins, and thus may be involved in either binding or causing pore formation. More research needs to be done to determine how each protein of the Cry operon is involved in the complex's toxicity.

Future directions for this research include purifying Cry17 and performing a binding assay. Cry16 may help to facilitate binding of Cry17, this hypothesis arises from the Cry16 and Cry11A competition assay. The competition assay should be run again to validate the results, and a competition with Cry17 should be performed to see if this is the case. As stated earlier, aegerolysin proteins have been shows to be pore forming, this may also be part of the mechanism of the Cry operon, and a pore formation assay should be performed with Cbm17.1 and Cbm17.2 alone, and also together as all proteins are necessary for toxicity. Another direction this project could go is to introduce *Anopheles* toxicity into the Cry operon by using the loop regions of other Cry toxins that target *Anopheles* mosquitoes. Integrating other toxin loop regions into the putative loop 1 region of Cry17 could change toxicity of the Cry operon all together.

References

Abdullah, M.A.F., Alzate, O., Mohammad, M., McNall, R.J., Adang, M.J., Dean, D.H., 2003. Introduction of Culex Toxicity into Bacillus thuringiensis Cry4Ba by Protein Engineering. Appl. Environ. Microbiol. 69, 5343–5353. https://doi.org/10.1128/AEM.69.9.5343-5353.2003

Adang, M.J., Crickmore, N., Jurat-Fuentes, J.L., 2014. Chapter Two - Diversity of Bacillus thuringiensis Crystal Toxins and Mechanism of Action, in: Dhadialla, T.S., Gill, S.S. (Eds.), Advances in Insect Physiology, Insect Midgut and Insecticidal Proteins. Academic Press, pp. 39–87. https://doi.org/10.1016/B978-0-12-800197-4.00002-6

Barloy, F., Delécluse, A., Nicolas, L., Lecadet, M.M., 1996. Cloning and expression of the first anaerobic toxin gene from Clostridium bifermentans subsp. malaysia, encoding a new mosquitocidal protein with homologies to Bacillus thuringiensis delta-endotoxins. J. Bacteriol. 178, 3099–3105.

Barloy, F., Lecadet, M.M., Delécluse, A., 1998. Cloning and sequencing of three new putative toxin genes from Clostridium bifermentans CH18. Gene 211, 293–299. https://doi.org/10.1016/s0378-1119(98)00122-x

Ben-Dov, E., 2014. Bacillus thuringiensis subsp. israelensis and Its Dipteran-Specific Toxins. Toxins 6, 1222–1243. https://doi.org/10.3390/toxins6041222

Bravo, A., Soberón, M., Gill, S.S., 2005. 6.6 - Bacillus thuringiensis: Mechanisms and Use, in: Gilbert, L.I. (Ed.), Comprehensive Molecular Insect Science. Elsevier, Amsterdam, pp. 175–205. https://doi.org/10.1016/B0-44-451924-6/00081-8

CDC, 2020. Disease of the Week - Zika [WWW Document]. Cent. Dis. Control Prev. URL https://www.cdc.gov/dotw/zika/index.html (accessed 6.28.22).

Charles, J.F., Nicolas, L., Sebald, M., de Barjac, H., 1990. Clostridium bifermentans serovar malaysia: sporulation, biogenesis of inclusion bodies and larvicidal effect on mosquito. Res. Microbiol. 141, 721–733. https://doi.org/10.1016/0923-2508(90)90066-y

Chikungunya fact sheet [WWW Document], 2020. URL https://www.who.int/news-room/fact-sheets/detail/chikungunya (accessed 6.28.22).

Contreras, E., Masuyer, G., Qureshi, N., Chawla, S., Dhillon, H.S., Lee, H.L., Chen, J., Stenmark, P., Gill, S.S., 2019. A neurotoxin that specifically targets Anopheles mosquitoes. Nat. Commun. 10, 2869. https://doi.org/10.1038/s41467-019-10732-w

de Barjac, H., Sebald, M., Charles, J.F., Cheong, W.H., Lee, H.L., 1990. [Clostridium bifermentans serovar malaysia, a new anaerobic bacterium pathogen to mosquito and blackfly larvae]. C. R. Acad. Sci. III 310, 383–387.

Dengue Fever | NIH: National Institute of Allergy and Infectious Diseases [WWW Document], 2016. URL https://www.niaid.nih.gov/diseases-conditions/dengue-fever (accessed 6.28.22).

Georghiou, G.P., Wirth, M.C., 1997. Influence of Exposure to Single versus Multiple Toxins of Bacillus thuringiensis subsp. israelensis on Development of Resistance in the Mosquito Culex quinquefasciatus (Diptera: Culicidae). Appl. Environ. Microbiol. 63, 1095–1101.

Global Health - Newsroom - Yellow Fever [WWW Document], 2019. URL https://www.cdc.gov/globalhealth/newsroom/topics/yellowfever/index.html (accessed 6.28.22).

Gray, V.E., Hause, R.J., Fowler, D.M., 2017. Using large-scale mutagenesis to guide single amino acid scanning experiments (preprint). Molecular Biology. https://doi.org/10.1101/140707

Jones, G.W., Wirth, M.C., Monnerat, R.G., Berry, C., 2008. The Cry48Aa-Cry49Aa binary toxin from Bacillus sphaericus exhibits highly restricted target specificity. Environ. Microbiol. 10, 2418–2424. https://doi.org/10.1111/j.1462-2920.2008.01667.x

Juárez-Pérez, V., Delécluse, A., 2001. The Cry toxins and the putative hemolysins of Clostridium bifermentans ser. malaysia are not involved in mosquitocidal activity. J. Invertebr. Pathol. 78, 57–58. https://doi.org/10.1006/jipa.2001.5042

Lee, H.L., Seleena, P., 1990a. Isolation of indigenous larvicidal microbial control agents of mosquitos: the Malaysian experience. Southeast Asian J. Trop. Med. Public Health 21, 281–287.

Lee, H.L., Seleena, P., 1990b. Isolation and evaluation of larvicidal Clostridium bifermentans against mosquitoes of public health importance. Trop. Biomed. 7, 103–106.

Liu, L., Li, Z., Luo, X., Zhang, X., Chou, S.-H., Wang, J., He, J., 2021. Which Is Stronger? A Continuing Battle Between Cry Toxins and Insects. Front. Microbiol. 12.

Masson, L., Schwab, G., Mazza, A., Brousseau, R., Potvin, L., Schwartz, J.-L., 2004. A Novel Bacillus thuringiensis (PS149B1) Containing a Cry34Ab1/Cry35Ab1 Binary Toxin Specific for the Western Corn Rootworm Diabrotica virgifera virgifera LeConte Forms Ion Channels in Lipid Membranes. Biochemistry 43, 12349–12357. https://doi.org/10.1021/bi048946z

Nielsen-Leroux, C., Pasteur, N., Prètre, J., Charles, J.-F., Sheikh, H.B., Chevillon, C., 2002. High resistance to Bacillus sphaericus binary toxin in culex pipiens (Diptera: Culicidae): the complex situation of west Mediterranean countries. J. Med. Entomol. 39, 729–735. https://doi.org/10.1603/0022-2585-39.5.729

Panevska, A., Hodnik, V., Skočaj, M., Novak, M., Modic, Š., Pavlic, I., Podržaj, S., Zarić, M., Resnik, N., Maček, P., Veranič, P., Razinger, J., Sepčić, K., 2019. Pore-forming protein complexes from Pleurotus mushrooms kill western corn rootworm and Colorado potato beetle through targeting membrane ceramide phosphoethanolamine. Sci. Rep. 9, 5073. https://doi.org/10.1038/s41598-019-41450-4

Pérez, C., Fernandez, L.E., Sun, J., Folch, J.L., Gill, S.S., Soberón, M., Bravo, A., 2005. Bacillus thuringiensis subsp. israelensis Cyt1Aa synergizes Cry11Aa toxin by functioning as a membrane-bound receptor. Proc. Natl. Acad. Sci. 102, 18303–18308. https://doi.org/10.1073/pnas.0505494102

Qureshi, N., Chawla, S., Likitvivatanavong, S., Lee, H.L., Gill, S.S., 2014. The Cry Toxin Operon of Clostridium bifermentans subsp. malaysia Is Highly Toxic to Aedes Larval Mosquitoes. Appl. Environ. Microbiol. 80, 5689–5697. https://doi.org/10.1128/AEM.01139-14

Silva Filha, M.H.N.L., Berry, C., Regis, L., 2014. Chapter Three - Lysinibacillus sphaericus: Toxins and Mode of Action, Applications for Mosquito Control and Resistance Management, in: Dhadialla, T.S., Gill, S.S. (Eds.), Advances in Insect Physiology, Insect Midgut and Insecticidal Proteins. Academic Press, pp. 89–176. https://doi.org/10.1016/B978-0-12-800197-4.00003-8

Sinègre, G., Babinot, M., Quermel, J.M., Gavon, B., 1994. First field occurrence of Culex pipiens resistance to Bacillus sphaericus in southern France. 8th Eur. Meet. Soc. Vector Ecol.

Souza-Neto, J.A., Powell, J.R., Bonizzoni, M., 2019. Aedes aegypti vector competence studies: A review. Infect. Genet. Evol. 67, 191–209. https://doi.org/10.1016/j.meegid.2018.11.009

Thiery, I., Hamon, S., Gaven, B., De Barjac, H., 1992. Host range of Clostridium bifermentans serovar. malaysia, a mosquitocidal anaerobic bacterium. J. Am. Mosq. Control Assoc. 8, 272–277.

Wirth, M.C., Georghiou, G.P., Malik, J.I., Abro, G.H., 2000. Laboratory Selection for Resistance to Bacillus sphaericus in Culex quinquefasciatus (Diptera: Culicidae) from California, USA. J. Med. Entomol. 37, 534–540. https://doi.org/10.1603/0022-2585-37.4.534

Yiallouros, M., Storch, V., Thiery, I., Becker, N., 1994. Efficacy of Clostridium bifermentans serovar Malaysia on target and nontarget organisms. J. Am. Mosq. Control Assoc. 10, 51–55.

Chapter 3

Purification of Ptox progenitor complex from *Paraclostridium bifermentans* serovar *malaysia.*

Abstract

Anopheles mosquitoes are responsible for vectoring Plasmodium and in turn infecting hundreds of thousands of people with malaria annually. A bacteria called *Paraclostridium bifermentans* serovar *malaysia* was found to have mosquitocidal activity against *Anopheles.* This bacterium was found in mangrove swamp soil in Malaysia in an anopheline environment which allowed for the co-evolution of its toxins to target *Anopheles* mosquitoes. The component that is toxic to *Anopheles* is found in a toxin locus within a plasmid. The toxin locus contains genes related to those found with botulinum neurotoxin. This chapter aims to determine the size of this toxin complex, speculate the protein ratio of all proteins involved, as well as purify the complex as a whole using multiple purification methods.

Introduction

Malaria has been and continues to be a global problem (World Health Organization, 2019). The organism responsible for this disease, plasmodium, is transferred from person to person by *Anopheles* mosquito vectors(Becker et al., 2010). One method utilized to decrease the global burden is through controlling the mosquito vector. Current *Anopheles* mosquito control methods include the use of pesticides on nets or spraying indoors ("Malaria vector control," n.d.) . Although, they are effective, pesticides can lead to resistance development, have off target or long-term effects on other organisms, the environment and on human health (Oliveira et al., 2017). Biological methods have been used to target other mosquito vectors, these include *Bacillus thuringiensis israelensis* (*Bti*) and *Lysinibacillus sphaericus* (*Ls*), however, they are mostly effective against *Aedes* and *Culex* mosquitoes respectively and are not as effective against *Anopheles* mosquitoes (Becker, 1997; CDC, 2020; Fillinger et al., 2008).

Paraclostridium bifermentans serovar *malaysia (Pbm)* was found in mangrove swamp soil in 1990 (de Barjac et al., 1990). *Pbm* is toxic to both *Aedes* and *Anopheles* mosquitoes, and interestingly, the type strain is not toxic to vertebrates (Contreras et al., 2019; Qureshi et al., 2014; Thiery et al., 1992). Mosquitocidal activity against *Aedes* is due to the Cry operon encoded in the bacteria's large 109kb plasmid. The Ptox locus of the same 109kb plasmid is credited with activity against *Anopheles* mosquitoes. The Ptox locus contains five genes under the same promoter, *pmp1* (paraclostridial mosquitocidal protein 1) a neurotoxin, *ntnh*, *orfx1*, *orfx2*, and *orfx3*. This operon is flanked on one side by a *p47* protein and on the other, a putative metallophosphatase family protein (*mpp*)

(Contreras et al., 2019). Pmp1 shows 36% similarity to other clostridial neurotoxins, like botulinum toxin, and the locus it is in mimics other clostridial neurotoxin loci. The other genes involved in the toxin loci show 35-57% amino acid identity to those found in other clostridial neurotoxin loci (Contreras et al., 2019).

When botulinum neurotoxin is ingested, it must survive in the gut of its target organism and migrate to presynaptic neurons where it can cleave its target SNARE protein. The neurotoxins survive the gut environment by forming progenitor toxin complexes. Of the seven botulinum neurotoxin (BoNT) serotypes, five are clustered with hemagglutinin genes, while the other two are clustered with *orfx* genes. Although the role of the *orfx* genes is still unknown, they are known to be part of the progenitor toxin complex. Both clusters are associated with a non-toxic non-hemagglutinin (NTNH) protein (Eswaramoorthy et al., 2015; Gu and Jin, 2013). In a similar vein, the pmp operon which includes *pmp1, ntnh, orfx1, orfx2,* and *orfx3.* It is this full complex that is most toxic to *Anopheles* larvae when fed (Contreras et al., 2019). In contrast, Pmp1 and NTNH when expressed together do confer significant toxicity, while Pmp1 alone, is not toxic when ingested by mosquito larvae. When injected, however, the Pmp1 toxin alone is toxic to mosquito larvae both *Aedes* and *Anopheles*. Further study of the Pmp1 toxin shows that it acts similarly to BoNT in that it cleaves the SNARE protein syntaxin (Contreras et al., 2019). Collectively this data suggests the complex that is formed is critical for oral toxicity to mosquito larvae.

This chapter details attempts to purify the Ptox complex formed by Pmp1, NTNH, OrfX1, OrfX2, and OrfX3. Using multiple extractions and purification techniques, some

purification was successful, while complete purification and crystallization of the complex was not. The aim of purifying the toxin complex was to determine the size, potential stoichiometry, and crystal structure of the toxin complex. An approximate size was calculated using multiple methods and will also be described in this chapter.

Materials and Methods

Pbm culture

Pbm colonies were plated on TYG plates (7.5g Tryptone, 5g Yeast Extract, 2.5g Dextrose, .125g L-cysteine, 5g Agar, 250mL water, pH to 7.0 ± .2. All growth of *Pbm* bacteria was done at 30°C in a GasPak™ anaerobic chamber with a GasPak™ Anaerobe Container System with Indicator, by Becton Dickinson. *Pbm* plates were replated monthly to keep the bacteria alive.

Expression of toxins

One loop full of plate grown bacteria (TYG plate) was inoculated into TYG media. The media was left at 30°C for the allotted amount of time (1hr, 2hrs, 4hrs, 8hrs, 16hrs, 24hrs). Incubation occurred in a GasPak™ anaerobic chamber with a GasPak™ Anaerobe Container System with Indicator, by BD.

Antibodies for toxins

Rabbit antibodies were made either by Pacific Immunology Corp. (Ramona, CA) or by Genscript (Piscataway, NJ). All antibodies (Pmp1, orfX1, orfX2, Mpp) were used in a 1:1000 dilution.

SDS-Page

A 10% SDS page (Stacking Gel: 1.5mm, 2.329ml water, .375ml 1M Tris pH 6.8, 281µl 40% acrylamide, 15µl 20% SDS, 30µl 10% APS, 5µl Temed. for one, 1.5mm gel; Separating Gel: 1.5mm, 10%, 3.75mL 1M Tris pH 8.8, .05ml 20% SDS, 2.5 mL 40% acrylamide, 3.7mL water, 200µl 10% APS, 8µl Temed for one, 1.5mm gel) gel was prepared and 30µl of sample was loaded into each well. The gel was run at 80V until the loading dye reached the end of the gel. The proteins of the SDS-PAGE were then transferred to a PVDF membrane overnight at 21V at 4°C or for 2-3 h at 40V and 4°C.

Native-PAGE

Native-PAGE, 8%, were prepared ((Stacking Gel: 1.5mm, 2.329ml water, .375ml 1M Tris pH 6.8, 281µl 40% Acrylamide, 30µl 10% APS, 5µl Temed, for one, 1.5mm gel; Separating Gel: 1.5mm, 10%, 3.75mL 1M Tris pH 8.8, 2.0 mL 40% acrylamide, 3.7mL water, 100µl 10% APS, 6µl Temed for one, 1.5mm gel). Twenty µl of sample was loaded into the gel. The gel was run at 90V until the native loading dye reached the bottom of the gel. Most gels were transferred to a PVDF membrane, following the same protocol as for SDS-PAGE. The membrane was then developed following the same protocols as for SDS western blot membranes.

Using protein antibody to detect protein in western blot

After the transfer of proteins to the PVDF membrane, each membrane was blocked with 5% skim milk in PBST (1X PBS pH 7.4, 1% Tween-20) for 1 h at room temperature. Then the membrane was incubated with primary antibody (1:1000 – orfX1, Pmp1, orfX2, MPP) in 1% skim milk in PBST for 2 h at room temperature. After

incubation with primary antibody the membrane was washed quickly 3 times with water, and then incubated for 5 min shaking with water. Those same steps are repeated using PBST. Next the membrane was incubated with secondary antibody (anti-rabbit at 1:5000 dilution). The membrane was then washed following the same water and PBST protocol. The membrane was developed using SuperSignal™ West Dura by Thermo Scientific using the ImageQuant LAS 4000 mini by GE and chemiluminescence.

Size exclusion chromatography

A size exclusion column, HiLoad™ 26/600 Superdex™ was used for purification of the Ptox and Cry operon complex from *Paraclostridium bifermentans malaysia* overnight culture. 50ml of overnight culture was spun down at 6260 rpm for 10 min at 4°C, the supernatant was the filtered through a 115ml gravity filter (Falcon), and then concentrated using the Amicon® Stirred Cell. Fifty ml using an Ultracel® 5kDa Ultrafiltration disc. The overnight culture was concentrated from either 50ml or 100ml to 5ml. The concentrated supernatant was then loaded onto the Superdex size exclusion column. A flow rate of 1ml/min was used and a 20mM Bis-Tris Propane, 100mM NaCl, pH 7.2 was used at the running buffer. The column was allowed to run for 2 full column volumes and peaks were collected in 1ml fractions. Samples were run in a native-PAGE and transferred to a PVDF membrane. The membranes were then probed with orfX1 antibody and Cry16 antibody to detect proteins within the membrane.

Size exclusion standards

Standards were used to determine the void volume as well as the volumes when specific sized proteins would elute from the column. Blue dextran, β- galactosidase,

bovine serum albumin and p-nitrophenol were used as standards. The blue dextran and p-nitrophenol are both colored and helped to visualize separation within the column as well as in the eluted fractions. These also indicate the void and inclusion limits respectively, of the column. The volumes at which each chemical or protein eluted was noted and used to determine a standard curve to help calculate the size of the pmp complex based on its elution volume.

Anion-exchange chromatography

The MonoQ 4.6/100PE was used to separate *Pbm* proteins based on charges. The column was equilibrated using 20mM Bis Tris Propane pH 6.7. The sample of *Pbm* culture was grown for 24 h at 30°C in an anaerobic chamber. The culture was then spun down at 6260 rpm for 10 min. The resulting supernatant was filtered in a115ml gravity filtration device and the resulting supernatant was concentrated to 5ml in the Amicon® Stirred Cell 50ml using an Ultracel® 5kDa Ultrafiltration disc. The concentrated culture was then loaded onto the MonoQ column. A flow rate of 0.25ml/min was used, and elution fractions were collected in 1ml fractions. The gradient was set to take 2 h to reach 100% B buffer (20mM Bis Tris Propane, pH 6.8 with 1M NaCl). Fractions were run on a native-PAGE and SDS-PAGE and then transferred to a PVDF membrane. OrfX1 and Cry16 antibodies were used to detect protein within the membrane.

Acid precipitation

A 24 h culture grown at 30°C (1L) was spun for 10 min at 4°C and 15,300 g. The pellet was discarded, and the supernatant was titrated with 1M H_2SO_4 to pH 3.5. The solution was then spun again for 30 min at 4°C and 15,300 g. The pellet was then

resuspended in .1M Sodium Citrate buffer pH 5.5 and kept on ice for 2 h. Then the solution was spun for 10 min at 4°C and 15,300 g. The supernatant was then used for anion-exchange chromatography.

Ammonium sulfate extraction

Sodium citrate extracted proteins were incubated in a saturated ammonium sulfate solution where the total volume of ammonium sulfate was 20%. The samples were incubated for 1 h and then spun at 15,300 g at 4°C. The supernatant from this spinning step was then incubated in a 60% total ammonium sulfate solution on ice for 1 h. The sample was then spun again at 15,300 g at 4°C. The 20% ammonium sulfate pellet, 60% ammonium sulfate pellet and 60% ammonium sulfate supernatant were kept for analysis in a native-PAGE.

Mass spectrometry

Samples were sent to the Biomolecular and Proteomics Mass Spectrometry Facility for Mass Spec analysis at UC San Diego. Samples were sent in aqueous form as well as bands cut from a Native-PAGE.

CRYO-EM

The same sample that was sent for Mass Spectrometry was sent to the Stenmark Group at Stockholm University for crystallization using CryOEM.

Complex size calculations

Two experiments were done to calculate the size of the *Pbm* complex. Twenty four hour culture of *Pbm* was run in a native-PAGE. The proteins were then transferred to a PVDF membrane and probed with Pmp1, orfX1, orfX2, and Mpp antibodies.

Concurrently a native gel was run using a NativeMark Unstained Protein marker. This native gel was stained with Coomassie. The distance from the top of the separating gel to each of the molecular markers was measured in millimeters. A plot was made of the distance vs the size of each marker, a best fit line was determined on excel. Then the distance from the top of the separating gel to each band detected with an antibody was measured. This distance was then used to calculate the size of each band.

The second experiment utilized the size exclusion column. Four standard sized proteins were used, as stated above. The volume at which the protein or chemical eluted from the column was plotted against the molecular size of each protein or chemical standard. A best fit line equation was determined on excel. This equation was then used to determine the size of the protein based on the volume during the peak when the protein eluted. This protein was detected using the orfX1 antibody when run in a native-PAGE and transferred to a PVDF membrane.

Results

Ptox complex protein expression

Paraclostridium bifermentans serovar *malaysia* was grown for 4, 8 and 24 h. Each culture was analyzed to determine if the MPP proteins as well as Ptox loci proteins are found in either the pellet or supernatant (Figure 3-1). Pmp1 and orfX1 antibody detect proteins in the pellet and supernatant in the 24 h culture but not 4 or 8 h. MPP antibody detects proteins in the pellet at 4 and 8 h and in both pellet and supernatant of 24 h culture.

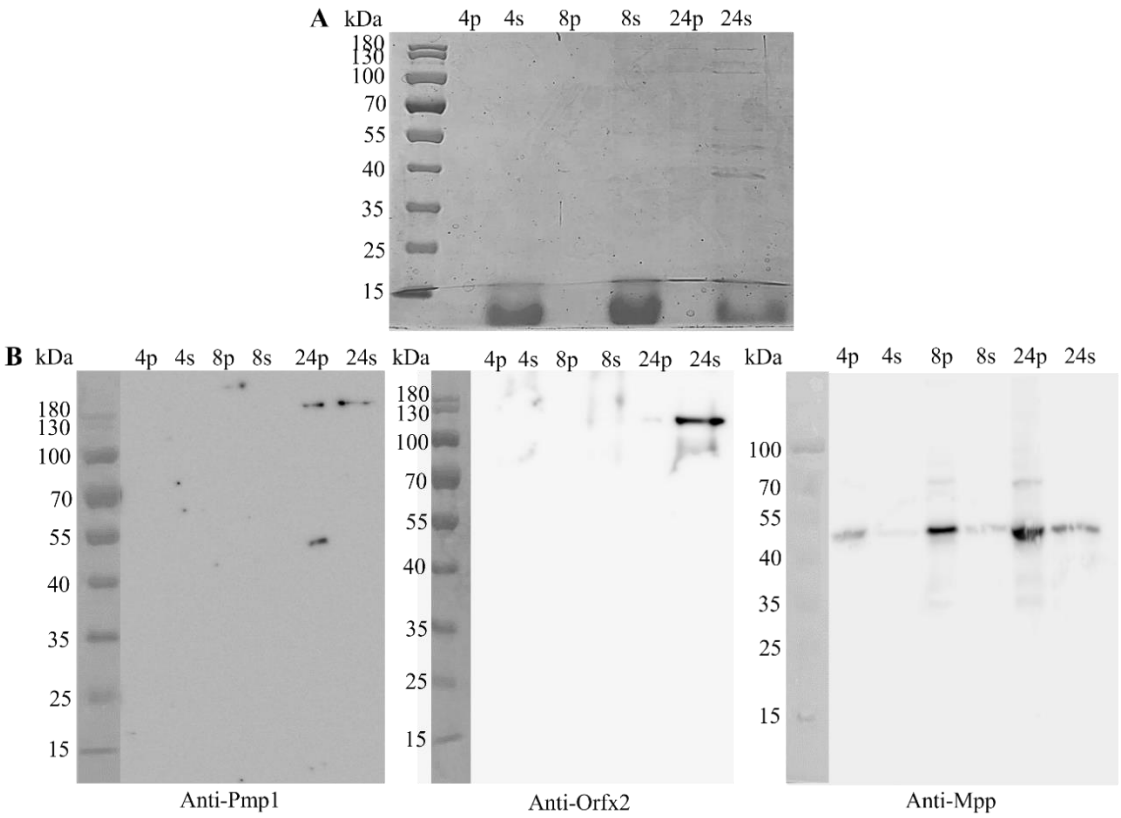

Figure 3-1. Expression of Ptox loci proteins.
This figure shows an SDS-PAGE and western blot containing samples of *Pbm* culture grown for different amounts of time; 4h, 8h and 24h. Figure A contains samples run in an SDS-PAGE and stained with Coomassie. B shows three western membranes containing a pelleted sample and a supernatant sample each from the 4h, 8h and 24h cultured bacteria; these membranes were probed with anti-Pmp1, anti-Orf2, and anti-Mpp respectively.

Ptox complex size

A 24 h cultured *Pbm* was run in a Native-PAGE. The culture proteins were transferred to a PVDF membrane and then probed with Pmp1, orfX1, orfX2, and Mpp antibodies (Figure 3-2**)**.

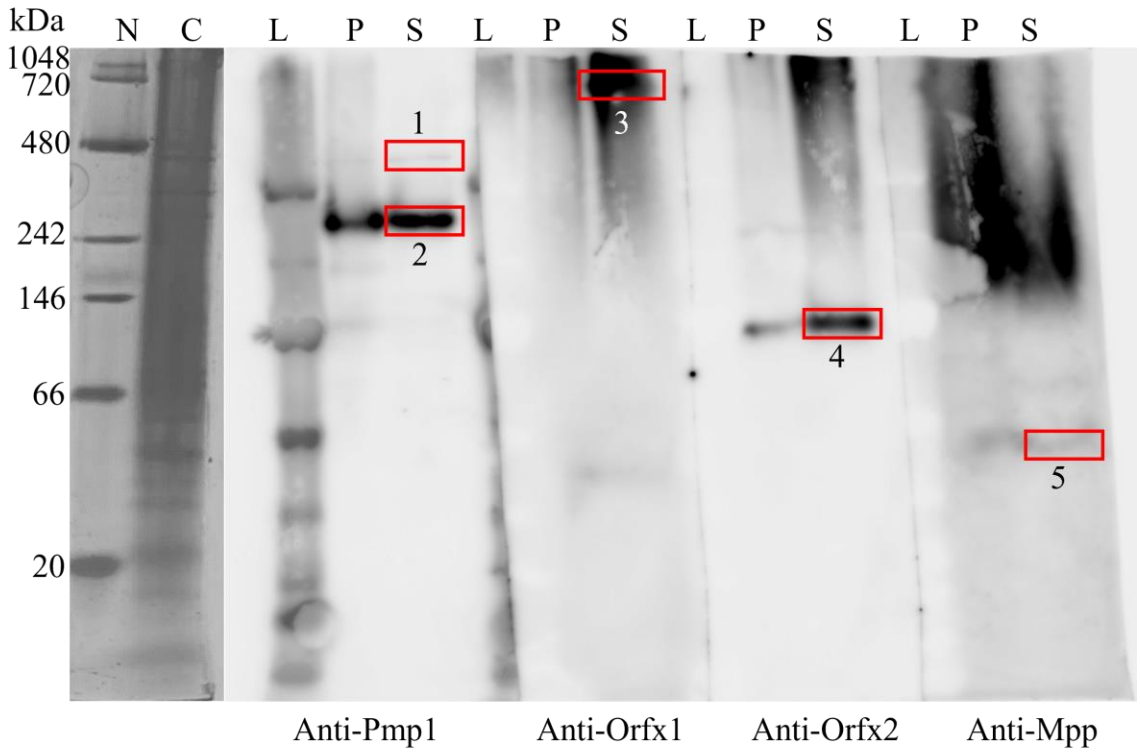

Figure 3-2. Western of *Pbm* culture probed with Ptox complex antibodies.
This figure shows a Coomassie stained Native gel as well as 4 PVDF membranes probed with different Ptox complex antibodies, Pmp1, Orf1, Orf2, and Mpp respectively. The N indicates the native ladder, C is *Pbm* whole culture, L indicates SDS ladder (used to visualize how far the gel has run), P indicates pelleted 24h culture, and S indicates 24h supernatant. The bands indicated by the red boxes were used to help determine the size of the Ptox protein complex. The numbers next to each box correlate to a value measured from the top of the gel to the band and are indicated in Table 3-2.

The native protein ladder was used as a standard, the size of each band and the distance from the top of the gel to each protein standard was measured in millimeters, this data was plotted, and a best fit linear equation was determined from the data points (Table 3-1, Figure 3-3).

Table 3-1. Standard protein values of native ladder.

Distance (mm)	MW (Da)	log MW
2	1048000	6.020361
4	720000	5.857332
12.5	480000	5.681241
24.5	242000	5.383815
32	146000	5.164353
44	66000	4.819544
67	20000	4.30103

This table contains the distance in millimeters from the top of the gel to each band of the native protein standard. The distance, along with the log molecular weight were plotted in a graph and a best fit equation was determined (Figure 3-3).

This equation was used to calculate the size of protein bands detected with each antibody as indicated in Figure 3-2 (Table 3-2); the calculated sizes can be seen in Table 3-2.

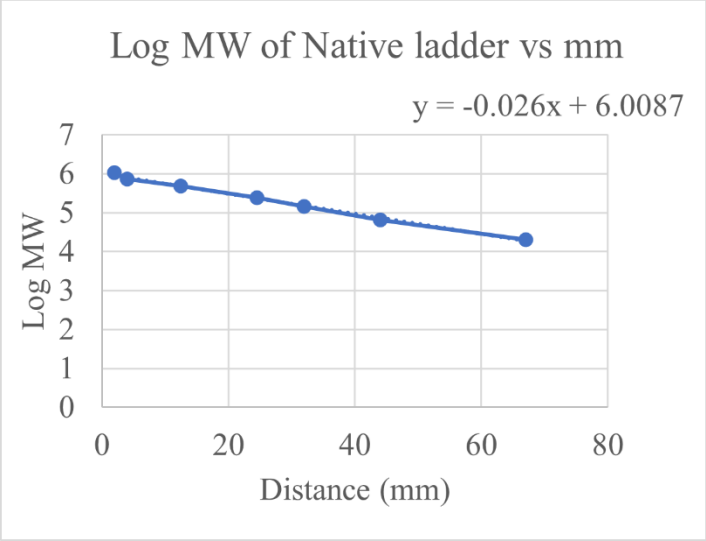

Figure 3-3. Log MW of native ladder vs distance.
This graph shows a scatter plot of the data from Table 3-1, and the calculated best fit linear line. This equation was used to determine the size of each band detected by the Ptox complex protein antibodies in Figure 3-2.

Table 3-2. Calculated size of detected bands in western blot.

Band Number	Distance (mm)	Calculated Log (MW)	Size (Da)	Calculated Size (kDa)	Expected Elution Volume (ml)
1	14	5.6447	441265.5	441	145.79
2	22	5.4367	273338	273	165.23
3	5	5.8787	756310.3	756	123.93
4	35	5.0987	125516.3	125	196.82
5	50	4.7087	51132.85	51	233.27

This table shows the steps to determine the calculated size of each band detected by Ptox protein complex antibodies. The band numbers correspond to the bands indicated in Figure 3-2. The distance indicates the distance from the top of the gel to each band, this value was used as the x value in the equation, and the calculated log MW is the y value used to find the calculated size. The expected elution value will be discussed later.

Size exclusion for standard proteins

Standard sized proteins were prepared and run through a Size Exclusion column. The standard proteins chosen for this experiment were blue dextran (2,000 kDa), β-galactosidase (465 kDa), bovine serum albumin (66 kDa), and p-nitrophenol (139 Da). These proteins and a chemical were chosen because they cover a wide range of sizes and helped to determine the void and inclusion volumes of the size exclusion column as well as determine when small molecules would elute. Blue dextran and p-nitrophenol were easily identified due to their color, which could be seen in both the column as well as the fractions collected. The chromatogram and volumes at which the proteins were eluted from the size exclusion column can be found in Figure 3-4.

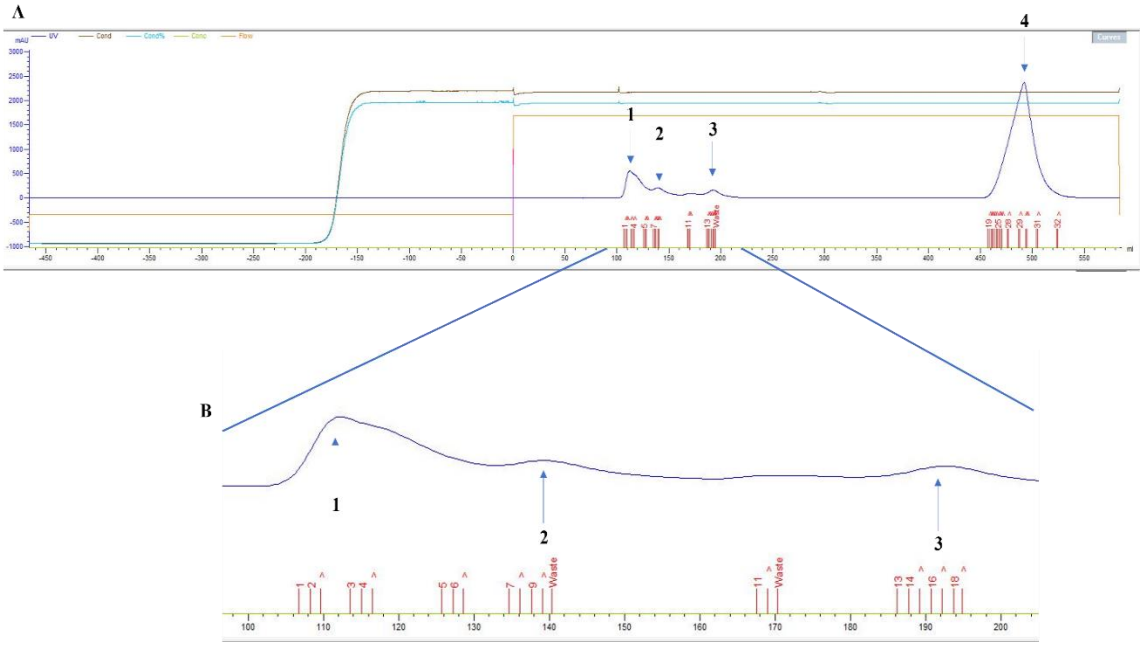

Figure 3-4. Chromatogram of standard proteins from size exclusion column. This figure shows the chromatogram associated with the standard proteins run through the size exclusion column. Panel A shows the full chromatogram while B shows a portion of the chromatogram. The peaks indicated with arrows and denoted 1, 2, 3, and 4 indicate blue dextran, β-galactosidase, bovine serum albumin, and p-nitrophenol respectively. The volume at which each peak was used to determine a best fit line and can be seen in Table 3-3, and a graph of the data can be seen in Figure 3-5.

Table 3-3 lists the elution volume of each protein that was plotted in Figure 3-5. The size of each protein and volume at which the proteins eluted from the size exclusion column were plotted. A best fit linear equation was determined from the graph and was used to determine the expected elution volume for the bands detected in Figure 3-2, that data can be found in Table 3-2.

Table 3-3. Volume of elution for each standard protein and their size

Protein	vol (ml)	MW (Da)	log (MW)
blue dextran	112	2000000	6.30103
β-galactosidase	140	465000	5.66745
bovine serum albumin	192	66000	4.81954
p-nitrophenol	480	139	2.14301

This table contains the elution volume for each protein standard from the size exclusion column as well as size of each protein. The size of each protein was converted to a log value to plot in Figure 3-5 where a best fit linear equation was determined.

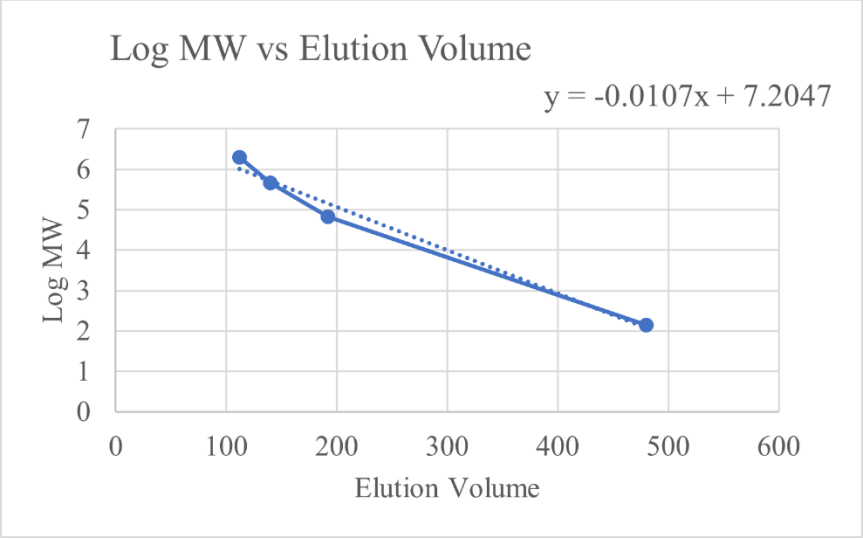

Figure 3-5. Log MW vs elution volume of protein standards from size exclusion column.

This figure contains a graph of the Log MW of each of the standard proteins used in the size exclusion column plotted with the elution volume. This data is listed in Table 3-3. A best fit equation was determined and used as a guide to determine the expected elution volume of the proteins detected in Figure 3-2, these values can be seen in the last column of Table 3-2.

Ptox complex size

Using the calculated protein size from the Table 3-2 found from Figure 3-2, the expected volume at which each protein would elute was calculated using the equation in Figure 3-5 and can be found in Table 3-2. Figure 3-6A and 3-6C shows 2 chromatograms different 24h *Pbm* cultures run through the size exclusion column along with the corresponding western blot (Figure 3-6B and 3-6D) detected with anti-OrfX1 antibody.

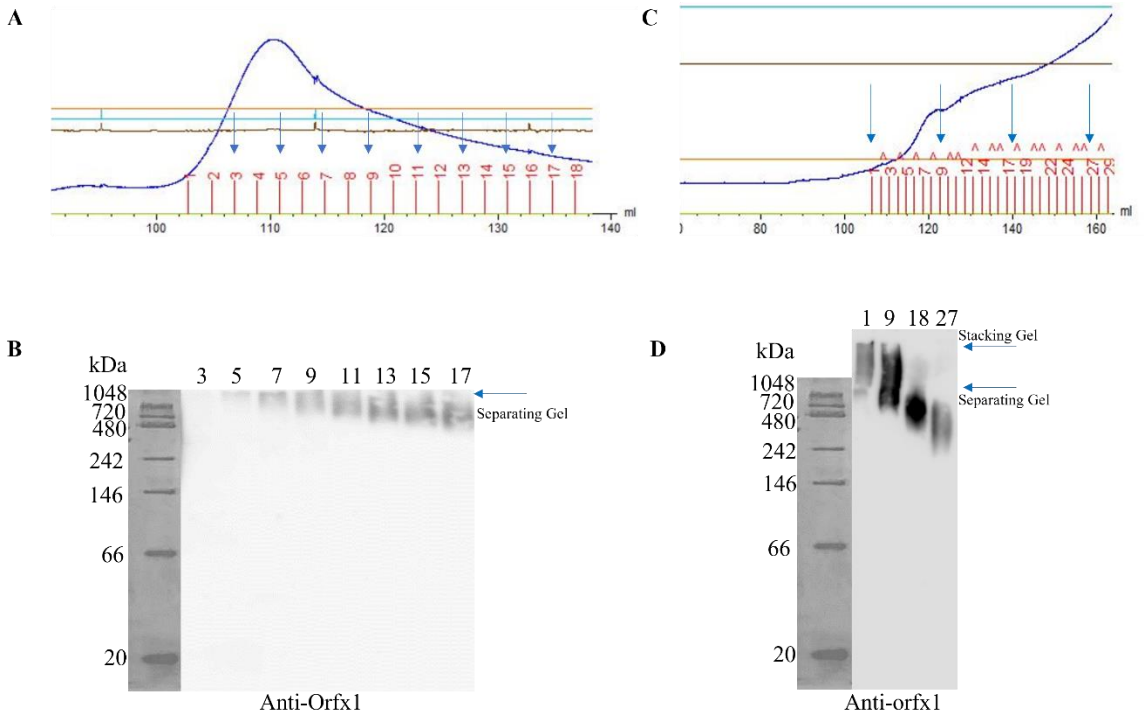

Figure 3-6. Chromatogram and native western of *Pbm* run through size exclusion column.

Figure A and C are two chromatograms when 24h *Pbm* culture was run through a size exclusion column for gel filtration. Figures B and D are the corresponding native western blot membranes with proteins detected using anti-orfX1 antibody, where B relates to A, and D relates to C. The numbers at the top of each blot indicate the fraction loaded from the size exclusion elution fractions; they are noted on the chromatogram with arrows. The volumes of figure B sample 5, and figure D sample 9 were used to determine the size of the complex detected.

Based off the size exclusion chromatogram and the volume at which proteins can be detected using the orf1 antibody two values were calculated. Elution at 111ml resulted in a complex size of 1039.92kDa, while elution at 122ml results in a complex size of 793.05 kDa, which is closer to the size determined from the original native-PAGE, 756.31kDa.

Three samples were sent for mass spectrometry analysis, 19-21, PbmF and PbmG. Sample 19-21 was a gel slice cut from a native-PAGE, PbmF was a 4 times concentrated sample of size exclusion fractions thought to contain the Ptox complex, and PbmG was

the 4 times concentrated sample of size exclusion fractions run through and cut from a native-PAGE. However, when the bands seen in the native protein gel were sent for Mass Spectrometry analysis at the University of California, San Diego, many other proteins were still present, and proteins from both the Ptox complex and the Cry operon complex were present Table 3-4. Further purification was necessary to better elucidate the exact size and structure of only the Ptox complex.

If both the Cry operon proteins and Ptox proteins are present in the complex that was seen in the highest band in the native-PAGE, my analysis is that the complex of 1040 kDa consist of both the Cry operon and the Ptox loci. In this case I predict the stoichiometry is 1 of each Cry operon proteins, 1 Pmp1 and NTNH protein and 3 of each of the OrfX proteins for the larger complex size (1:1:1:1:1:1:3:3:6; Cry16:Cry17:Cbm17.1:Cbm17.2:Pmp1:NTNH:OrfX1:OrfX2:OrfX3). The 793 kDa band is likely a complex of the Ptox complex, and I hypothesize it has a stoichiometry of 1:1:6:3:3, pmp1:NTNH:orfX1:orfX2:orfX3. While band 2, in Figure 3-2 of 273 kDa would be a complex of the Pmp1 and NTNH proteins. Band 1, in Figure 3-2 of 441 kDa could have an even stoichiometry of 1:1:1:1:1, Pmp1:NTNH:OrfX1:Orfx2:Orfx3.

Table 3-4. Analysis of Ptox and Cry complex proteins from samples sent for mass spectrometry.

Sample	Sample Type	Preparation	Number proteins found	Cry16	Cry17	Cbm17.1	Cbm17.2	Pmp1	NTNH	OrfX1	OrfX2	OrfX3	P-47	Mpp
19-21	Gel	SEC fractions	115											X
PbmF	Liquid	SEC 4X concentrated	519	X	X	X	X	X	X		X		X	
PbmG	Gel	SEC 4X concentrated	261	X	X	X	X	X			X			
S10	Gel	Na citrate +SEC	217						X					
S36B	Gel	Na citrate +SEC	160	X		X	X		X		X			
S36T	Gel	Na citrate +SEC	159	X		X	X	X	X		X			
F10L	Liquid	Na citrate +SEC	670	X	X	X	X	X	X		X		X	
P10-18	Liquid	Na citrate + SEC (pooled fractions 10-18)	317	X	X	X	X	X			X			
PmpH	Gel	Na citrate + anion-exchange+ SEC	12											
PmpL	Gel	Na citrate + anion-exchange + SEC	8											

This table shows which proteins of the Cry operon and Ptox complex were found in each of the samples sent for mass spectrometry. This table also indicates whether the sample was sent in gel or liquid form, the preparation procedure for each sample sent, as well as how many proteins were detected total from the sample. Each sample and their preparation are discussed in subsequent sections.

Sodium citrate with size exclusion chromatography

The first technique used to increase purification of the Ptox complex was using acid precipitation figure 3-7 followed by sodium citrate extraction.

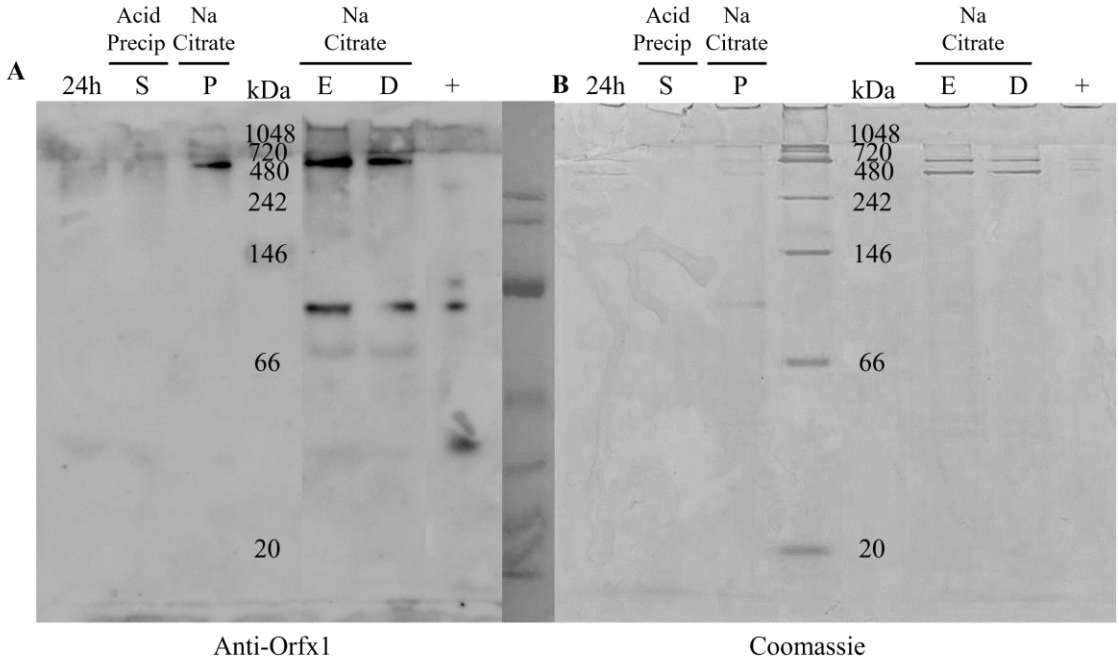

Figure 3-7. Acid precipitation and sodium citrate extraction
This figure shows a western membrane and native-PAGE containing acid precipitation supernatant, S, sodium citrate pellet, P, sodium citrate extract, E, dialyzed sodium citrate extract, D, 24 h *Pbm* culture, and a *Pbm* Ptox complex control, +. The western membrane was probed using an anti-orfX1 antibody.

The resulting extract was determined to be advantageous because more protein was detected in the sodium citrate extract than in the pellet, or earlier samples. The sodium citrate extract was loaded into a size exclusion column and separated via gel filtration. The chromatogram and resulting native-PAGE and western membrane can be seen in Figure 3-8**.** The fractions used in the native-PAGE were chosen based off the size at which the Ptox complex was expected to elute from the size exclusion column.

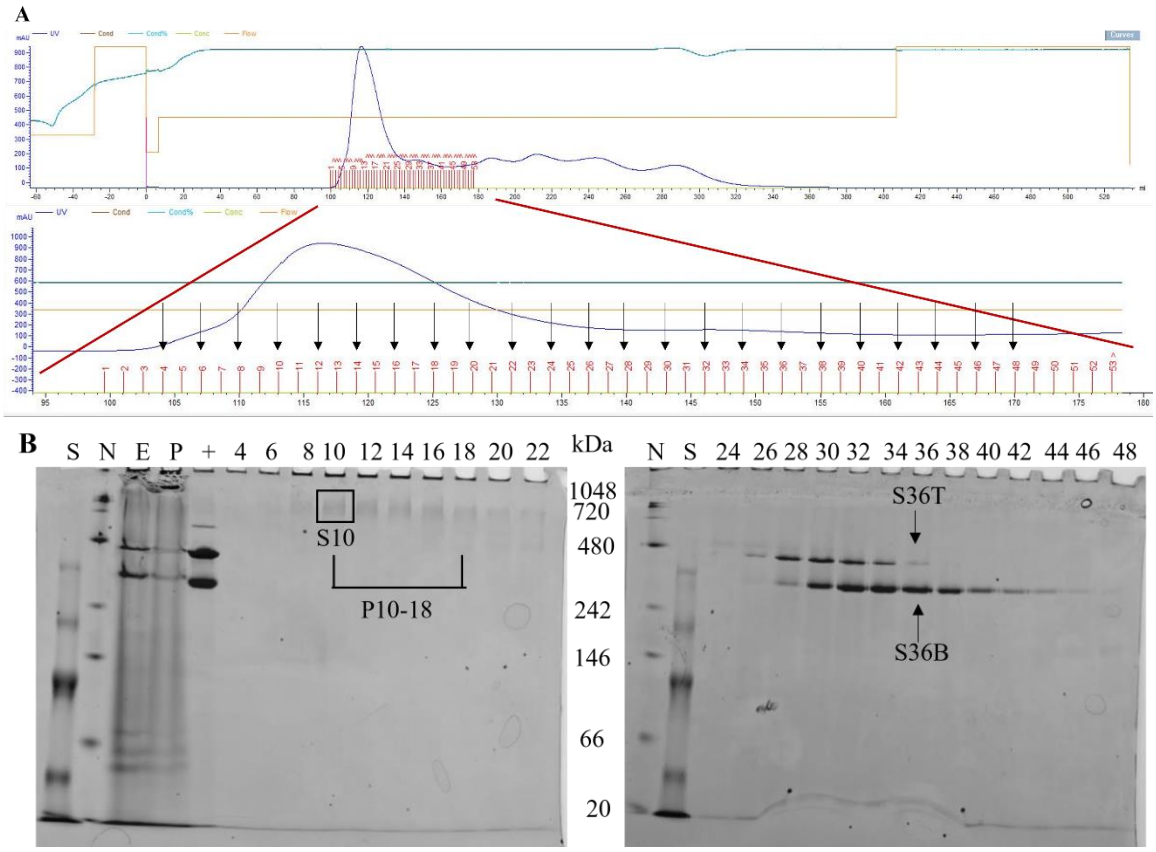

Figure 3-8. Chromatogram and native-PAGE of *Pbm* culture after sodium citrate extraction and gel filtration

This figure shows the chromatogram for size exclusion chromatography after protein extraction with sodium citrate. Figure A has the full chromatogram as well as a zoomed in portion showing the fractions that were loaded, indicated by arrows, into the Native-Page in Figure B. The numbers correspond to the fraction collected during gel filtration. N is the native ladder while S in an SDS ladder used to determine how far the proteins have run during the separation. E is the sodium citrate extract, P is the pellet from the sodium citrate extract, and + was a 4x concentrated size exclusion fraction used as a positive control. The size indicated in kDa corresponds to the bands from the native ladder, the column labeled N.

Five samples were sent using this preparation for mass spectrometry analysis. S10, S36B, S36T, F10L, and P10-18. S10 was fraction 10 from Figure 3-8 run in a native-PAGE and cut, S36B and S36T are fraction 36 from Figure 3-8 run in a native-PAGE, S36B is the bottom band, while S36T is the top band, both were cut from the gel and sent for analysis Figure 3-9. F10L was a liquid sample of fraction 10, because most of the Cry operon and

Ptox complex proteins were not present, a liquid sample was sent for further analysis to verify the proteins were not there. P10-18 is fractions 10 through 18 pooled together and sent for analysis. Analysis of the Mass spectrometry data found from these samples can be seen in Table 3-4. Interestingly Cry17 protein was not detected in either of the fraction 36 samples, but the rest of the Cry operon complex proteins were present. Similarly, Pmp1 was not detected in the bottom band of fraction 36, but it was detected in the top band. Here, however, we still see Cry operon proteins found along with some of the Ptox locus proteins.

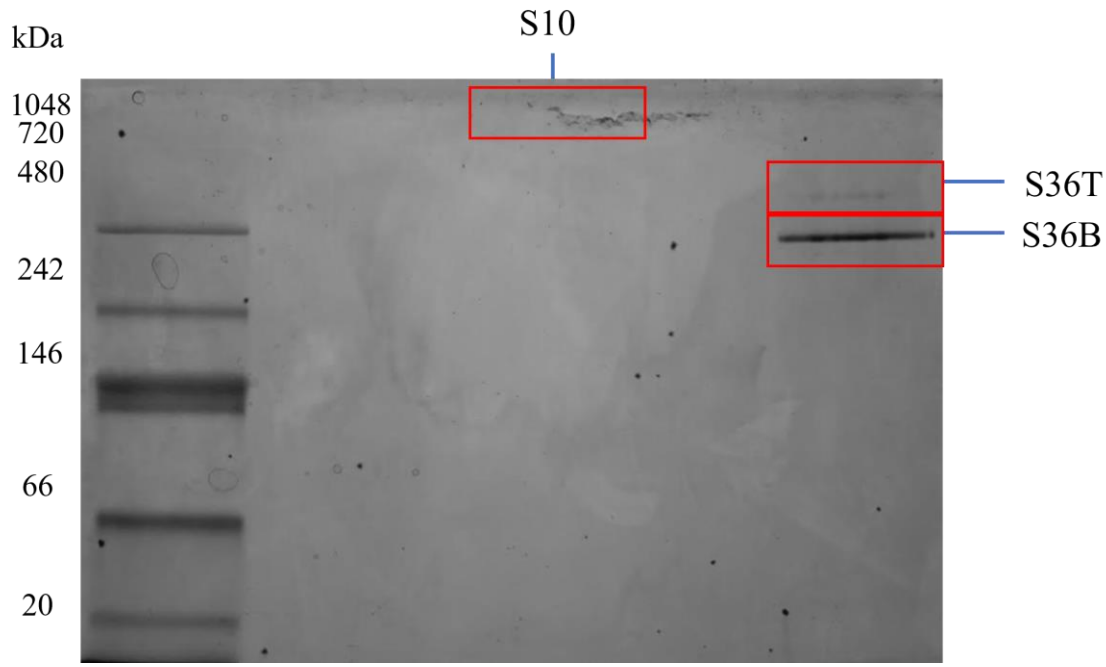

Figure 3-9. Samples sent for mass spectrometry analysis
This figure shows a native-PAGE run with fraction 10 and fraction 36 from Figure 3-8. The boxes indicate where the gel was cut, and the sample name of the cut gel that was sent for mass spectrometry analysis. The kDa values on the left correspond to band sizes of a Native protein ladder, the ladder in the image was used to visualize how far the samples had run during separation.

Sodium citrate extraction with anion-exchange chromatography

An attempt to separate the Cry operon complex proteins and the Ptox complex proteins was made by using anion-exchange chromatography with sodium citrate extraction. Samples were first extracted using acid precipitation as detailed earlier, samples were then dialyzed overnight and loaded onto a MonoQ anion-exchange column the following day. Although it appeared separation occurred, the Cry16 antibody and orfX1 antibody detected the same bands in all samples. The chromatogram, native-PAGE, SDS-PAGE and western membranes can be seen in Figure 3-10**.** These samples were not sent for mass spectrometry analysis.

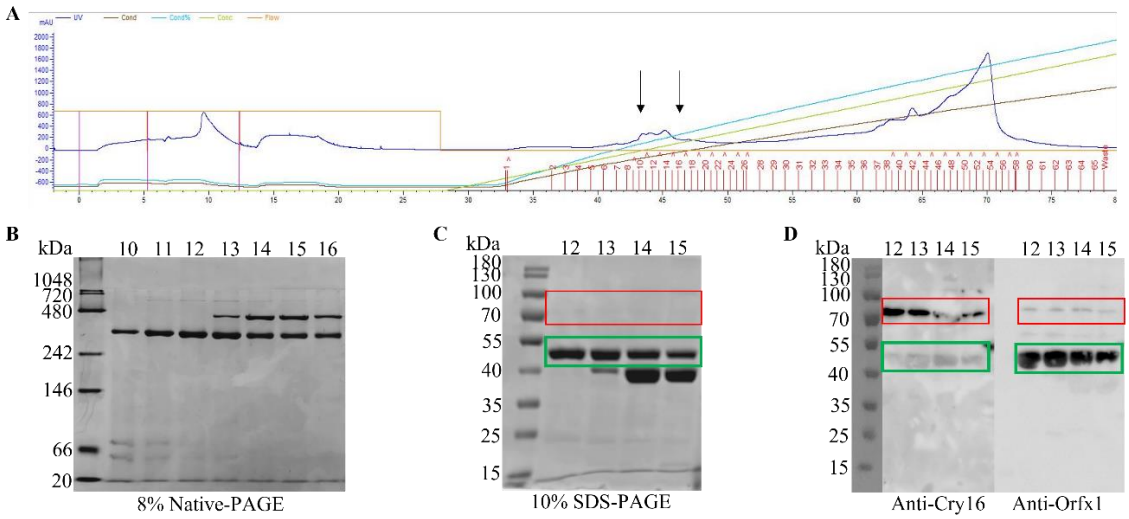

Figure 3-10. Sodium citrate extract with anion-exchange chromatography
This figure shows a sodium citrate extract separated by anion-exchange chromatography. A contains the chromatogram from the separation, the two black arrows indicate the fractions that are loaded into the gels in B, C and D. B is an 8% Native-PAGE stained with Coomassie containing fractions 10 through 16. C is a 10% SDS-PAGE stained with Coomassie containing fractions 12 through 15. D contains two western blot membranes that have fractions 12 through 15, probed with anti-Cry16 antibody and anti-orfX1 antibody respectively.

Ammonium sulfate extraction

The next technique used to purify the Ptox complex was to add a step of ammonium citrate extraction between acid precipitation and gel filtration through size exclusion chromatography (Figure 3-11). Although the ammonium sulfate extraction did appear to help purification, it was deemed not to be advantageous due to the resulting high salt content. This high salt content caused the proteins to stick to the filter during filtration prior to injection for size exclusion chromatography, and the resulting Coomassie stained native-PAGE and western blot membrane showed no bands for any of the loaded size exclusion chromatography fractions. The western blot from the ammonium sulfate extraction indicated Cry16 and thus the Cry operon may still be present as well, and thus this technique was not helpful in separating the Cry operon complex proteins from the Ptox complex proteins.

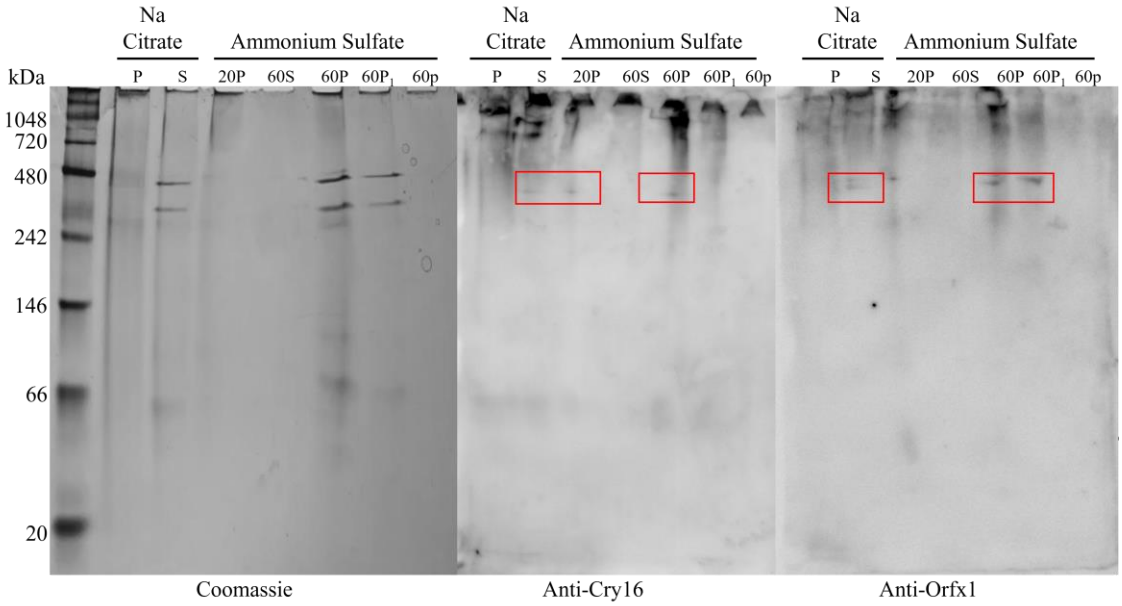

Figure 3-11. Ammonium sulfate extraction samples in Native-PAGE and western blot.
This figure contains a Coomassie stained Native-PAGE, and two western blot membranes probed with anti-Cry16 antibody and anti-orfX1 antibody respectively. Two sodium citrate samples were loaded for reference, a pellet and a supernatant. Five ammonium sulfate samples were loaded, 20% pellet (20P), 60% supernatant (60S), 60% pellet resuspended in phosphate buffer then spun down, supernatant (60P), 60% pellet resuspended in phosphate buffer supernatant filtered ($60P_1$), and the resulting pellet from the resuspension of 60% pellet (60p).

Sodium citrate, anion-exchange, and size exclusion

The next technique utilized sodium citrate extraction, and two chromatography methods. In this case, the goal was to separate the Cry operon proteins and the Ptox locus proteins. For this set of purification methods 2 L of overnight culture were used for sodium citrate extraction, the extract was dialyzed and loaded into an anion-exchange column, the fractions containing the Ptox complex was then loaded into a size exclusion column. Figure 3-12 shows SDS and native-PAGE after each step in the process as well as the resulting chromatogram from both chromatography steps.

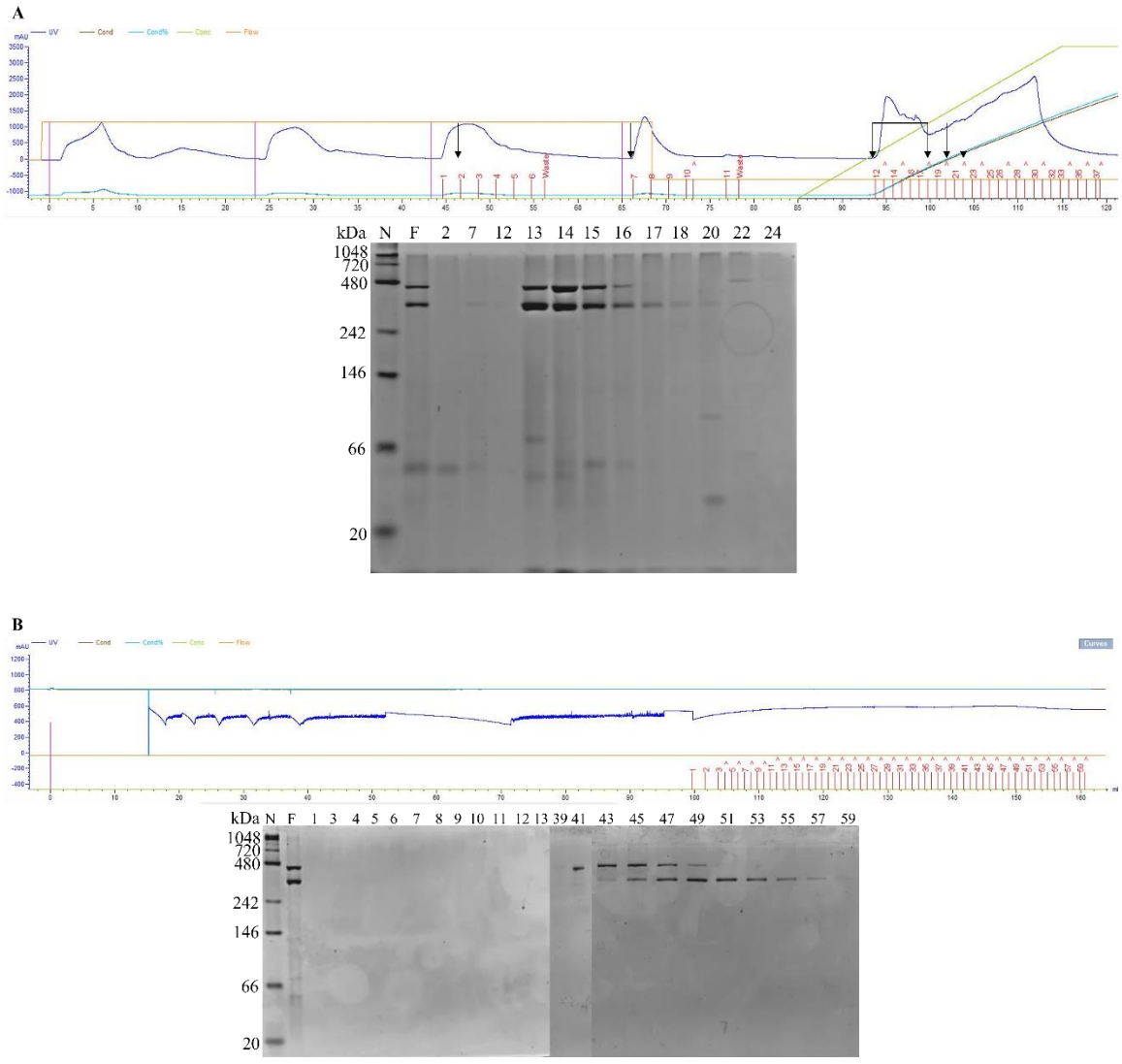

Figure 3-12. Anion-exchange and size exclusion chromatography and native-PAGE. Panel A shows the chromatogram and Native-PAGE associated with anion-exchange chromatography of the sodium citrate extract. The arrows indicate the fractions that were loaded into the gel. Fractions 13 through 16 from anion-exchange chromatography were pooled and filtered then loaded into the size exclusion column. B shows the chromatogram and resulting native-PAGE from that separation.

Fractions 39 through 41 from the size exclusion chromatography were pooled together, fractions 43 through 49 were also pooled together, and fractions 51 through 59 were pooled together; these pooled samples were named A, B and C respectively. These three

pooled samples were run in an SDS-PAGE and a native-PAGE and also detected in a western blot using anti-Cry16 antibody, anti-Pmp1 antibody, and anti-orfX1 antibody (Figure 3-13**).** Bands separated by native-PAGE were cut and sent for mass spectrometry analysis (Table 3-4**)**, these samples were called PmpH and PmpL. Pooled A, B and C were also sent to the Stenmark Group at Stockholm University for crystallization by CryOEM. Although bands can be seen in the native and SDS-Page, no proteins from either the Cry operon complex or the Ptox complex were found in the samples sent, and CryOEM data validated the lack of toxin complex proteins.

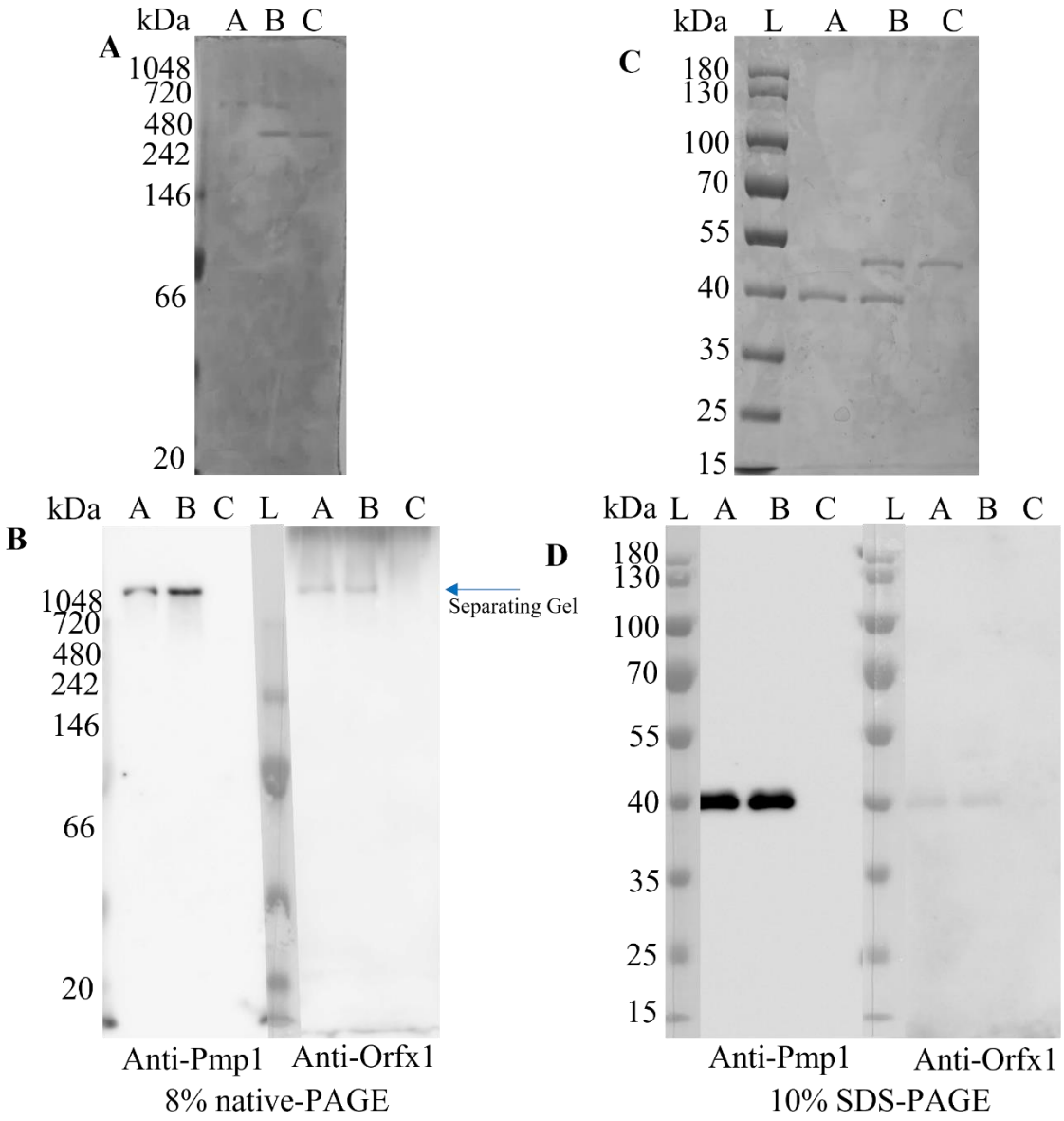

Figure 3-13. Native-PAGE and SDS-PAGE of pooled samples
Figure A is an 8% Native-PAGE stained with Coomassie, proteins from that gel were transferred to a PVDF membrane and probed with Anti-Pmp1 and anti-orfX1 antibodies shown in figure B. Figure C is a 10% SDS-PAGE stained with Coomassie, proteins from that gel were transferred to a PVDF membrane and also probed with Anti-Pmp1 and Anti-orfX1 antibodies. A, B and C labels in the figures refer to the pooled samples discussed in this section. Membranes probed with anti-Cry16 antibody are not shown because no bands were detected.

Mass Spectrometry data

Mass Spectrometry analysis was performed for many samples including gel filtration, sodium citrate extraction followed by gel filtration, and sodium citrate extraction followed by anion-exchange chromatography followed by size exclusion chromatography. Each of these attempted purification processes were sent in either liquid aliquots or separated further by native-PAGE and then sent for mass spectrometry analysis. Table 3-5 contains the proteins involved in both the Cry operon as well as the Ptox locus. This table also contains GO terms, the molecular weight and theoretical pI of the protein, their NCBI protein ID and locus tag, and the entry they can be found under in the Uniprot database.

Table 3-5. Cry operon and Ptox locus proteins

Gene Name	NCBI protein ID	NCBI locus tag/ Uniprot gene name	Uniprot Entry Name	Protein Name	AA	MW (Da)	pI	GO Annotations (uniprot)
Cry16	QEZ70817.1	D4A35_17940	A0A5P3XKC6_PARBF	Pesticidal crystal-like protein Cry16Aa	617	71,398	5.04	extracellular region, signaling receptor binding, toxin activity, cytolysis by symbiont of host cell, sporulation resulting in formation of a cellular spore
Cry17	QEZ70818.1	D4A35_17945	A0A5P3XKB6_PARBF	Pesticidal crystal-like protein Cry17Aa	618	71,651	5.45	extracellular region, signaling receptor binding, toxin activity, cytolysis by symbiont of host cells, sporulation resulting in formation of a cellular spore
Cbm17.1	QEZ70819.1	D4A35_17950	O32337_PARBF	Hemolysin-like protein	153	17,200	5.41	hemolysis by symbiont of host erythrocytes
Cbm17.2	QEZ70820.1	D4A35_17955	O32338_PARBF	Hemolysin-like protein	152	17,463	5.82	hemolysis by symbiont of host erythrocytes
Pmp1	QEZ70852.1	D4A35_18120	A0A5P3XKQ1_PARBF	LlaJI family restriction endonuclease (100%) paraclostridium bifermentans (Clostridium bifermentans)	1260	146,320	5.5	extracellular region, metalloendopeptidase activity, protein transmembrane transporter activity, toxin activity, zinc ion binding, negative regulation of neurotransmitter secretion, proteolysis

NTNH	QEZ70856.1	D4A35_18140	A0A5P3XKL4_PARBF	Peptidase M27	1167	136,455	5.15	extracellular region, metalloendopeptidase activity, zinc ion binding, negative regulation of neurotransmitter secretion, proteolysis
OrfX1	QEZ70855.1	D4A35_18135	A0A5P3XKM0_PARBF	Toxin	142	16,839	9.12	
OrfX2	QEZ70854.1	D4A35_18130	A0A5P3XKJ3_PARBF	DUF3289 family protein	740	84,007	5.05	
OrfX3	QEZ70853.1	D4A35_18125	A0A5P3XKL3_PARBF	Toxin	491	55,007	4.63	Integral component of membrane, Transmembrane
p-47	QEZ70857.1	D4A35_18145	A0A5P3XKG5_PARBF	P-47	426	48,091	5.24	integral component of membrane
MPP	QEZ70851.1	D4A35_18115	A0A5P3XKH7_PARBF	Metallophos domain-containing protein	450	51,489	6.27	Hydrolase activity, carbohydrate metabolic process

Listing of proteins in the Cry operon and the Ptox locus and associated NCBI protein ID, locus tag, Uniprot entry name, protein name, number of amino acids, size, theoretical pI, and GO terms.

The Mass spectrometry data that was obtained can be found in Table 3-4**.** This table notes which of the Cry operon or Ptox locus proteins are present in the samples that were sent for analysis. This table also contains the preparation of each sample, the number of proteins found in each analysis. It is interesting that two of the liquid samples sent for Mass Spectrometry still included the p-47 protein that is located near the pmp operon. For some samples, all Cry operon proteins were present, while in others only Cry16, Cbm17.1 and Cbm17.2 were present. None of the data from any of the samples included data for either orfX1 or orfX3, and NTNH and Pmp1 were only present in some samples.

Discussion

Although purification of the entire Ptox progenitor complex was not achieved, valuable information was gathered. We saw Ptox does form a complex and can be seen in the pellet and supernatant after 24h of growth. We also saw detection of proteins at various sizes using Ptox complex specific proteins. This allowed for an estimate of the size of the Ptox complex. The size of the complex was estimated through two different means, use of proteins standards in a Native-PAGE, and through size exclusion chromatography. The estimated sized of the Ptox complex was 756.31 kDa for the first method, and 793.05 kDa for the size exclusion method. The complex with the calculated size of 1039.92 kDa had both Ptox complex proteins and Cry operon complex proteins in it. The values of approximately 750 kDa to 800 kDa are consistent with the size of botulinum neurotoxin progenitor complexes. Some botulinum neurotoxin progenitor complexes can be up to about 900 kDa, while others are about 300 kDa (Gu and Jin, 2013). These progenitor complexes include the botulinum neurotoxin, non-toxic non-

hemagglutinin (NTNH), and either three hemagglutinin proteins (Ha) or three orfX proteins. There have been three different size classifications of progenitor toxin complexes; they are M-PTC, L-PTC, and LL-PTC which are approximately 300 kDa, 500kDa and 900kDa respectively (Gu and Jin, 2013). The M complex is said to be a minimally functional complex and is only the association of the neurotoxin and NTNH, while the L-PTC has at least three neurotoxin associated proteins (Eswaramoorthy et al., 2015). The LL-PTC, also called the 19S or extra-large, is thought to be a dimer of the L complex with an additional HA protein cross-linking two L-PTC (Inoue et al., 1996). Two proposed ratios for the 16S progenitor toxin complex are 1:1:6:3:3 or 1:1:4:4:2 of neurotoxin:NTNH:Ha-33:Ha-17:Ha-70 (Fujinaga, 2010; Hasegawa et al., 2007; Mutoh et al., 2003). These ratios are similar to the values found when speculating about the stoichiometry of proteins in the Ptox complex.

Botulinum neurotoxin progenitor complexes have been purified through a variety of means. One method included ammonium sulfate precipitation and purification using cation-exchange chromatography. The resulting samples were then purified further through gel filtration (DasGupta and Sathyamoorthy, 1984; Mutoh et al., 2003). Another method also included sucrose density gradient centrifugation (Inoue et al., 1996; Sugii and Sakaguchi, 1975). Although cation-exchange chromatography was performed, more attempts may have been beneficial in helping to purify the Ptox complex, along with sucrose density gradient centrifugation.

Considering the mass spectrometry data, it appears P-47 is not part of the protein complex like we have previously thought as it is coded in a reverse direction (Contreras

et al., 2019). This conclusion stems from P-47 being present only in liquid samples, not the samples that were separated in a native-PAGE prior to analysis. It is interesting that orfX1 and orfX3 were never detected in the samples sent. This may be a function of the conditions used during analysis, or poor fragmentation (Kim et al., 2016). Nonspecific and missed cleavages or lack of recognition of peptide sequences may have also caused a lack of identification of orfX1 or orfX3 (Lubec and Afjehi-Sadat, 2007). These issues may have also led to the lack of identification of Cry17 when the rest of the Cry operon proteins were present in the samples.

It was interesting that the Cry operon complex proteins were present with the Ptox complex proteins when analyzed using mass spectrometry. One theory could be that the two toxin complexes work together, or at least associate together. This theory stems from both toxin loci being located on the same bacterial plasmid. Similar to the toxins found in *Bti* that synergize together to increase toxicity (Adang et al., 2014; Silva Filha et al., 2014). Another theory is the isoelectric point of the complexes is too close together to be able to separate using anion-exchange chromatography. Anion-exchange chromatography would cause the two complexes to congregate in the same fractions because they would be eluted at around the same salt concentration (Fritz, 1987).

Future directions for this project should include other purification methods like sucrose density gradient centrifugation and cation-exchange chromatography. Multiple methods must be used to purify the complex from its native bacteria. Once purified the crystal structure can be determined and a more exact complex size can be calculated.

References

Adang, M.J., Crickmore, N., Jurat-Fuentes, J.L., 2014. Chapter Two - Diversity of Bacillus thuringiensis Crystal Toxins and Mechanism of Action, in: Dhadialla, T.S., Gill, S.S. (Eds.), Advances in Insect Physiology, Insect Midgut and Insecticidal Proteins. Academic Press, pp. 39–87. https://doi.org/10.1016/B978-0-12-800197-4.00002-6

Becker, N., 1997. Microbial control of mosquitoes: Management of the upper rhine mosquito population as a model programme. Parasitology Today 13, 485–487. https://doi.org/10.1016/S0169-4758(97)01154-X

Becker, N., Petrić, D., Zgomba, M., Boase, C., Madon, M., Dahl, C., Kaiser, A., 2010. Mosquitoes and Their Control, 2nd ed. Springer-Verlag, Heidelberg, Germany.

CDC, 2020. Bti \ CDC [WWW Document]. Centers for Disease Control and Prevention. URL https://www.cdc.gov/mosquitoes/mosquito-control/community/bti.html (accessed 6.22.22).

Contreras, E., Masuyer, G., Qureshi, N., Chawla, S., Dhillon, H.S., Lee, H.L., Chen, J., Stenmark, P., Gill, S.S., 2019. A neurotoxin that specifically targets Anopheles mosquitoes. Nature Communications 10, 2869. https://doi.org/10.1038/s41467-019-10732-w

DasGupta, B.R., Sathyamoorthy, V., 1984. Purification and amino acid composition of type A botulinum neurotoxin. Toxicon 22, 415–424. https://doi.org/10.1016/0041-0101(84)90085-0

de Barjac, H., Sebald, M., Charles, J.F., Cheong, W.H., Lee, H.L., 1990. [Clostridium bifermentans serovar malaysia, a new anaerobic bacterium pathogen to mosquito and blackfly larvae]. C R Acad Sci III 310, 383–387.

Eswaramoorthy, S., Sun, J., Li, H., Singh, B.R., Swaminathan, S., 2015. Molecular Assembly of Clostridium botulinum progenitor M complex of type E. Sci Rep 5, 17795. https://doi.org/10.1038/srep17795

Fillinger, U., Kannady, K., William, G., Vanek, M.J., Dongus, S., Nyika, D., Geissbühler, Y., Chaki, P.P., Govella, N.J., Mathenge, E.M., Singer, B.H., Mshinda, H., Lindsay, S.W., Tanner, M., Mtasiwa, D., de Castro, M.C., Killeen, G.F., 2008. A toolbox for operational mosquito larval control: preliminary results and early lessons from the Urban Malaria Control Programme in Dar es Salaam, Tanzania. Malaria Journal 7, 20. https://doi.org/10.1186/1475-2875-7-20

Fritz, J.S., 1987. Ion Chromatography. Anal. Chem. 59, 335A-344A. https://doi.org/10.1021/ac00131a737

Fujinaga, Y., 2010. Interaction of botulinum toxin with the epithelial barrier. J Biomed Biotechnol 2010, 974943. https://doi.org/10.1155/2010/974943

Gu, S., Jin, R., 2013. Assembly and Function of the Botulinum Neurotoxin Progenitor Complex. Curr Top Microbiol Immunol 364, 10.1007/978-3-642-33570–9_2. https://doi.org/10.1007/978-3-642-33570-9_2

Hasegawa, K., Watanabe, T., Suzuki, T., Yamano, A., Oikawa, T., Sato, Y., Kouguchi, H., Yoneyama, T., Niwa, K., Ikeda, T., Ohyama, T., 2007. A novel subunit structure of Clostridium botulinum serotype D toxin complex with three extended arms. J Biol Chem 282, 24777–24783. https://doi.org/10.1074/jbc.M703446200

Inoue, K., Fujinaga, Y., Watanabe, T., Ohyama, T., Takeshi, K., Moriishi, K., Nakajima, H., Inoue, K., Oguma, K., 1996. Molecular composition of Clostridium botulinum type A progenitor toxins. Infection and Immunity 64, 1589–1594. https://doi.org/10.1128/iai.64.5.1589-1594.1996

Kim, M.-S., Zhong, J., Pandey, A., 2016. Common errors in mass spectrometry-based analysis of post-translational modifications. Proteomics 16, 700–714. https://doi.org/10.1002/pmic.201500355

Lubec, G., Afjehi-Sadat, L., 2007. Limitations and Pitfalls in Protein Identification by Mass Spectrometry. Chem. Rev. 107, 3568–3584. https://doi.org/10.1021/cr068213f

Malaria vector control [WWW Document], n.d. URL https://www.who.int/teams/global-malaria-programme/prevention/vector-control (accessed 11.25.22).

Mutoh, S., Kouguchi, H., Sagane, Y., Suzuki, T., Hasegawa, K., Watanabe, T., Ohyama, T., 2003. Complete subunit structure of the Clostridium botulinum type D toxin complex via intermediate assembly with nontoxic components. Biochemistry 42, 10991–10997. https://doi.org/10.1021/bi034996c

Oliveira, S., Caleffe, R., Conte, H., 2017. Chemical control of Aedes aegypti: a review on effects on the environment and human health. Revista Eletrônica em Gestão, Educação e Tecnologia Ambiental - REGET 21, 240–247. https://doi.org/10.5902/2236117027692

Qureshi, N., Chawla, S., Likitvivatanavong, S., Lee, H.L., Gill, S.S., 2014. The Cry Toxin Operon of Clostridium bifermentans subsp. malaysia Is Highly Toxic to Aedes Larval Mosquitoes. Appl. Environ. Microbiol. 80, 5689–5697. https://doi.org/10.1128/AEM.01139-14

Silva Filha, M.H.N.L., Berry, C., Regis, L., 2014. Chapter Three - Lysinibacillus sphaericus: Toxins and Mode of Action, Applications for Mosquito Control and Resistance Management, in: Dhadialla, T.S., Gill, S.S. (Eds.), Advances in Insect

Physiology, Insect Midgut and Insecticidal Proteins. Academic Press, pp. 89–176. https://doi.org/10.1016/B978-0-12-800197-4.00003-8

Sugii, S., Sakaguchi, G., 1975. Molecular construction of Clostridium botulinum type A toxins. Infect Immun 12, 1262–1270.

Thiery, I., Hamon, S., Gaven, B., De Barjac, H., 1992. Host range of Clostridium bifermentans serovar. malaysia, a mosquitocidal anaerobic bacterium. J Am Mosq Control Assoc 8, 272–277.

World Health Organization, 2019. World malaria report 2019 [WWW Document]. URL https://www.who.int/publications/i/item/9789241565721 (accessed 3.15.21).

Chapter 4.

Genomic Editing of *Bacillus thuringiensis* subsp. *israelensis* to Increase Toxicity to *Anopheles* Mosquitoes

Abstract

Some species of mosquitoes are responsible for hundreds of thousands of deaths annually. Mosquitoes can serve as vectors for viruses that cause diseases like West Nile, dengue and yellow fevers among others. Currently a bacteria called *Bacillus thuringiensis israelensis* (*Bti*) is used domestically, commercially and in agricultural areas to fight these mosquito populations. *Bti* has been effective for many years against two of the three major mosquito vectors, *Aedes* and *Culex* but not *Anopheles*, due to the cocktail of toxins it produces. However, with longer exposure to the same toxins, these mosquito populations may develop resistance. Although no resistance has been seen against the full cocktail of toxins, some has been seen against single toxins in laboratory settings. Cross-resistance has also been seen between some toxins; thus, it would be advantageous to find or create new ways to combat mosquito populations. This chapter outlines a possible method to increase toxicity of *Bti* to *Anopheles* populations by using CRISPR/Cas9 technology to edit the genome of *Bti*.

Introduction

Three mosquito species are responsible for hundreds of thousands of deaths a year; they are *Aedes aegypti, Anopheles stephensi,* and *Culex quinquefaciatus.* These three mosquito species serve as vectors for dengue fever, malaria, and West Nice virus respectively among others ("Mosquito factsheets," n.d.). Work has been done to try to control these mosquito species in the hopes that it will prevent infection in the most effected parts of the world. The areas where these diseases are most prevalent do not always have the means to run large chemical pesticide sweeps, or government run programs to combat the issue (Benelli et al., 2016; Benelli and Beier, 2017; Busvine, 1978).

Bacillus thuringiensis serovar *israelensis* (*Bti*) is one such method that is used to control mosquito populations. This bacterial strain contains a plasmid that encodes at least four cry toxins; Cry4Ba, cry4Aa, Cry11Aa, and Cry10Aa, and two cyt toxins; cyt1Aa, and cyt2Ba (Ben-Dov, 2014). This cocktail of toxins is most effective against *Aedes* and *Culex* mosquito larvae but not *Anopheles* mosquito larvae. This bacterial strain has been used commercially and is sold as small pellets that can be left in standing bodies of water. The first stage of life for a mosquito is aquatic, and these cry and cyt toxins are toxic when ingested by mosquito larvae. The use of *Bti* is advantageous in that it is not toxic to humans, animals, honeybees, or the environment (Center for Disease Control, 2017). No resistance has been seen against the full cocktail of toxins however some resistance has been seen in the laboratory against single toxins (Georghiou and Wirth, 1997; Tetreau et al., 2013). *Bti* is registered and approved by the EPA for use in

residential, commercial and agricultural settings (Center for Disease Control, 2017; Silva-Filha et al., 2021)

Bacillus thuringiensis subsp. *jegathesan* (*Btj*) is another strain that contains mosquitocidal toxins. *Btj* was isolated from Malaysia and shows toxicity to *Aedes aegypti, Culex pipiens*, and *Anopheles stephensi* (Wirth et al., 1998). This bacteria produces a combination of eight toxin proteins including Cry11Ba, Cry25Aa, Cry24Aa, Cry19Aa, Cry30Ca, Cry60Ba, Cry60Aa, and Cyt2Bb (Silva-Filha et al., 2021; Wirth et al., 2004). Cry11B shows 58% identity to Cry11A which is produced in *Bti* and shows similar toxicity to parasporal crystals produced by *Btj* (Wirth et al., 1998). A current problem seen amongst cry toxins is cross resistance, which ultimately could lead to resistance against current control methods. Cross resistance has been seen between Cry4 and Cry11, both produced by *Bti* (Wirth and Georghiou, 1997). Cross resistance has also been seen among lepidoptera targeting Cry proteins (Gould et al., 1992; McGaughey and Johnson, 1994; Tabashnik et al., 1996).

Cry11B produces more toxin activity against *Ae. aegypti* and *An. stephensi* than native crystals of *Btj* or Cry11A alone (Delécluse et al., 1995). Although LC50 values vary in the hands of different research groups, no one can dispute that *Bti,* and its individual toxins are active against *Ae. aegypti* and *Cx. quinquefaciatus* (Otieno-Ayayo et al., 2008).

Gene editing has become a useful tool within the molecular biology community. A new technique involving clustered regularly interspaced short palindromic repeats (CRISPR) has been used to edit the genome of many organisms. CRISPR was originally

found in *Escherichia coli* in 1987 by Ishino et al. CRISPR- Cas systems have functioned as part of the immune system of some archaea and bacteria. Immunity produced through CRISPR-Cas systems involves integrating sequences of foreign DNA, which can include invasive genetic elements like viral DNA or plasmids, into a CRISPR locus. This integration of foreign DNA allows the cell to recognize, remember, and destroy the invasive element if seen again. The type-II-system of CRISPR/Cas9 has been utilized as a gene editing tool. The Cas9 protein is guided by a small RNA, which is made up of two parts, a CRISPR RNA (crRNA) and a trans-activating CRISPR RNA (tracrRNA), that can be linked together to make a single guide RNA (gRNA). The Cas protein also recognizes a Protospacer Adjacent motif (PAM) (Tetsch, 2017). The PAM region involves any nucleotide followed by two G nucleotides (Shah et al., 2013). This PAM sequence is essential for causing the double strand break made by the Cas9 protein. When the Cas9 protein finds a PAM sequence, the crRNA pairs with the unwound target DNA. The base pairing for the crRNA and the target DNA causes a conformational change in the Cas9 protein which allows the nuclease domain to contact the target DNA resulting in a double strand break. Cells in which CRISPR/Cas9 are being used will then repair the cleaved DNA through two repair methods; homologous recombination or nonhomologous end joining (Ran et al., 2013). Depending on the goal of the gene editing, a plasmid can be provided to allow the cell to go through homologous recombination in which a new sequence of DNA can be put into the original sequence. Nonhomologous end joining results in the disruption of sequence whether through frameshift of a small

deletion within the DNA, which can cause inactivity of a gene (Lieber, 2010; Ran et al., 2013; Toymentseva and Altenbuchner, 2019).

Toymentseva and Altenbuchner (2019) engineered a plasmid, pJoe9282.1, with the ability to perform CRISPR/Cas9 editing of *Bacillus subtilis*. This plasmid encodes a Cas9 gene under a xylose inducible promoter. The plasmid also contains a cloning site for a homologous region and another cloning site for insertion of a guide RNA with a semi-synthetic promoter. To knock in a new gene using CRISPR/Cas9 a homologous region must be provided for us as a template during the repair mechanism. (Toymentseva and Altenbuchner, 2019).

This chapter looks at using CRISPR/Cas9 technology to increase the toxicity of *Bti* against *Anopheles* mosquitoes by editing the toxin containing plasmid, pBtoxis. The goal of this project was to edit pBtoxis to also include Cry11B, a toxin produced by *Btj*. Two proof of concept experiments will be discussed in this chapter along with the tools created for further screening and future directions.

Materials and Methods

gRNA (synthesis and ligation)

Guide RNA (gRNA) was designed using CRISPOR (http://crispor.tefor.net/) to target the sequence 1.1kb upstream of the *cry10A* gene in the pBtoxis plasmid (Figure 4-1). A forward and reverse primer (Table 4-1) were ordered from IDT and were annealed to integrate into the pJoe9282.1 plasmid (Bacillus Genetic Stock Center in Columbus, OH; Figure 4-2).

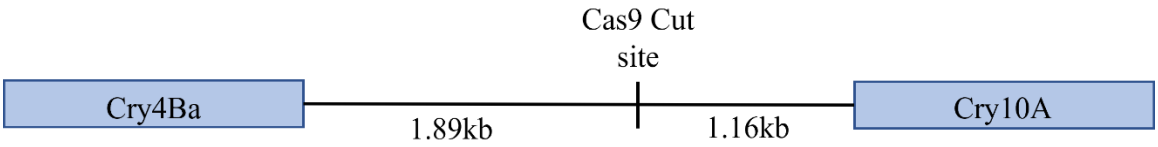

Figure 4-1. Schematic of Cas9 cut site.
This figure shows the gRNA target region in the pBtoxis plasmid. The gRNA targets a region 1.89kb downstream of *cry4Ba*, and 1.16kb upstream of *cry10A*.

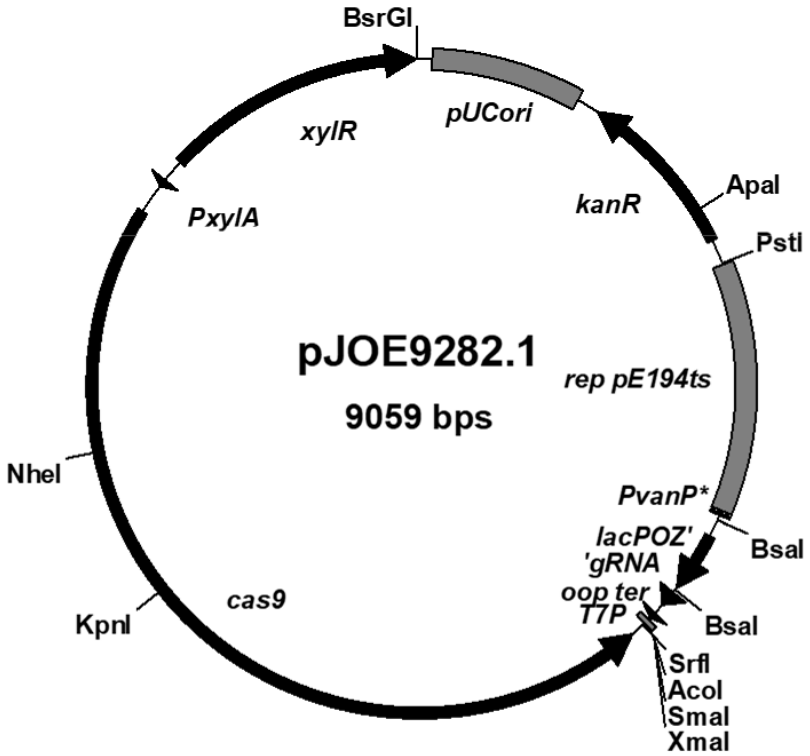

Figure 4-2. pJoe9282.1 plasmid map.
This plasmid was used as a template for homologous recombination and contains the Cas9 gene. PxylA – xylose inducible promoter for Cas9, PvanP* - semisynthetic promoter with high identity to the improved PvanABK promoter of *Corynebacterium glutamicum*, BASI sites – used to clone in gRNA, SfiI sites (near XmaI) – used to clone homologous cassette.

Table 4-1. Primers used to create gRNA sequence

Primer	Direction	Sequence
D52	Forward	CGGTACGCGAGACCTCAGAATGCACAAAGTA AAG CTG**GGG TCGGTCTCACGG**
D53	Reverse	CCGTGAGACCGACCCCAGCTTTACTTTGTGCATTCTGA GGTCTCGCGTACCG

Forward and reverse primers that were self-annealed and inserted into the pJoe9282.1 plasmid for use as a gRNA template. Both contain cut sites for BsaI for ease of cloning into the plasmid The underlined area indicates the area that will anneal together.

Four µl of each Primer (10mM) and 42µl of annealing buffer (10mM Tris pH 7.5-8, 50mM NaCl, 1mM EDTA) were heated to 95°C for 3 min, then incubated at room temperature for 45 min. The annealed primers were then digested with BsaI at 37°C for 1 h. Concurrently, pJoe9282.1 was cut with BsaI for 1 h at 37°C, then treated with antarctic phosphatase for 30 min at 37°C which was then inactivated for 2 mins at 80°C. Both digests were run in a 1% agarose gel to verify size. Correct sized bands (69 bps for the gRNA and 8.78kb for the plasmid) were excised from the gel and gel purified using the Zymoclean™ Gel DNA recovery kit (Irvine, CA). The digested annealed DNA primer and pJoe9282.1 plasmid were ligated using T4 Ligase (Thermo Fisher) over night at 16°C. The ligated DNA was transformed into Top10 *E. coli* cells and grown on LB plates supplemented with Kanamycin. A Colony PCR was performed to check for the insert. Plasmid was purified from positive colonies and digested with BseYI and BtsI-v2 to confirm gRNA insert. Insertion was further verified with DNA sequencing at EtonBio.

Homologous recombination cassette

The homologous region was synthesized in two parts and then was cloned into the pJoe9282.1 plasmid. The first contains the left and right homologous arms, approximately 1Kb upstream and downstream of the designated gRNA/Cas9 cut site in the pBtoxis plasmid. The left and right arms were synthesized in a construct containing

the LacZ alpha subunit in between the 2 arms. LacZ was chosen to utilize blue/white screening for selection of colonies with new inserts in a SK+ plasmid (GenScript). To allow for cloning into pJoe9282.1 plasmid, 2 SfiI cut sites flank the left and right arms, one upstream of the left arm and one downstream of the right arm. To further enable cloning of eGFP, LacZ and Cry11B between the homologous arms, SacI and BamHI cut sites downstream of the left arm, and a HindIII cut site upstream of the right arm were introduced, pLaRa (Figure 4-3A).

The second construct was synthesized in pUC57 to contain 1.1kb of the Cry11A promoter region followed by the eGFP gene. The construct also contained a SacI and HindIII cut site downstream of the eGFP, pInsert (Figure 4-3B) to facilitate ligation between the left and right arm in pLaRA plasmid. The Cry11A promoter and eGFP were cloned into pLARA plasmid and named pCombined (Figure 4-3C). pCombined was also used as the backbone to create the homologous cassettes for LacZ and Cry11B.

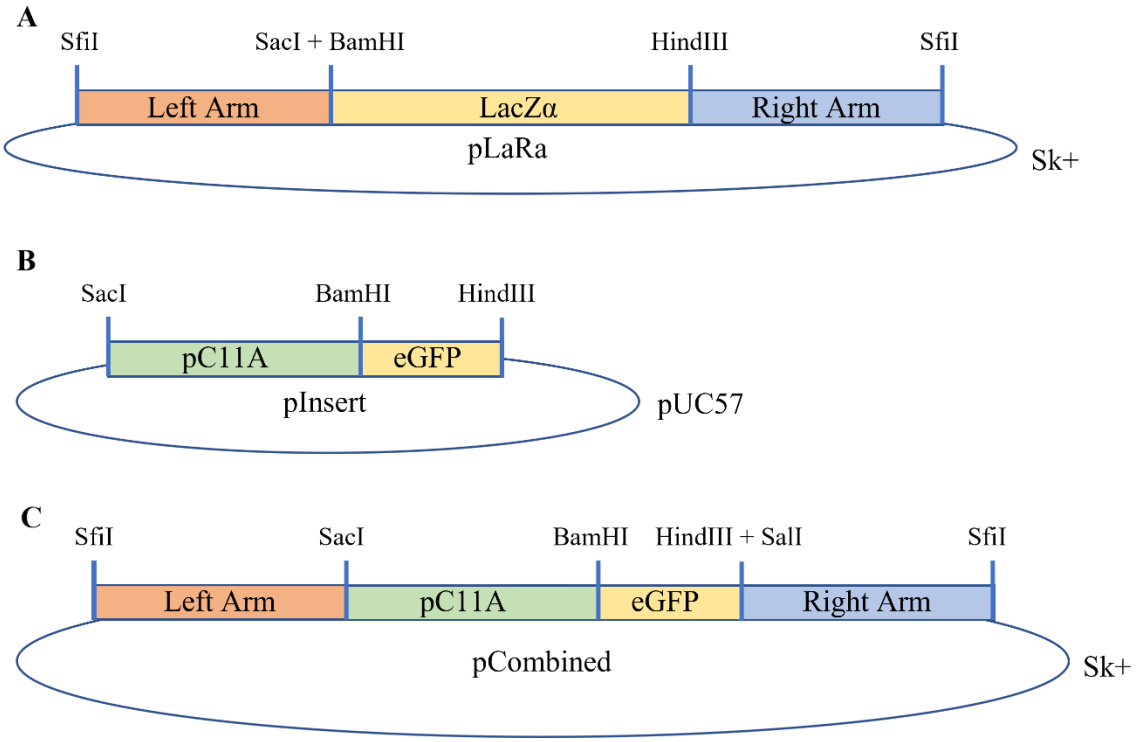

Figure 4-3. Synthesized and cloned plasmids for homologous cassette assembly
A. Shows a schematic of a SK+ plasmid synthesized with left and right arms that are homologous to the regions upstream and downstream of the guideRNA cut site in the pBtoxis plasmid and a LacZα subunit to be utilized for blue/white screening. B. Shows a schematic of a pUC57 plasmid synthesized with the Cry11A promoter and eGFP. Both plasmids contain restriction sites to allow for easy replacement of construct components. C. shows a schematic of sk+ with the full homologous cassette combined and is called pCombined. This plasmid was used as the backbone to build each homologous cassette that was eventually cloned into the pJoe9282.1 plasmid.

LacZ was cloned from the p8op LacZ plasmid, and Cry11B from pHT315-Cry11B using primers described in Table 4-2 and ligated into Topo Ta-2.1 vector. Each gene was digested to verify size and sequenced by EtonBio. SacI and BamHI upstream of the gene, and a HindIII cut site downstream the gene were used to clone the gene into the pCombined plasmid.

Table 4-2. Primers for LacZ and Cry11B isolation

Primer	Direction	Sequence	Use
D36	Forward	ggtaccggatccATGACCATGATTAC GGATTCACTGG	LacZ isolation with BamHI upstream
D37	Reverse	aagcttTTATTTTTGACACCAGACC AACTGG	LacZ isolation with HindIII downstream
D44	Forward	GGATCCTTAATTATGAAAAGAT TTCGTTTATATTAGTAAATTGTT TAAAGAAGAGGGG	Cry11B isolation with BamHI upstream
D45	Reverse	AAGCTTTTGTATGCCATCAAGA AAAAATATTATGGTTGAAAAAC TATTGAC	Cry11B isolation with HindIII downstream

This table contains the forward and reverse primers used to isolate LacZ and Cry11B from their respective plasmids as indicated. These primers were used in a PCR, the resulting PCR fragment contains a BamHI cut site upstream of the gene and a HindIII cut site downstream of the gene and can be used to clone each gene into the previously synthesized pUC57 plasmid.

Three final homologous cassettes were created containing either eGPF, LacZ, or Cry11B driven by cry11A promoter and bracketed by 1Kb homologous regions upstream and downstream of the Cas9/gRNA cut site in the pBtoxis plasmid (Figure 4-4). These cassettes were cloned into pJoe9282.1 using SfiI restriction sites resulting in plasmids pJoe-eGFP, pJoe-LacZ, and pJoe-Cry11B respectively.

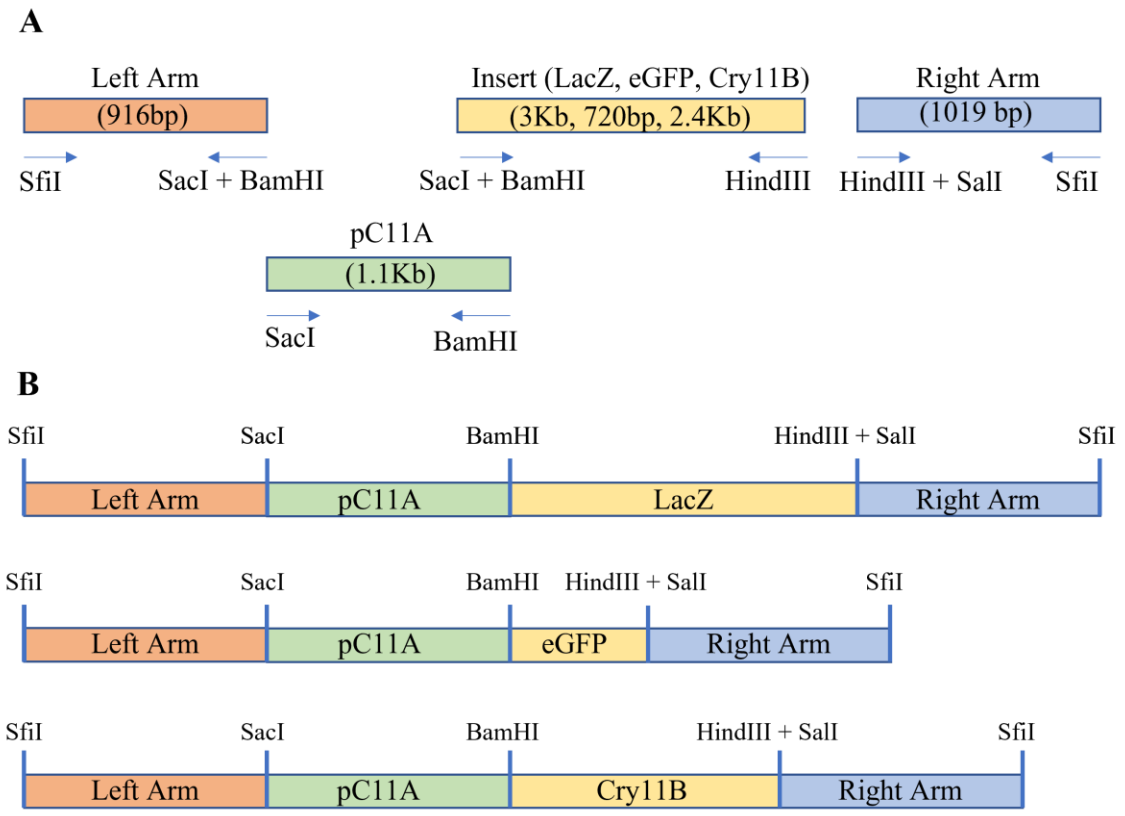

Figure 4-4. Schematic of each homologous recombination cassette.
A. Indicates the size and restriction sites included in each fragment. B. Shows a schematic of each of the homologous cassettes with the restriction sites indicated. These cassettes were cloned into pJoe9282.1 using SfiI sites to make pJoe-LacZ, pJoe-eGFP, and pJoe-Cry11B respectively. Each construct contains a 916bp left arm, a 1.0Kb right arm, the Cry11A promoter and the gene that is being inserted into the pBtoxis plasmid.

E. coli transformation

All constructs were transformed into Top10 (Invitrogen) cells first. The cells and DNA were incubated together on ice for 30 min. The cells were then shocked at 42°C for 1 min. Following heat shock, 250 µl of SOC (Super Optimal Broth) were added to the cells and they were incubated at 37°C shaking at 250rpm for 1 hr. Last, the cells were plated on LB plates supplemented with kanamycin.

_Bt_ (4Q7) and _Bti_ (4Q5) cell production

A single 4Q7 or 4Q5 colony was inoculated in 10mL of BHIG (Brain Heart Infusion + 0.5% glycerol) in a 250mL flask. The cells were incubated at 30°C overnight with moderate shaking. Then 5ml of overnight culture was diluted into 95ml of BHIG in a 1L flask. The dilutions were incubated for 1 h with vigorous shaking at 30°C. The cells were pelleted by centrifugation (17,000 g, 10 min, 4°C), in 2 separate 50mL falcon tubes. Ice cold EB (0.625M sucrose, 1mM $MgCl_2$) was used to resuspend the pellet and fill the falcon tube to 50ml. The centrifugation step was repeated, and the pellet was resuspended in 5ml of ice-cold EB again. Once resuspended 0.8ml aliquots of cells were stored at -80°C until use.

_Bt_ transformation

Prepared 4Q7 and 4Q5 cells were thawed on ice and incubated with DNA for 10 min. After transferring the cells to a cuvette, a single pulse at 2.5kV, 25μF, 1000 Ω was applied with the Bio-Rad Gene Pulser™ coupled with the Bio-Rad Pulse Controller and Bio-Rad Capacitance Extender. The cells were then diluted in 1.6ml of BHIG (Brain Heart Infusion media with 0.5% glycerol autoclaved) and then left to incubate for 2 h at 30°C with moderate shaking. The cells were then plated on nutrient agar or LB agar plates with the necessary antibiotic and incubated overnight at 30°C.

Cas9 expression and verification

Two ml of LB were inoculated with 4Q5 colonies containing an empty pJoe9282.1 plasmid and left overnight shaking at 30°C. Overnight culture was diluted 1:20 in LB broth and left shaking at 30°C. At OD_{600} of .3 the culture was induced with

either .2% or 1% xylose. Samples of uninduced culture as well as aliquots each hour after induction up to 6 h was saved for SDS page and western blot analysis.

SDS-PAGE

A 10% SDS-PAGE was prepared and 30µl of sample was loaded into each well. The gel was run at 90V until the loading dye reached the end of the gel. The proteins were transferred to a PVDF membrane by western blot run overnight at 21V at 4°C.

Western blot and protein detection

After transfer of proteins to the PVDF membrane, each membrane was blocked with 5% skim milk in PBST (1X Phosphate-buffered saline, 1% Tween-20) for 1 h at room temperature. The membrane was washed with water and PBST and then incubated with primary antibody (1:2000) in 1% skim milk in PBST for 2 h at room temperature. Anti-Cas9 (Genscript) and anti-eGFP (Thermo Fisher Scientific) were used as primary antibodies. After incubation with primary antibody, the membrane was washed quickly 3 times with water, and then incubated for 5 min shaking with water. Those same steps were repeated using PBST. Next the membrane was incubated with secondary antibody (anti-rabbit, GE Healthcare, at 1:5000 dilution). The membrane was then washed following the same water and PBST protocol and was developed using SuperSignal™ West Dura by Thermo Scientific, which detects horse radish peroxidase through chemiluminescence, using the ImageQuant LAS 4000 mini by GE.

In vitro cleavage assay

PCR was used to isolate DNA fragment templates using E31/E32 and F25/26 primers sets (Table 4-3). The DNA fragments were used as a template for an in vitro

cleavage assay. The cleavage assay reaction mixture contained 1µg of Cas9 protein, 200ng of sgRNA (generated by Genscript), 210ng of PCR purified DNA template and NEBuffer 3.1. The reaction mixture was incubated at 37°C for 1 h and then incubated at 65°C for 10 min to inactivate the Cas9 protein. The reaction mixture was analyzed on an agarose gel.

Table 4-3. PCR fragment primers for in vitro cleavage assay

Primer	Direction	Sequence	Use
E31	Forward	CCGCATCAGGACGGATC	PCR results in 1.93Kb fragment
E32	Reverse	CCATTGGATGGAGCATTG	PCR results in 1.93Kb fragment
F25	Forward	CCGTGCAGGATGATATCAATGG	PCR results in 900bp fragment
F26	Reverse	CTCACAGTTCTTCCGTAGTC	PCR results in 900bp fragment

This table provides the primer sequence used to isolate a fragment of the pBtoxis plasmid DNA. The fragments contain the cut site for Cas9 when guided by the designed gRNA. The table also indicates the expected size of the PCR fragments.

4Q5 plating screening protocol

pJoe9282.1 derived plasmids containing the correct homologous recombination cassette and guideRNA were transformed into 4Q5 cells. These cells were plated on LB agar supplemented with kanamycin and left overnight at 30°C. The next day single colonies were plated on LB agar with .2% xylose and left to grow overnight at 30°C. Colonies from these plates were replated on LB agar without antibiotic and grown overnight at 50°C. Lastly, colonies that grew were replated on LB agar with and without kanamycin antibiotic. Those bacteria that grew on plates without antibiotic but did not grow on plates containing antibiotic were further analyzed by PCR, SDS-PAGE, and bioassay.

4Q5 liquid screening protocol

The LacZ reporter gene causes a blue color to form when the bacteria is in the presence of X-Gal. To screen for colonies that were positively edited a more robust selection protocol was developed. A liquid screening method was utilized because it allowed for screening of larger numbers of colonies and was more time efficient. pJoe-LacZ was transformed into 4Q5 cells and plated on LB plates supplemented with kanamycin and X-Gal, and grown at 30°C After 2-4 days, blue colonies were grown in liquid culture at 30°C overnight as a primary culture. Blue colonies were chosen because they were positive transformants. The next day the primary culture was diluted 1:10 and allowed to grow to OD_{600} of .3-.4 The culture was then induced with 1% xylose and allowed to grow shaking at 30°C for 24 h. The culture was then cured by incubation at 50°C for 24 h, which should result in the loss of the pJoe plasmid. The resulting liquid culture was diluted 1:10,000 and plated on large LB plates. The next day single colonies were grown on LB plates with and without kanamycin. Those colonies that grew on the LB plate without antibiotic but not in the presence of antibiotic were then used in a colony PCR to determine if the LacZ insert was edited into the pBtoxis plasmid.

Mosquito rearing

Orlando wildtype, *Aedes aegypti* mosquitoes were used for bioassay experiments. These mosquitoes were grown in a room kept between 60% and 70% humidity using humidifiers. Eggs were hatched in water supplemented with fish food pellets (TetraMin, Tropical Tablets) as food for the larvae. Once the larvae reached pupation, they were moved to a larger cage where they are able to emerge as adults. The females of these

cages were blood fed on anesthetized mice and allowed to mate with male mosquitoes contained in the same cage. The insectary where mosquitoes are kept follows a 14:10h cycle of lights on:lights off.

Bioassay

Bioassays were performed by taking 20, 3rd instar *Orlando* wildtype larvae and placing them in 200ml of water. The larvae were then dosed with an overnight culture and after 24 h mortality was noted.

Results

pJoe plasmid

The pJoe plasmid was obtained from Bacillus Genetic Stock Center in Columbus, OH. A plasmid map can be found in Figure 4-2. The plasmid contains the Cas9 gene under a xylose inducible promoter. The plasmid also contains a region to cassette in a homologous region to be edited into the target DNA flanked by SfiI sites. The pJoe plasmid also contains a semi synthetic promoter denoted PvanP to promote transcription of the gRNA, this site is flanked by BsaI sites. The plasmid also contains a kanamycin resistance gene.

Schematic of constructs

A schematic of the constructs can be found in Figure 4-4 The schematic also includes restriction sites used to cassette in each homologous region with the gene slated to be used for insertion. For each construct, the left arm, right arm and Cry11A promoter are all the same, but only the gene is different. Three separate constructs were created one containing LacZ (pJoe-LacZ), one containing eGFP (pJoe-eGFP), and one containing

Cry11B (pJoe-Cry11B). These constructs were ultimately cloned into the pJoe plasmid between BsaI cut sites.

eGFP fluorescence

To verify *Bt* cells would fluoresce green and to verify the correct sequence of the promoter used, eGFP and the Cry11A promoter were cloned into pHT315, a shuttle vector that can be expressed in *Bt* cells. This plasmid was transformed into 4Q7, *Bt* cells, which do not contain the pBtoxis plasmid. Fluorescence was seen in cells using fluorescence microscopy from a Zeiss microscope. The fluorescent cells can be seen in Figure 4-5.

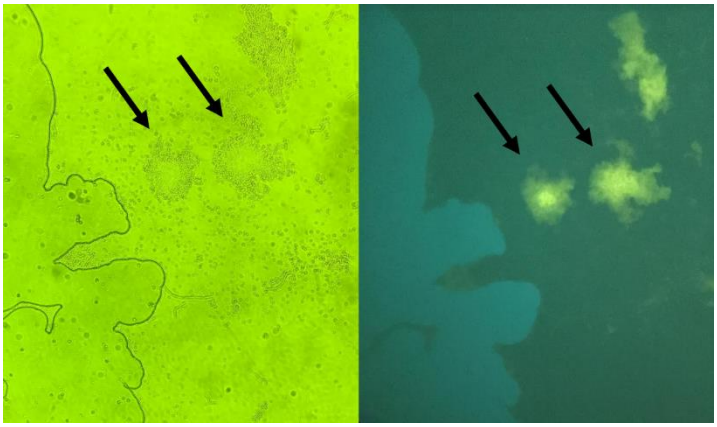

Figure 4-5. Fluorescent 4Q7 cells.
This figure shows florescent 4Q7 cells as indicated by the arrows. The image on the left utilized only light microscopy while the image on the right is the same field under florescence.

Blue color in 4Q7 (pHT315) and 4Q5 (pJoe)

To ensure blue color could be used to screen for LacZ production, the LacZ gene was cloned into pHT315 with the Cry11A promoter. This had a dual purpose, seeing the blue color in *Bacillus thuringiensis* bacteria as well as to be sure the promoter was correct and would work. pHT315 is a shuttle vector that can be used to express proteins in *Bt* and *E. coli* cells. In this case the pHT315 plasmid containing the promoter and LacZ gene

were transformed into 4Q7 cells. The pJoe plasmid containing LacZ was also used to check that the pJoe system works in 4Q5 cells. When the plates were supplemented with X-Gal, both systems 4Q7 (Figure 4-6A) and 4Q5 (Figure 4-6B) turned blue.

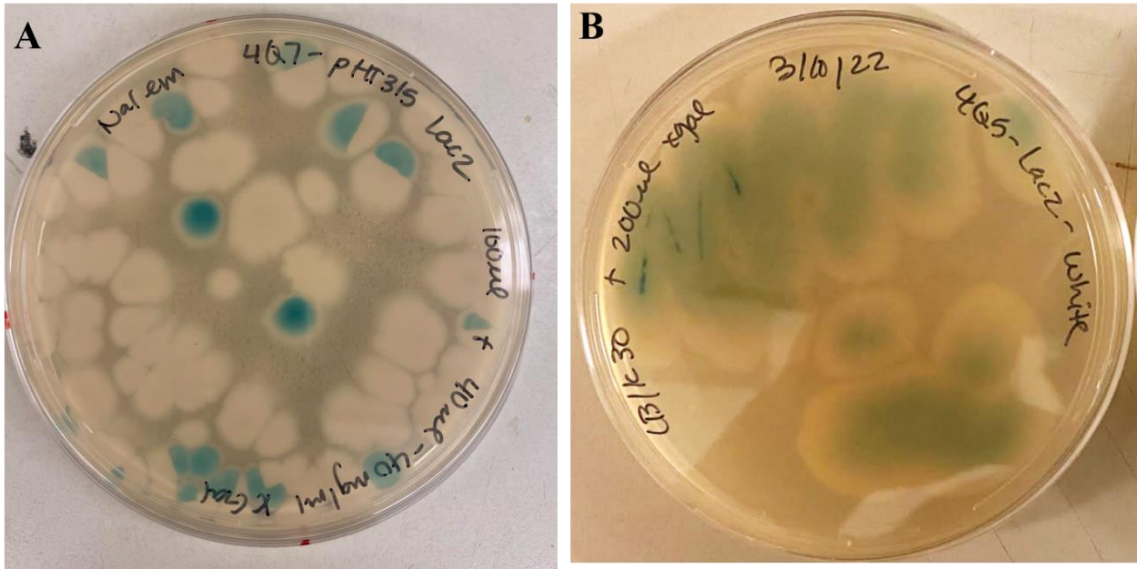

Figure 4-6. Verification of LacZ expression in 4Q7 and 4Q5 cells
This figure shows verification of LacZ expression in both A. 4Q7 cells and B. 4Q5 cells on nutrient agar (NA) and Luria agar (LB) plates respectively supplemented with antibiotic and X-Gal. The plasmid used in A is the shuttle vector pHT315 containing the Cry11A promoter and the full length LacZ gene. The plasmid used in B is pJoe9282.1 containing the homologous recombination cassette including LacZ and the guideRNA (pJoe-LacZ). B is a single 4Q5 colony replated in the presence of X-Gal.

eGFP in 4Q5

pJoe-eGFP, pJoe-LacZ, and pJoe-Cry11B were transformed into 4Q5 cells. These transformations were grown overnight on LB plates supplemented with Kanamycin. Single colonies were then plated on LB plates supplemented with Kanamycin and .2% total volume of 1M xylose and grown overnight. The following day single colonies were plated on LB agar without antibiotic and grown at 50°C to cure out the pJoe plasmid. Next, colonies that had grown were plated on LB agar both with and without kanamycin. These plates were analyzed, and those colonies that grew on plates without antibiotic but

did not grow in the presence of antibiotic were analyzed further. A schematic of this plate selection process can be seen in Figure 4-7**.**

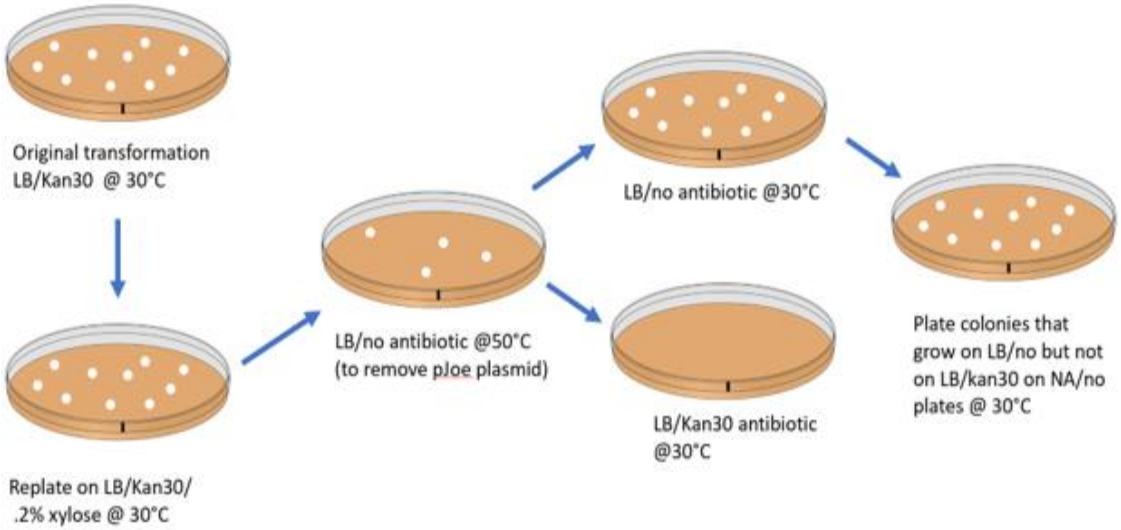

Figure 4-7. Schematic of single colony plate screening.
This figure shows a general schematic for screening for correct colonies after transformation of 4Q5 cells with the pJoe plasmid with the correct homologous recombination cassettes.

The three constructs were analyzed concurrently. Colonies lacking pJoe-LacZ were grown on nutrient agar plates supplemented with X-Gal and analyzed for blue color after 3 to 5 days. Colonies lacking pJoe-eGFP, were grown on nutrient agar plates and then analyzed using fluorescence microscopy (Figure 4-8**)**. These colonies were also analyzed by western blot using anti-eGFP as the primary antibody (Figure 4-9**)**. Finally, these colonies were also analyzed in an SDS-PAGE and bioassay against 3rd instar *Ae. aegypti* mosquito larvae to be sure the pBtoxis plasmid was not lost during curing.

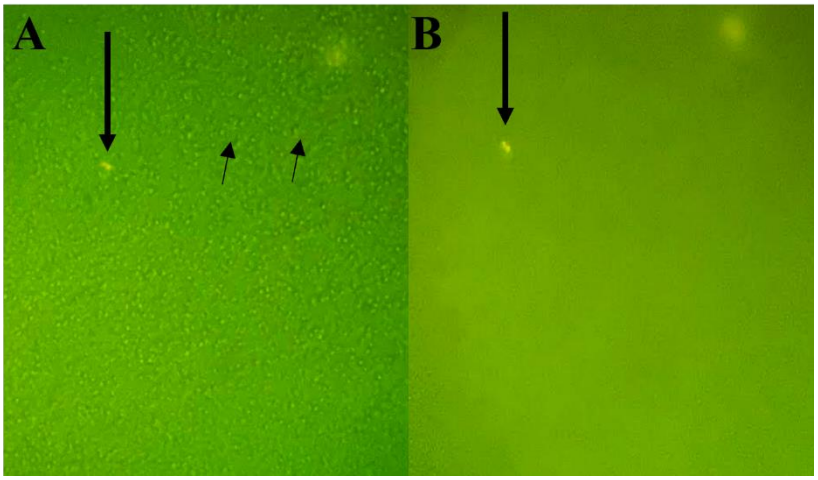

Figure 4-8. 4Q5 with eGFP under fluorescence microscopy.
This figure shows fluorescence microscopy using a Zeiss microscope. Both images are of the same section of a sample prepared. Potentially positive colonies are indicated in both images by an arrow. The image in figure A has contrast light in the background and allows for distinction of individual cells. Figure B does not have contrast light, and only the fluorescent light is used, and shows one or two cells showing fluorescence indicated by the downward arrow. This sample was made from eGFP sample 8, a western blot of the colony can be seen in Figure 4-9.

Colonies lacking pJoe-Cry11B were analyzed in an SDS-PAGE as well as a bioassay against 3rd instar *Ae. aegypti* mosquito larvae as well. The bioassay data for these colonies can be found in Table 4-4. A loss of pBoxis plasmid during curing can be determined by both SDS -PAGE analysis as well as a bioassay.

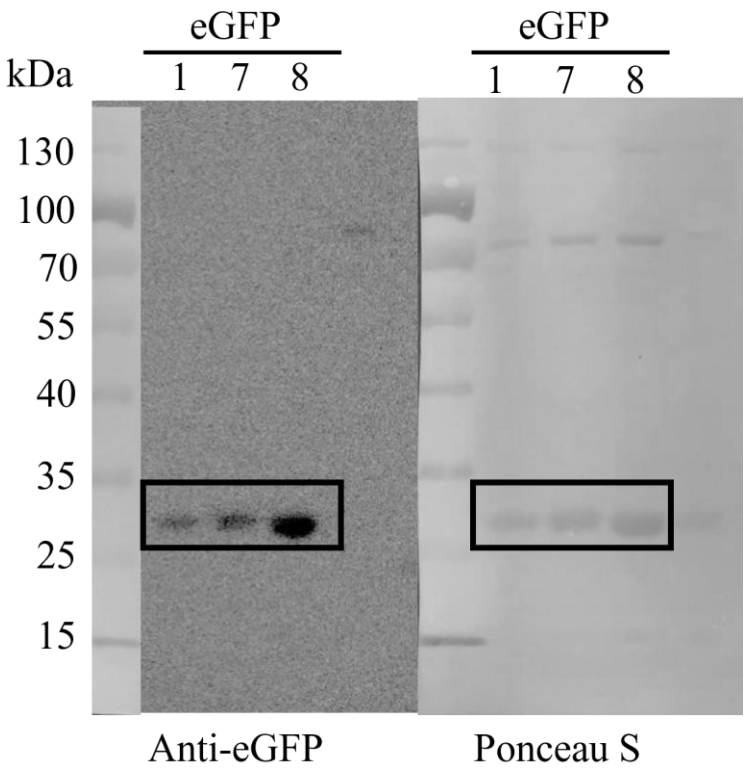

Figure 4-9. 4Q5 containing eGFP western membrane.
The western membrane detected with anti-eGFP as a primary antibody(left), and the same membrane stained with PonceauS (right). Bands detected between 25 and 35 kDa verify the presence of eGFP which is 26.9kDa. These samples correspond to the samples used in the SDS-PAGE in Figure 4-8 and the bioassay data in Table 4-4.

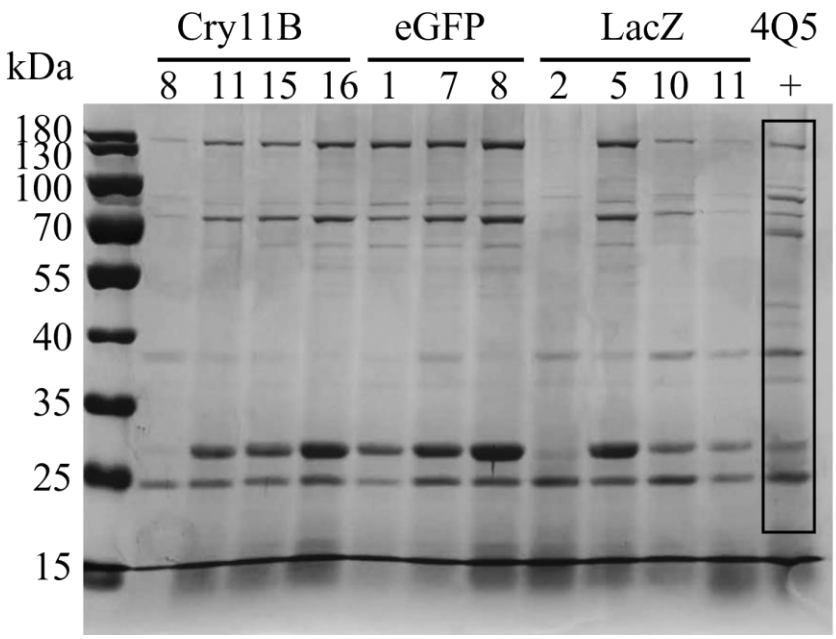

Figure 4-10. SDS-PAGE of 4Q5 screened bioassay cultures.
SDS-PAGE of cultures used in a bioassay against 3rd instar *Ae. aegypti* larvae. Four Cry11B colonies, three eGFP colonies, four LacZ colonies, and one 4Q5 positive control colony were tested in a bioassay. Each number represents a different colony. The 4Q5 sample was used as a control to compare band patterns and verify the pBtoxis plasmid was still present, these bands are indicated by the box. These samples correspond to the samples indicated in Table 4-4 used for the bioassay.

Bti is very toxic to *Aedes* mosquitoes. In Figure 4-10 a loss of pBtoxis plasmid can be seen in LacZ sample 2 indicated by a loss of protein bands and verified by a loss of toxicity., where the band pattern is different than the other lanes in the gel; this also corresponds to a lack of toxicity seen in the bioassay.

Table 4-4. Bioassay of 4Q5 samples.

Construct	Toxicity against Aedes
Cry11B – 8	100%
Cry11B – 11	100%
Cry11B – 15	100%
Cry11B – 16	100%
eGFP – 1	100%
eGFP – 7	100%
eGFP – 8	100%
LacZ – 2	0
LacZ – 5	100%
LacZ - 10	100%
Lac Z – 11	100%
4Q5	100%

This table indicates the percent mortality of each 4Q5 sample against 3rd instar *Ae. aegypti* larvae to ensure the pBtoxis plasmid is still present.

Unfortunately, potentially positive eGFP colonies could not be isolated, and potentially positive Cry11B colonies could not be verified by western blot analysis using an anti-Cry11B antibody. To further determine if this technique could be used to edit the pBtoxis plasmid, only the pJoe-LacZ was analyzed further.

Cas9 expression

Expression of Cas9 was checked to ensure all parts of the experiment were functional. Bacteria were grown and induced with 1% xylose. Samples of culture were taken every hour after induction and loaded into an SDS-PAGE. One gel was stained with Coomassie, and the other was transferred to a PVDF membrane in a western blot (Figure 4-11**)**. The membrane was developed using anti-Cas9 as the primary antibody. Cas9 is expressed, and the highest amount of Cas9 was detected after 6 h. This led to the decision to induce bacterial culture for 24 h, as it appears more Cas9 is produced the longer the bacteria expresses Cas9.

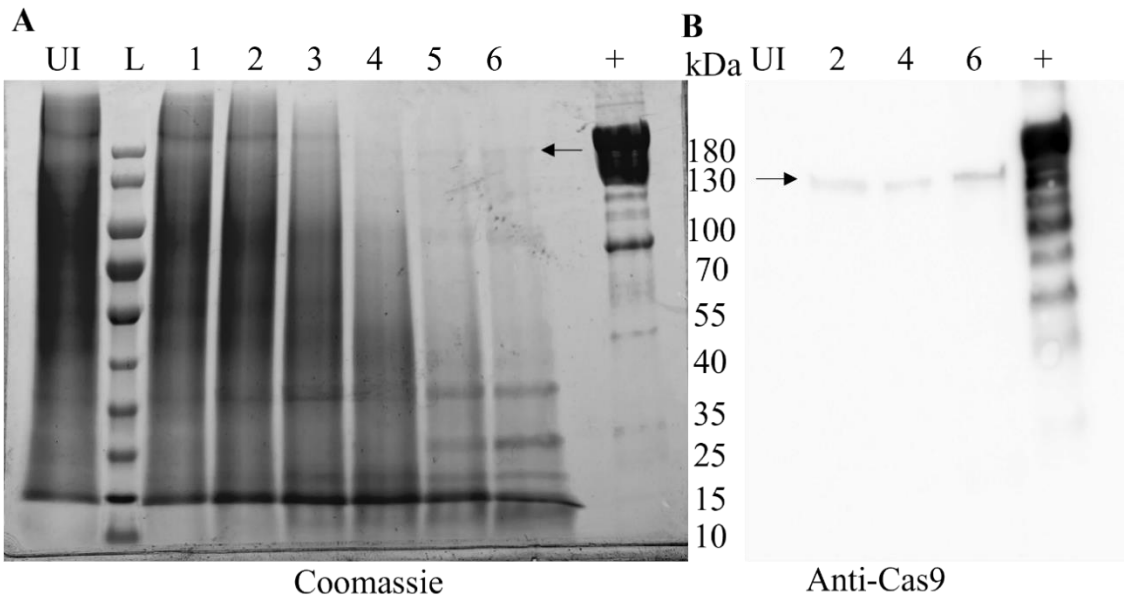

Figure 4-11. Cas9 expression in 4Q5.
This figure shows an SDS-PAGE and western membrane of 4Q5 cells transformed with the pJoe9282.1 plasmid induced with 1% xylose. Aliquots were taken 1 to 6 h after induction, indicated by the number at the top of the images, and run in an SDS-PAGE. The western blot in B is probed with anti-Cas9 antibody as the primary antibody. Cas9 protein is approximately 160 kDa. The last lane in both images indicates a positive control, purified Cas9 protein.

In vitro cleavage

An in vitro cleavage assay was performed to verify the gRNA would work. The cleavage assay indicates that the guide RNA is sufficient to guide Cas 9 to the target site. The cleavage assay was performed by isolating a DNA fragment from the pBtoxis plasmid, either 900bp or 1.93kb. This fragment was purified and incubated with Cas9 and the guide RNA, the appearance of two bands in the DNA gel indicates that the Cas9 will cleave DNA in the presence of the guide RNA (Figure 4-12**)**. Cas9 did cleave the DNA fragment isolated from the pBtoxis plasmid through PCR.

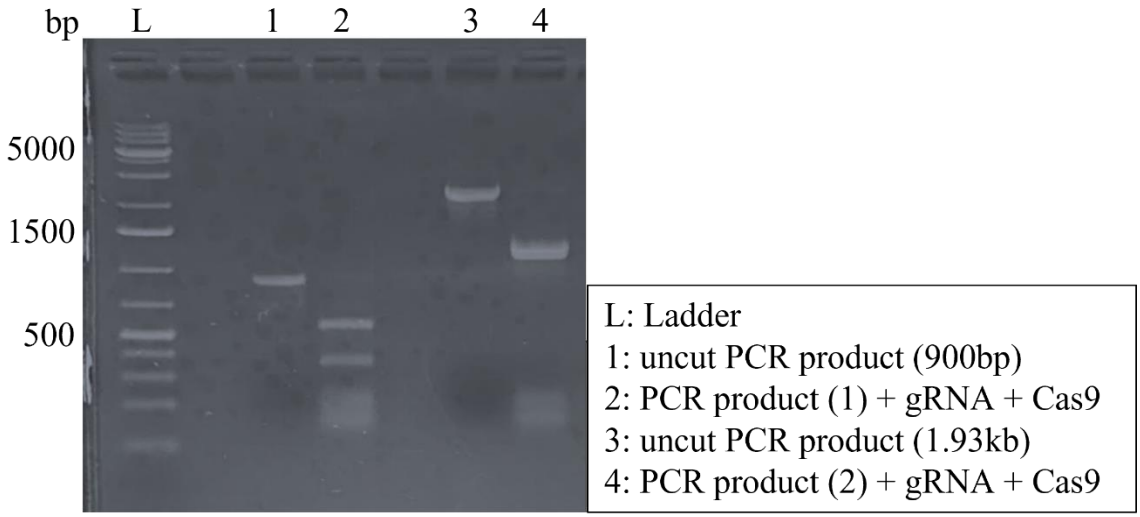

Figure 4-12. In vitro cleavage assay.
This gel contains DNA that is uncut and cut. Lanes 1 and 3 contain PCR products, of 900bp and 1.93kb used as the template DNA for the in vitro cleavage assay. Lanes 2 and 4 contain the template DNA, guide RNA, and Cas9 protein. The smaller bands in lanes 2 and 4 indicate that the cleavage was successful. Cleavage of the DNA fragment in lane 1 results in a 350bp fragment and a 550bp fragment, while cleavage of the fragment in lane 3 results in a 916bp fragment and 1016bp.

LacZ liquid screening

A blue color can be seen in 4Q5 cells when the pJoe plasmid containing LacZ is used in a transformation. Figure 4-6B shows blue color when transformed cells are plated in the presence of X-gal. These blue colonies were used as the primary culture for subsequent experiments for Cas9 cleavage. The primary culture containing one blue colony was diluted and grown to an OD_{600} of 0.3-0.4. The culture was then induced using 1M xylose to a final concentration of 1%. The culture was allowed to grow for 24 h at 30°C before increasing the temperature to 50°C for another 24 h. These cultures were then diluted and plated on plates with and without antibiotic (Figure 4-13).

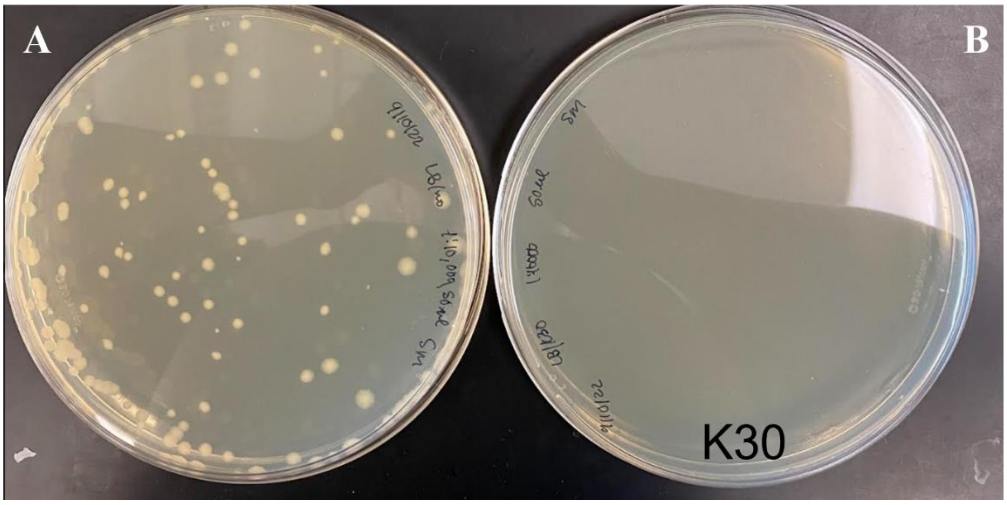

Figure 4-13. Curing efficiency
This figure shows three LB agar plates without (A) antibiotic and one with (B) Kanamycin. This image depicts the effectivity of the curing process. Very few or no colonies grew on plates with antibiotic while some grew on plates without antibiotic. Those colonies that grew on plates without antibiotic were further screened to see which of the colonies had lost only the pJoe plasmid.

To screen for positive colonies single colonies were grown on plates with and without antibiotic (Figure 4-14). Those colonies that grew on the plate without antibiotic but did not grow in the presence of antibiotic were screen further using colony PCR. One thousand colonies were screened for curing of the pJoe plasmid. Of those 1000 colonies 465 had lost the pJoe plasmid, however, a positively edited, blue colored, was never found.

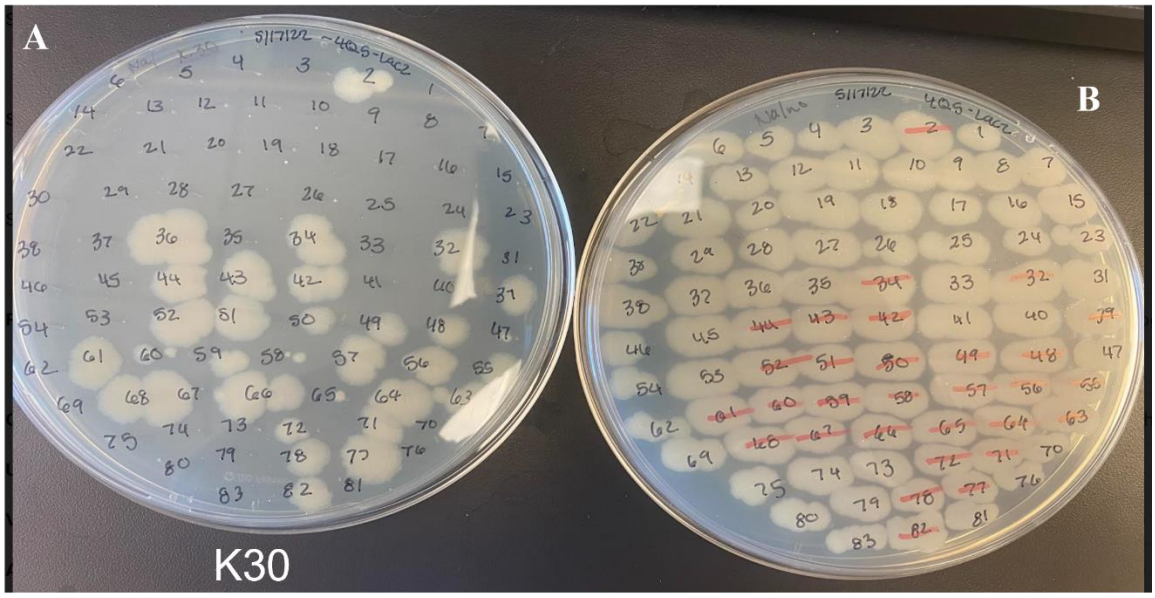

Figure 4-14. Single colony screening.
Screening of single colonies on LB agar plates with(A) or without (B) antibiotic. Those colonies that grew without antibiotic but not on plates supplemented with antibiotic were analyzed further to determine if editing occurred.

Discussion

Although a fully edited colony was not found, all the parts associated with CRISPR/Cas9 editing worked. Cas9 was being expressed, gRNA was efficient in cleaving PCR fragments, and the reporter genes were successfully expressed in both *Bt* and *Bti* cells. The curing process was also successful in removing the pJoe plasmid from some cells with about 46% efficiency. Trevors (1986) suggests using 5-7°C above the normal growing temperature is sufficient in removing plasmids from bacteria. The culture should be grown at the elevated temperature until it reaches late log phase, where it should be diluted and incubated again at the elevated temperature. This elevated growth temperature was successful in *Staphylococcus aureus* in removing a plasmid that provided tetracycline-resistance (Trevors, 1986).

All parts of the CRISPR-Cas technology up to homologous recombination worked, this suggests the efficiency of editing within these cells is very low. This issue may be multi-fold in that homologous recombination as a repair mechanism requires a homologous DNA sequence for use as a template (Jasin and Rothstein, 2013), different repair mechanisms are used during different life stages in bacteria (Ayora et al., 2011), and homologous recombination as a repair process takes longer than non-homologous end joining (Mao et al., 2008). Spatial distribution of the pJoe plasmid containing the homologous cassette may have caused a low efficiency in editing. In bacteria, non-homologous end joining is used more often during mitosis and G_1, while homologous recombination is more active during S and G_2 stages (Ayora et al., 2011; Liu et al., 2019). In *B. subtilis* most double strand breaks are repaired using homologous recombination (Cardenas et al., 2009), however if no homologous region or donor plasmid is present, or early stages of the homologous repair mechanism are impaired, the bacteria will utilize non-homologous end joining to repaid double strand breaks (Cardenas et al., 2009; Lieber, 2010). Although *B. subtilis* is within the same family as *Bti* the mechanism and requirements for repair may be altered slightly. There has been work done to try and enhance homologous recombination as a repair mechanism associated with Cas9 cleavage as well as determine what strategies could increase homologous recombination efficiency. Some enhancement strategies include timed delivery of the CRISPR/Cas9 system, fusing Cas9 with a protein required for signaling and starting homologous recombination, changing the Cas9 promoter for expression at a specific time, and using

chemical modulation to arrest cells during specific phases (Liu et al., 2019; Sun et al., 2022; Wolabu et al., 2020)

Future directions of this project should include attempting to increase the efficiency of homology direct repair within the bacteria. This technology could be used to edit other toxins into *Bti* bacterial plasmids, or other bacterial plasmids in general. Successful editing of the *Bti* plasmid would allow other toxins to be removed or replaced as well to help combat cross resistance in mosquito populations in the future and help to continually subject mosquito populations to different toxins and prevent resistance.

References

Ayora, S., Carrasco, B., Cárdenas, P.P., César, C.E., Cañas, C., Yadav, T., Marchisone, C., Alonso, J.C., 2011. Double-strand break repair in bacteria: a view from Bacillus subtilis. FEMS Microbiol. Rev. 35, 1055–1081. https://doi.org/10.1111/j.1574-6976.2011.00272.x

Ben-Dov, E., 2014. Bacillus thuringiensis subsp. israelensis and Its Dipteran-Specific Toxins. Toxins 6, 1222–1243. https://doi.org/10.3390/toxins6041222

Benelli, G., Beier, J.C., 2017. Current vector control challenges in the fight against malaria. Acta Trop. 174, 91–96. https://doi.org/10.1016/j.actatropica.2017.06.028

Benelli, G., Jeffries, C.L., Walker, T., 2016. Biological Control of Mosquito Vectors: Past, Present, and Future. Insects 7, 52. https://doi.org/10.3390/insects7040052

Busvine, J.R., 1978. Current problems in the control of mosquitoes. Nature 273, 604–607. https://doi.org/10.1038/273604a0

Cardenas, P.P., Carrasco, B., Sanchez, H., Deikus, G., Bechhofer, D.H., Alonso, J.C., 2009. Bacillus subtilis polynucleotide phosphorylase 3′-to-5′ DNase activity is involved in DNA repair. Nucleic Acids Res. 37, 4157–4169. https://doi.org/10.1093/nar/gkp314

Center for Disease Control, 2017. Mosquito Control: What you need to know about BTI [WWW Document]. Mosq. Control What You Need Know BTI. URL https://www.cdc.gov/zika/pdfs/bti_fact_sheet.pdf

Delécluse, A., Rosso, M.L., Ragni, A., 1995. Cloning and expression of a novel toxin gene from Bacillus thuringiensis subsp. jegathesan encoding a highly mosquitocidal protein. Appl. Environ. Microbiol. 61, 4230–4235.

Georghiou, G.P., Wirth, M.C., 1997. Influence of Exposure to Single versus Multiple Toxins of Bacillus thuringiensis subsp. israelensis on Development of Resistance in the Mosquito Culex quinquefasciatus (Diptera: Culicidae). Appl. Environ. Microbiol. 63, 1095–1101.

Gould, F., Martinez-Ramirez, A., Anderson, A., Ferre, J., Silva, F.J., Moar, W.J., 1992. Broad-spectrum resistance to Bacillus thuringiensis toxins in Heliothis virescens. Proc. Natl. Acad. Sci. 89, 7986–7990. https://doi.org/10.1073/pnas.89.17.7986

Jasin, M., Rothstein, R., 2013. Repair of Strand Breaks by Homologous Recombination. Cold Spring Harb. Perspect. Biol. 5, a012740. https://doi.org/10.1101/cshperspect.a012740

Lieber, M.R., 2010. The mechanism of double-strand DNA break repair by the nonhomologous DNA end-joining pathway. Annu. Rev. Biochem. 79, 181–211. https://doi.org/10.1146/annurev.biochem.052308.093131

Liu, M., Rehman, S., Tang, X., Gu, K., Fan, Q., Chen, D., Ma, W., 2019. Methodologies for Improving HDR Efficiency. Front. Genet. 9.

Mao, Z., Bozzella, M., Seluanov, A., Gorbunova, V., 2008. Comparison of nonhomologous end joining and homologous recombination in human cells. DNA Repair 7, 1765–1771. https://doi.org/10.1016/j.dnarep.2008.06.018

McGaughey, W.H., Johnson, D.E., 1994. Influence of crystal protein composition of Bacillus thuringiensis strains on cross-resistance in Indianmeal moths (Lepidoptera: Pyralidae). J. Econ. Entomol. 87, 535–540. https://doi.org/10.1093/jee/87.3.535

Mosquito factsheets [WWW Document], n.d. . Eur. Cent. Dis. Prev. Control. URL https://www.ecdc.europa.eu/en/disease-vectors/facts/mosquito-factsheets (accessed 11.16.22).

Otieno-Ayayo, Z.N., Zaritsky, A., Wirth, M.C., Manasherob, R., Khasdan, V., Cahan, R., Ben-Dov, E., 2008. Variations in the mosquito larvicidal activities of toxins from Bacillus thuringiensis ssp. israelensis. Environ. Microbiol. 10, 2191–2199. https://doi.org/10.1111/j.1462-2920.2008.01696.x

Ran, F.A., Hsu, P.D., Wright, J., Agarwala, V., Scott, D.A., Zhang, F., 2013. Genome engineering using the CRISPR-Cas9 system. Nat. Protoc. 8, 2281–2308. https://doi.org/10.1038/nprot.2013.143

Shah, S.A., Erdmann, S., Mojica, F.J.M., Garrett, R.A., 2013. Protospacer recognition motifs. RNA Biol. 10, 891–899. https://doi.org/10.4161/rna.23764

Silva-Filha, M.H.N.L., Romão, T.P., Rezende, T.M.T., Carvalho, K. da S., Gouveia de Menezes, H.S., Alexandre do Nascimento, N., Soberón, M., Bravo, A., 2021. Bacterial Toxins Active against Mosquitoes: Mode of Action and Resistance. Toxins 13, 523. https://doi.org/10.3390/toxins13080523

Sun, W., Liu, H., Yin, W., Qiao, J., Zhao, X., Liu, Y., 2022. Strategies for Enhancing the Homology-Directed Repair Efficiency of CRISPR-Cas Systems. CRISPR J. 5, 7–18. https://doi.org/10.1089/CRISPR.2021.0039

Tabashnik, B.E., Malvar, T., Liu, Y.B., Finson, N., Borthakur, D., Shin, B.S., Park, S.H., Masson, L., de Maagd, R.A., Bosch, D., 1996. Cross-resistance of the diamondback moth indicates altered interactions with domain II of Bacillus thuringiensis toxins. Appl. Environ. Microbiol. 62, 2839–2844. https://doi.org/10.1128/aem.62.8.2839-2844.1996

Tetreau, G., Stalinski, R., David, J.-P., Després, L., 2013. Monitoring resistance to Bacillus thuringiensis subsp. israelensis in the field by performing bioassays with each Cry toxin separately. Mem. Inst. Oswaldo Cruz 108, 894–900. https://doi.org/10.1590/0074-0276130155

Tetsch, L., 2017. The adaptive bacterial immune system CRISPR-Cas and its therapeutic potential. Med. Monatsschr. Pharm. 40, 17–23.

Toymentseva, A.A., Altenbuchner, J., 2019. New CRISPR-Cas9 vectors for genetic modifications of Bacillus species. FEMS Microbiol. Lett. 366. https://doi.org/10.1093/femsle/fny284

Trevors, J.T., 1986. Plasmid curing in bacteria. FEMS Microbiol. Rev. 1, 149–157. https://doi.org/10.1111/j.1574-6968.1986.tb01189.x

Wirth, M.C., Delécluse, A., Federici, B.A., Walton, W.E., 1998. Variable Cross-Resistance to Cry11B from Bacillus thuringiensis subsp. jegathesan in Culex quinquefasciatus (Diptera: Culicidae) Resistant to Single or Multiple Toxins of Bacillus thuringienisis subsp. israelensis. Appl. Environ. Microbiol. 64, 4174–4179.

Wirth, M.C., Delécluse, A., Walton, W.E., 2004. Laboratory Selection for Resistance to Bacillus thuringiensis subsp. jegathesan or a Component Toxin, Cry11B, in Culex quinquefasciatus (Diptera: Culicidae). J. Med. Entomol. 41, 435–441. https://doi.org/10.1603/0022-2585-41.3.435

Wirth, M.C., Georghiou, G.P., 1997. Cross-Resistance Among CryIV Toxins of Bacillus thuringiensis subsp. israelensis in Culex quinquefasciatus (Diptera: Culicidae). J. Econ. Entomol. 90, 1471–1477. https://doi.org/10.1093/jee/90.6.1471

Wolabu, T.W., Park, J.-J., Chen, M., Cong, L., Ge, Y., Jiang, Q., Debnath, S., Li, G., Wen, J., Wang, Z., 2020. Improving the genome editing efficiency of CRISPR/Cas9 in Arabidopsis and Medicago truncatula. Planta 252, 15. https://doi.org/10.1007/s00425-020-03415-0

Chapter 5

General Conclusions

The goal of this dissertation was to better understand the two toxin loci found within *Paraclostridium bifermentans* serovar *malaysia* and increase activity of *Bacillus thuringiensis israelensis* against *Anopheles* mosquitoes. This research investigated the mechanism of action of the Cry Operon, and the size, stoichiometry, and structure of the Ptox complex from *Paraclostridium bifermentans malaysia*. The research also utilized a genome editing technique, CRISPR-Cas9 to attempt to increase the activity of *Bti* against specific vector mosquito species. Each of these projects, although different, still focus on the toxicity of bacterial toxins against mosquito vector species and aim to broaden the knowledge in each situation.

Some mosquito species can serve as vectors for diseases like dengue fever, malaria, and West Nile fever among others. Three major mosquito species are responsible for the transmission of these diseases they are *Aedes aegypti, Anopheles stephensi,* and *Culex quinquefasciatus* respectively (Becker et al., 2010; Braack et al., 2018; Kraemer et al., 2015; Murray et al., 2013). These diseases and other arbovirus caused diseases are responsible for hundreds of thousands of infections and deaths per year. One method of controlling deaths from these diseases is through controlling the mosquito vector (Baldacchino et al., 2015; Brady and Hay, 2020; Oliveira et al., 2017). Pesticide use is used most widely, however these chemicals can have off target effects on other organisms, the environment and even human health (Oliveira et al., 2017). Another method of controlling mosquito populations is through biological means including

bacteria, specifically *Bacillus thuringiensis israelensis* (*Bti*) and *Lysinibacillus sphaericus* (*Ls*) (Becker, 1997; Ben-Dov, 2014; Davidson et al., 1984; de Barjac, 1978; Silva Filha et al., 2014). These two bacteria target *Aedes* and *Culex* mosquitoes but not *Anopheles*. *Bti* and *Ls* are safe for other aquatic animals like fish, as well as for mammals and humans which makes them advantageous as a control method (Lacey and Mulla, 1990; Siegel and Shadduck, 1990). Although these bacteria have proven to be effective at controlling mosquito populations, prolonged exposure of mosquito populations to the same bacterial toxins has allowed for the evolution of resistance as seen both in the field and in a laboratory setting (Rao et al., 1995; Rodcharoen and Mulla, 1994; Wirth, 2010; Wirth and Georghiou, 1997). This development of resistance indicates a need to find other methods or mechanisms of control. Moreover, there are currently no biological control methods that primarily target *Anopheles* mosquitoes. *Paraclostridium bifermentans* serovar m*alaysia* (*Pbm*) could bridge that gap.

Pbm is toxic to both *Aedes* and *Anopheles* mosquitoes. The goal of specific aim 1 of this dissertation was to better understand the two toxin loci that are responsible for *Pbm*s toxicity to *Aedes* and *Anopheles* mosquitoes. The Cry operon is the component that is toxic to *Aedes* mosquitoes while the Ptox locus is responsible for *Anopheles* toxicity. Chapter 2 of this dissertation looks at the mechanism of action of the Cry operon. Previous work has shown that all for genes of the Cry operon must be expressed to cause toxicity to mosquito larvae (Qureshi et al., 2014). The general mechanism of Cry toxins includes loop regions within Domain II binding to receptors in the midgut of the target organism, after binding the alpha-helices of Domain I insert into the membrane causing a

pore to form leading to osmotic imbalance and eventual death (Bravo et al., 2004; Gómez et al., 2002). The Cry operon contains *cry16, cry17, cbm17.1,* and *cbm17.2* all expressed under the same promoter. I created two constructs with a mutated *cry17*, the resulting Cry17 protein either contained a deletion of 212 amino acids, or a truncated protein of only 213AA compared to the original which is 618AA. Interestingly, neither of these constructs were toxic when fed to *Aedes* mosquito larvae. This indicated Cry17 was involved in the mechanism of toxicity. Taking this idea one step further, I created loop substitution constructs. These constructs were designed to cause the putative loop regions involved in receptor binding to be unreactive. Constructs with loop regions containing alanine were made for both Cry16 and Cry17. Of the 6 constructs made, one completely lost toxicity when fed to mosquito larvae. This helped to validate that Cry17 is likely involved in receptor binding. In contrast, constructs with mutations within Cry16 were still toxic. To further this idea Cry16 was purified and labeled with biotin. This biotin labeled protein was used in a biding assay using brush border membrane fractions created from *Aedes* mosquitoes. No binding was seen between Cry16 and brush border membrane fractions, which supports the data that Cry17 is involved in receptor binding, and Cry16 may be involved in pore formation. All four proteins are necessary for toxicity, which means it is likely they all have a specific role in the mechanism of toxicity. Further research should be done to elucidate the role of each individual protein. No work has been done to determine the role of Cbm17.1 or Cbm17.2, but they do show similarity to aegerolysin proteins which have been shown to interact with other proteins and create pores (Panevska et al., 2019).

The first aim also encompassed furthering our knowledge of the Ptox locus, specifically the size of the Ptox complex. The Ptox complex is responsible for toxicity to *Anopheles* mosquitoes. It contains a neurotoxin, Pmp1, a non-toxic non hemagglutinin, NTNH, and three orfX genes (Contreras et al., 2019). The components of the Ptox complex are similar to those found in Botulinum toxin progenitor complexes (Gu and Jin, 2013). Using two different techniques the size of the Ptox complex was estimated. The first technique involved using the protein standards of a native-PAGE ladder and estimating the size of protein bands detected using Ptox protein complex antibodies. This method estimated the Ptox protein complex to be about 756kDa. The other method utilized a size exclusion column and protein standards. The protein standards were used to create a plot of elution volume vs protein size. The volume at which proteins detected by Ptox protein complex antibodies were eluted determined the estimated size of the Ptox complex. For this second method the protein complexes are estimated to be between 793kDa and 1040kDa. However, the latter complex also included the Cry operon complex, which on its own is 177.7kDa. Thus the value of 756-793 kDa is consistent with botulinum neurotoxin progenitor complexes, which can range from 500 kDa to 900 kDa depending on their composition (Gu and Jin, 2013). Attempts were made to purify the Ptox complex through multiple methods including acid precipitation, ammonium sulfate extraction, anion-exchange chromatography, and size exclusion chromatography. Although these attempts were not completely successful if was found that acid precipitation is advantageous while ammonium sulfate extraction is not. Anion-exchange chromatography and size exclusion chromatography are not sufficient to separate the Cry

operon complex from the Ptox complex and other methods should be utilized. Further purification should include cation-exchange chromatography and could include sucrose density gradient centrifugation in conjunction with methods that were attempted.

The second aim of this dissertation was to increase the toxicity of *Bti* against *Anopheles* mosquitoes. As stated earlier there is no biological control method whose primary activity targets *Anopheles* mosquitoes. My goal was to introduce *Anopheles* toxicity to *Bti* using Crispr-Cas9. To achieve this goal a plasmid called pJoe9282.1 (Toymentseva and Altenbuchner, 2019) was used. The plasmid was developed with a xylose inducible promoter in front of the Cas9 gene, and two restriction cloning sites, one for a homologous cassette, for use in homologous recombination repair, and another for guide RNA production which contained a semisynthetic promoter upstream of the gRNA insertion point. The gRNA was to be integrated into the plasmid as DNA and would be transcribed into gRNA. Although the plasmid was originally created for use in *Bacillus subtilis* I wanted to utilize the system for *Bti.* Here I was able to successfully express Cas9 in the *Bti* system. I also confirmed the gRNA I designed was sufficient to guide Cas9 to a cleavage site and cut DNA. I also verified that *Bti* could express a functional β-galactosidase and will hydrolyze X-Gal to form 5-bromo-4-chloro-indoxyl and after dimerization blue pigment in the bacteria. Although an edited bacteria was not isolated, all of the parts were functional, and screening of more colonies would likely lead to a positive colony. Further research for this project should include using the pJoe plasmid containing Cry11B. Introducing Cry11B to pBtoxis of *Bti* would increase the bacteria's

activity against *Anopheles* mosquitoes. This method could also be used to introduce other toxins into the pBtoxis plasmid including other Cry toxins or other pest targeting toxins.

This data has helped to fill gaps in the current knowledge of the mechanism of the Cry operon, the size of the Ptox complex, methods for purifying the Ptox complex, and methods for increasing toxicity of *Bti*. Taken together this data has increased knowledge regarding toxin activity and synthesis in two bacterial systems, *Pbm* and *Bti*. This will help to move research forward in finding new ways to target vector mosquito populations and can provide a new means of control.

References

Adang, M.J., Crickmore, N. and Jurat-Fuentes, J.L. (2014) 'Chapter Two - Diversity of Bacillus thuringiensis Crystal Toxins and Mechanism of Action', in T.S. Dhadialla and S.S. Gill (eds) *Advances in Insect Physiology*. Academic Press (Insect Midgut and Insecticidal Proteins), pp. 39–87. Available at: https://doi.org/10.1016/B978-0-12-800197-4.00002-6.

Allen, G. (2016) 'Florida Keys Approves Trial Of Genetically Modified Mosquitoes To Fight Zika', *NPR*, 20 November. Available at: https://www.npr.org/sections/health-shots/2016/11/20/502717253/florida-keys-approves-trial-of-genetically-modified-mosquitoes-to-fight-zika (Accessed: 22 June 2022).

Ayora, S. *et al.* (2011) 'Double-strand break repair in bacteria: a view from Bacillus subtilis', *FEMS Microbiology Reviews*, 35(6), pp. 1055–1081. Available at: https://doi.org/10.1111/j.1574-6976.2011.00272.x.

Baldacchino, F. *et al.* (2015) 'Control methods against invasive Aedes mosquitoes in Europe: a review', *Pest Management Science*, 71(11), pp. 1471–1485. Available at: https://doi.org/10.1002/ps.4044.

de Barjac, H. (1978) '[Toxicity of Bacillus thuringienses var. israelensis for larvae of Aedes aegypti and Anopheles stephensi]', *Comptes Rendus Hebdomadaires Des Seances De l'Academie Des Sciences. Serie D: Sciences Naturelles*, 286(15), pp. 1175–1178.

de Barjac, H. *et al.* (1990) '[Clostridium bifermentans serovar malaysia, a new anaerobic bacterium pathogen to mosquito and blackfly larvae]', *Comptes rendus de l'Academie des sciences. Serie III, Sciences de la vie*, 310(9), pp. 383–387.

Barloy, F. *et al.* (1996) 'Cloning and expression of the first anaerobic toxin gene from Clostridium bifermentans subsp. malaysia, encoding a new mosquitocidal protein with homologies to Bacillus thuringiensis delta-endotoxins.', *Journal of Bacteriology*, 178(11), pp. 3099–3105.

Barloy, F., Lecadet, M.M. and Delécluse, A. (1998) 'Cloning and sequencing of three new putative toxin genes from Clostridium bifermentans CH18', *Gene*, 211(2), pp. 293–299. Available at: https://doi.org/10.1016/s0378-1119(98)00122-x.

Baumann, P. *et al.* (1985) 'Purification of the larvicidal toxin of Bacillus sphaericus and evidence for high-molecular-weight precursors', *Journal of Bacteriology*, 163(2), pp. 738–747. Available at: https://doi.org/10.1128/jb.163.2.738-747.1985.

Beard, J. (2006) 'DDT and human health', *Science of The Total Environment*, 355(1), pp. 78–89. Available at: https://doi.org/10.1016/j.scitotenv.2005.02.022.

Becker, N. (1997) ‘Microbial control of mosquitoes: Management of the upper rhine mosquito population as a model programme’, *Parasitology Today*, 13(12), pp. 485–487. Available at: https://doi.org/10.1016/S0169-4758(97)01154-X.

Becker, N. *et al.* (2010) *Mosquitoes and Their Control*. 2nd edn. Heidelberg, Germany: Springer-Verlag.

Ben-Dov, E. (2014) ‘Bacillus thuringiensis subsp. israelensis and Its Dipteran-Specific Toxins’, *Toxins*, 6(4), pp. 1222–1243. Available at: https://doi.org/10.3390/toxins6041222.

Benelli, G. and Beier, J.C. (2017) ‘Current vector control challenges in the fight against malaria’, *Acta Tropica*, 174, pp. 91–96. Available at: https://doi.org/10.1016/j.actatropica.2017.06.028.

Benelli, G., Jeffries, C.L. and Walker, T. (2016) ‘Biological Control of Mosquito Vectors: Past, Present, and Future’, *Insects*, 7(4), p. 52. Available at: https://doi.org/10.3390/insects7040052.

Berry, C. (2012) ‘The bacterium, Lysinibacillus sphaericus, as an insect pathogen’, *Journal of Invertebrate Pathology*, 109(1), pp. 1–10. Available at: https://doi.org/10.1016/j.jip.2011.11.008.

Bifenthrin - ScienceDirect (no date). Available at: https://www.sciencedirect.com/science/article/pii/B9780123864543011696 (Accessed: 26 December 2021).

Braack, L. *et al.* (2018) ‘Mosquito-borne arboviruses of African origin: review of key viruses and vectors’, *Parasites & Vectors*, 11(1), p. 29. Available at: https://doi.org/10.1186/s13071-017-2559-9.

Brady, O.J. and Hay, S.I. (2020) ‘The Global Expansion of Dengue: How Aedes aegypti Mosquitoes Enabled the First Pandemic Arbovirus’, *Annual Review of Entomology*, 65(1), pp. 191–208. Available at: https://doi.org/10.1146/annurev-ento-011019-024918.

Bravo, A. *et al.* (2004) ‘Oligomerization triggers binding of a Bacillus thuringiensis Cry1Ab pore-forming toxin to aminopeptidase N receptor leading to insertion into membrane microdomains’, *Biochimica Et Biophysica Acta*, 1667(1), pp. 38–46. Available at: https://doi.org/10.1016/j.bbamem.2004.08.013.

Bravo, A., Soberón, M. and Gill, S.S. (2005) ‘6.6 - Bacillus thuringiensis: Mechanisms and Use’, in L.I. Gilbert (ed.) *Comprehensive Molecular Insect Science*. Amsterdam: Elsevier, pp. 175–205. Available at: https://doi.org/10.1016/B0-44-451924-6/00081-8.

Busvine, J.R. (1978) ‘Current problems in the control of mosquitoes’, *Nature*, 273(5664), pp. 604–607. Available at: https://doi.org/10.1038/273604a0.

Cardenas, P.P. *et al.* (2009) ‘Bacillus subtilis polynucleotide phosphorylase 3′-to-5′ DNase activity is involved in DNA repair’, *Nucleic Acids Research*, 37(12), pp. 4157–4169. Available at: https://doi.org/10.1093/nar/gkp314.

Carlysue, #038;r=pg’ and Loading=’lazy’/>carylsue, #038;r=pg 2x’ Class=’avatar Avatar-20 Photo’ Height=’20’ Width=’20’ (2017) ‘Are Mosquitoes Outsmarting Mosquito Nets?’, *National Geographic Education Blog*, 3 April. Available at: https://blog.education.nationalgeographic.org/2017/04/03/are-mosquitoes-outsmarting-mosquito-nets/ (Accessed: 15 March 2021).

CDC (2020a) *Bti \ CDC, Centers for Disease Control and Prevention*. Available at: https://www.cdc.gov/mosquitoes/mosquito-control/community/bti.html (Accessed: 22 June 2022).

CDC (2020b) *Disease of the Week - Zika, Centers for Disease Control and Prevention*. Available at: https://www.cdc.gov/dotw/zika/index.html (Accessed: 28 June 2022).

CDC-Centers for Disease Control (2020) *CDC - Malaria - About Malaria - Biology*. Available at: https://www.cdc.gov/malaria/about/biology/index.html (Accessed: 22 June 2022).

Center for Disease Control (2017) *Mosquito Control: What you need to know about BTI, Mosquito Control: What you need to know about BTI*. Available at: https://www.cdc.gov/zika/pdfs/bti_fact_sheet.pdf.

Charles, J.F. *et al.* (1990) ‘Clostridium bifermentans serovar malaysia: sporulation, biogenesis of inclusion bodies and larvicidal effect on mosquito’, *Research in Microbiology*, 141(6), pp. 721–733. Available at: https://doi.org/10.1016/0923-2508(90)90066-y.

Charles, J.F. and Nicolas, L. (1986) ‘Recycling of Bacillus sphaericus 2362 in mosquito larvae: a laboratory study’, *Annales De l’Institut Pasteur. Microbiologie*, 137B(1), pp. 101–111. Available at: https://doi.org/10.1016/s0769-2609(86)80097-7.

Chatterjee, N. and Walker, G.C. (2017) ‘Mechanisms of DNA damage, repair and mutagenesis’, *Environmental and molecular mutagenesis*, 58(5), pp. 235–263. Available at: https://doi.org/10.1002/em.22087.

Cheong, H. and Gill, S.S. (1997) ‘Cloning and characterization of a cytolytic and mosquitocidal delta-endotoxin from Bacillus thuringiensis subsp. jegathesan’, *Applied and Environmental Microbiology*, 63(8), pp. 3254–3260. Available at: https://doi.org/10.1128/aem.63.8.3254-3260.1997.

Chikungunya fact sheet (2020). Available at: https://www.who.int/news-room/fact-sheets/detail/chikungunya (Accessed: 28 June 2022).

Clements, A.N. (1999) *The Biology of Mosquitoes*. Cabi Publishing.

Contreras, E. *et al.* (2019) 'A neurotoxin that specifically targets Anopheles mosquitoes', *Nature Communications*, 10(1), p. 2869. Available at: https://doi.org/10.1038/s41467-019-10732-w.

Cowman, A.F. *et al.* (2016) 'Malaria: Biology and Disease', *Cell*, 167(3), pp. 610–624. Available at: https://doi.org/10.1016/j.cell.2016.07.055.

DasGupta, B.R. and Sathyamoorthy, V. (1984) 'Purification and amino acid composition of type A botulinum neurotoxin', *Toxicon*, 22(3), pp. 415–424. Available at: https://doi.org/10.1016/0041-0101(84)90085-0.

Davidson, E.W. *et al.* (1984) 'Fate of Bacillus sphaericus 1593 and 2362 spores used as larvicides in the aquatic environment', *Applied and Environmental Microbiology*, 47(1), pp. 125–129. Available at: https://doi.org/10.1128/aem.47.1.125-129.1984.

'DDT (General Fact Sheet)' (1999). National Pesticide Information Center. Available at: http://npic.orst.edu/factsheets/ddtgen.pdf.

Delécluse, A., Rosso, M.L. and Ragni, A. (1995) 'Cloning and expression of a novel toxin gene from Bacillus thuringiensis subsp. jegathesan encoding a highly mosquitocidal protein.', *Applied and Environmental Microbiology*, 61(12), pp. 4230–4235.

Dengue Fever | NIH: National Institute of Allergy and Infectious Diseases (2016). Available at: https://www.niaid.nih.gov/diseases-conditions/dengue-fever (Accessed: 28 June 2022).

Dhiman, R.C., Pahwa, S. and Dash, A.P. (2008) 'Climate change and malaria in India: Interplay between temperatures and mosquitoes', 12(1), p. 6.

Eswaramoorthy, S. *et al.* (2015) 'Molecular Assembly of Clostridium botulinum progenitor M complex of type E', *Scientific Reports*, 5(1), p. 17795. Available at: https://doi.org/10.1038/srep17795.

Fernández, L.E. *et al.* (2005) 'Cry11Aa toxin from Bacillus thuringiensis binds its receptor in Aedes aegypti mosquito larvae through loop alpha-8 of domain II', *FEBS letters*, 579(17), pp. 3508–3514. Available at: https://doi.org/10.1016/j.febslet.2005.05.032.

Ferreira, L.M. and Silva-Filha, M.H.N.L. (2013) 'Bacterial larvicides for vector control: mode of action of toxins and implications for resistance', *Biocontrol Science and*

Technology, 23(10), pp. 1137–1168. Available at: https://doi.org/10.1080/09583157.2013.822472.

Figtree, M. *et al.* (2010) 'Plasmodium knowlesi in human, Indonesian Borneo', *Emerging Infectious Diseases*, 16(4), pp. 672–674. Available at: https://doi.org/10.3201/eid1604.091624.

Fillinger, U. *et al.* (2008) 'A tool box for operational mosquito larval control: preliminary results and early lessons from the Urban Malaria Control Programme in Dar es Salaam, Tanzania', *Malaria Journal*, 7(1), p. 20. Available at: https://doi.org/10.1186/1475-2875-7-20.

Fritz, J.S. (1987) 'Ion Chromatography', *Analytical Chemistry*, 59(4), pp. 335A-344A. Available at: https://doi.org/10.1021/ac00131a737.

Fujinaga, Y. (2010) 'Interaction of botulinum toxin with the epithelial barrier', *Journal of Biomedicine & Biotechnology*, 2010, p. 974943. Available at: https://doi.org/10.1155/2010/974943.

Georghiou, G.P. and Wirth, M.C. (1997) 'Influence of Exposure to Single versus Multiple Toxins of Bacillus thuringiensis subsp. israelensis on Development of Resistance in the Mosquito Culex quinquefasciatus (Diptera: Culicidae)', *Applied and Environmental Microbiology*, 63(3), pp. 1095–1101.

Global Health - Newsroom - Yellow Fever (2019). Available at: https://www.cdc.gov/globalhealth/newsroom/topics/yellowfever/index.html (Accessed: 28 June 2022).

Goldberg, L.J. and Margalit, J. (1977) 'A bacterial spore demonstrating rapid larvicidal activity against Anopheles sergentii, Uranotaenia unguiculata, Culex univitattus, Aedes aegypti and Culex pipiens.', *Mosquito News*, 37(3), pp. 355–358.

Gómez, I. *et al.* (2002) 'Cadherin-like receptor binding facilitates proteolytic cleavage of helix α-1 in domain I and oligomer pre-pore formation of Bacillus thuringiensis Cry1Ab toxin', *FEBS Letters*, 513(2), pp. 242–246. Available at: https://doi.org/10.1016/S0014-5793(02)02321-9.

Gould, F. *et al.* (1992) 'Broad-spectrum resistance to Bacillus thuringiensis toxins in Heliothis virescens.', *Proceedings of the National Academy of Sciences*, 89(17), pp. 7986–7990. Available at: https://doi.org/10.1073/pnas.89.17.7986.

Gray, V.E., Hause, R.J. and Fowler, D.M. (2017) *Using large-scale mutagenesis to guide single amino acid scanning experiments*. preprint. Molecular Biology. Available at: https://doi.org/10.1101/140707.

Gu, S. and Jin, R. (2013) ‘Assembly and Function of the Botulinum Neurotoxin Progenitor Complex’, *Current topics in microbiology and immunology*, 364, p. 10.1007/978-3-642-33570–9_2. Available at: https://doi.org/10.1007/978-3-642-33570-9_2.

Gubler, D.J. (1998) ‘Dengue and Dengue Hemorrhagic Fever’, *Clinical Microbiology Reviews*, 11(3), pp. 480–496. Available at: https://doi.org/10.1128/CMR.11.3.480.

Guillet, P. *et al.* (1990) ‘Use of Bacillus thuringiensis israelensis for Onchocerciasis Control in West Africa’, in H. de Barjac and D.J. Sutherland (eds) *Bacterial Control of Mosquitoes & Black Flies: Biochemistry, Genetics & Applications of Bacillus thuringiensis israelensis and Bacillus sphaericus*. Dordrecht: Springer Netherlands, pp. 187–201. Available at: https://doi.org/10.1007/978-94-011-5967-8_11.

Hasegawa, K. *et al.* (2007) ‘A novel subunit structure of Clostridium botulinum serotype D toxin complex with three extended arms’, *The Journal of Biological Chemistry*, 282(34), pp. 24777–24783. Available at: https://doi.org/10.1074/jbc.M703446200.

Inoue, K. *et al.* (1996) ‘Molecular composition of Clostridium botulinum type A progenitor toxins’, *Infection and Immunity*, 64(5), pp. 1589–1594. Available at: https://doi.org/10.1128/iai.64.5.1589-1594.1996.

Ishino, Y., Krupovic, M. and Forterre, P. (2018) ‘History of CRISPR-Cas from Encounter with a Mysterious Repeated Sequence to Genome Editing Technology’, *Journal of Bacteriology*, 200(7), pp. e00580-17. Available at: https://doi.org/10.1128/JB.00580-17.

Iwamura, T., Guzman-Holst, A. and Murray, K.A. (2020) ‘Accelerating invasion potential of disease vector Aedes aegypti under climate change’, *Nature Communications*, 11(1), p. 2130. Available at: https://doi.org/10.1038/s41467-020-16010-4.

Ja, N. (2001) ‘Malaria control: achievements, problems and strategies.’, *Parassitologia*, 43(1–2), pp. 1–89.

Jasin, M. and Rothstein, R. (2013) ‘Repair of Strand Breaks by Homologous Recombination’, *Cold Spring Harbor Perspectives in Biology*, 5(11), p. a012740. Available at: https://doi.org/10.1101/cshperspect.a012740.

Jones, G.W. *et al.* (2008) ‘The Cry48Aa-Cry49Aa binary toxin from Bacillus sphaericus exhibits highly restricted target specificity’, *Environmental Microbiology*, 10(9), pp. 2418–2424. Available at: https://doi.org/10.1111/j.1462-2920.2008.01667.x.

Juárez-Pérez, V. and Delécluse, A. (2001) ‘The Cry toxins and the putative hemolysins of Clostridium bifermentans ser. malaysia are not involved in mosquitocidal activity’,

Journal of Invertebrate Pathology, 78(1), pp. 57–58. Available at: https://doi.org/10.1006/jipa.2001.5042.

Kalfon, A. *et al.* (no date) 'Sporulation of Bacillus sphaericus 2297: an Electron Microscope Study of Crystal-like Inclusion Biogenesis and Toxicity to Mosquito Larvae', *Microbiology*, 130(4), pp. 893–900. Available at: https://doi.org/10.1099/00221287-130-4-893.

Kawalek, M.D. *et al.* (1995) 'Isolation and Identification of novel toxins from a new mosquitocidal isolate from Malaysia, Bacillus thuringiensis subsp. jegathesan', *Applied and Environmental Microbiology*, 61(8), pp. 2965–2969. Available at: https://doi.org/10.1128/aem.61.8.2965-2969.1995.

Kawalek, M.D. (1998) *Cloning and characterization of mosquitocidal genes from Bacillus thuringiensis subsp. jegathesan*. Ph.D. University of California, Riverside. Available at: https://www.proquest.com/docview/304413845/abstract/14DA36E0406E46BDPQ/1 (Accessed: 14 June 2022).

Kim, M.-S., Zhong, J. and Pandey, A. (2016) 'Common errors in mass spectrometry-based analysis of post-translational modifications', *Proteomics*, 16(5), pp. 700–714. Available at: https://doi.org/10.1002/pmic.201500355.

Knowles, B.H. and Ellar, D.J. (1987) 'Colloid-osmotic lysis is a general feature of the mechanism of action of Bacillus thuringiensis δ-endotoxins with different insect specificity', *Biochimica et Biophysica Acta (BBA) - General Subjects*, 924(3), pp. 509–518. Available at: https://doi.org/10.1016/0304-4165(87)90167-X.

Kraemer, M.U. *et al.* (2015) 'The global distribution of the arbovirus vectors Aedes aegypti and Ae. albopictus', *eLife*, 4, p. e08347. Available at: https://doi.org/10.7554/eLife.08347.

Lacey, L.A. and Mulla, M.S. (1990) *Safety of Bacillus thuringiensis ssp. israelensis and Bacillus sphaericus to nontarget organisms in the aquatic environment*. Available at: https://agris.fao.org/agris-search/search.do?recordID=US9105330 (Accessed: 16 June 2022).

Lederberg, J. (1992) 'The interface of science and medicine', in *The Mount Sinai journal of medicine. Human cancer : from precurable to curable. Symposium*, pp. 380–383. Available at: http://pascal-francis.inist.fr/vibad/index.php?action=getRecordDetail&idt=4451931 (Accessed: 16 March 2021).

Lee, H.L. and Seleena, P. (1990a) ‘Isolation and evaluation of larvicidal Clostridium bifermentans against mosquitoes of public health importance.’, *Tropical Biomedicine*, 7(1), pp. 103–106.

Lee, H.L. and Seleena, P. (1990b) ‘Isolation of indigenous larvicidal microbial control agents of mosquitos: the Malaysian experience’, *The Southeast Asian Journal of Tropical Medicine and Public Health*, 21(2), pp. 281–287.

Lieber, M.R. (2010) ‘The mechanism of double-strand DNA break repair by the nonhomologous DNA end-joining pathway’, *Annual Review of Biochemistry*, 79, pp. 181–211. Available at: https://doi.org/10.1146/annurev.biochem.052308.093131.

Likitvivatanavong, S., Aimanova, K. and Gill, S.S. (2009) ‘Loop residues of the receptor binding domain of Bacillus thuringiensis Cry11Ba toxin are important for mosquitocidal activity’, *FEBS letters*, 583(12), pp. 2021–2030. Available at: https://doi.org/10.1016/j.febslet.2009.05.020.

Liu, L. *et al.* (2021) ‘Which Is Stronger? A Continuing Battle Between Cry Toxins and Insects’, *Frontiers in Microbiology*, 12. Available at: https://www.frontiersin.org/article/10.3389/fmicb.2021.665101 (Accessed: 28 June 2022).

Liu, M. *et al.* (2019) ‘Methodologies for Improving HDR Efficiency’, *Frontiers in Genetics*, 9. Available at: https://www.frontiersin.org/articles/10.3389/fgene.2018.00691 (Accessed: 16 November 2022).

López-Diaz, J.A. *et al.* (2013) ‘Oligomerization is a key step in Cyt1Aa membrane insertion and toxicity but not necessary to synergize Cry11Aa toxicity in Aedes aegypti larvae’, *Environmental Microbiology*, 15(11), pp. 3030–3039. Available at: https://doi.org/10.1111/1462-2920.12263.

Lubec, G. and Afjehi-Sadat, L. (2007) ‘Limitations and Pitfalls in Protein Identification by Mass Spectrometry’, *Chemical Reviews*, 107(8), pp. 3568–3584. Available at: https://doi.org/10.1021/cr068213f.

Malaria vector control (no date). Available at: https://www.who.int/teams/global-malaria-programme/prevention/vector-control (Accessed: 25 November 2022).

Mao, Z. *et al.* (2008) ‘Comparison of nonhomologous end joining and homologous recombination in human cells’, *DNA repair*, 7(10), pp. 1765–1771. Available at: https://doi.org/10.1016/j.dnarep.2008.06.018.

Masson, L. *et al.* (2004) ‘A Novel Bacillus thuringiensis (PS149B1) Containing a Cry34Ab1/Cry35Ab1 Binary Toxin Specific for the Western Corn Rootworm Diabrotica

virgifera virgifera LeConte Forms Ion Channels in Lipid Membranes', *Biochemistry*, 43(38), pp. 12349–12357. Available at: https://doi.org/10.1021/bi048946z.

McGaughey, W.H. and Johnson, D.E. (1994) 'Influence of crystal protein composition of Bacillus thuringiensis strains on cross-resistance in Indianmeal moths (Lepidoptera: Pyralidae)', *Journal of economic entomology*, 87(3), pp. 535–540. Available at: https://doi.org/10.1093/jee/87.3.535.

Mordecai, E.A. *et al.* (2020) 'Climate change could shift disease burden from malaria to arboviruses in Africa', *The Lancet Planetary Health*, 4(9), pp. e416–e423. Available at: https://doi.org/10.1016/S2542-5196(20)30178-9.

Mosquito factsheets (no date) *European Centre for Disease Prevention and Control*. Available at: https://www.ecdc.europa.eu/en/disease-vectors/facts/mosquito-factsheets (Accessed: 16 November 2022).

Mulla, M.S. *et al.* (1984) 'Larvicidal activity and field efficacy of Bacillus sphaericus strains against mosquito larvae and their safety to nontarget organisms', *Mosquito news (USA)* [Preprint]. Available at: https://scholar.google.com/scholar_lookup?title=Larvicidal+activity+and+field+efficacy+of+Bacillus+sphaericus+strains+against+mosquito+larvae+and+their+safety+to+nontarget+organisms&author=Mulla%2C+M.S.&publication_year=1984 (Accessed: 16 June 2022).

Mulla, M.S. *et al.* (2003) 'Emergence of resistance and resistance management in field populations of tropical Culex quinquefasciatus to the microbial control agent Bacillus sphaericus', *Journal of the American Mosquito Control Association*, 19(1), pp. 39–46.

Murray, N.E.A., Quam, M.B. and Wilder-Smith, A. (2013) 'Epidemiology of dengue: past, present and future prospects', *Clinical Epidemiology*, 5, pp. 299–309. Available at: https://doi.org/10.2147/CLEP.S34440.

Mustafa, M.S. *et al.* (2015) 'Discovery of fifth serotype of dengue virus (DENV-5): A new public health dilemma in dengue control', *Medical Journal, Armed Forces India*, 71(1), pp. 67–70. Available at: https://doi.org/10.1016/j.mjafi.2014.09.011.

Mutoh, S. *et al.* (2003) 'Complete subunit structure of the Clostridium botulinum type D toxin complex via intermediate assembly with nontoxic components', *Biochemistry*, 42(37), pp. 10991–10997. Available at: https://doi.org/10.1021/bi034996c.

Myers, P., Yousten, A.A. and Davidson, E.W. (1979) 'Comparative studies of the mosquito-larval toxin of Bacillus sphaericus SSII-1 and 1593', *Canadian Journal of Microbiology*, 25(11), pp. 1227–1231. Available at: https://doi.org/10.1139/m79-193.

Nester, E.W. *et al.* (2002) *100 Years of Bacillus thuringiensis: A Critical Scientific Assessment: This report is based on a colloquium, "100 Years of Bacillis thuringiensis, a Paradigm for Producing Transgenic Organisms: A Critical Scientific Assessment," sponsored by the American Academy of Microbiology and held November 16–18, in Ithaca, New York*. Washington (DC): American Society for Microbiology (American Academy of Microbiology Colloquia Reports). Available at: http://www.ncbi.nlm.nih.gov/books/NBK559445/ (Accessed: 17 June 2022).

Nicolas, L., Darriet, F. and Hougard, J.M. (1987) 'Efficacy of Bacillus sphaericus 2362 against larvae of Anopheles gambiae under laboratory and field conditions in West Africa', *Medical and Veterinary Entomology*, 1(2), pp. 157–162. Available at: https://doi.org/10.1111/j.1365-2915.1987.tb00337.x.

Nicolopoulou-Stamati, P. *et al.* (2016) 'Chemical Pesticides and Human Health: The Urgent Need for a New Concept in Agriculture', *Frontiers in Public Health*, 4, p. 148. Available at: https://doi.org/10.3389/fpubh.2016.00148.

Nielsen-Leroux, C. *et al.* (2002) 'High resistance to Bacillus sphaericus binary toxin in culex pipiens (Diptera: Culicidae): the complex situation of west Mediterranean countries', *Journal of Medical Entomology*, 39(5), pp. 729–735. Available at: https://doi.org/10.1603/0022-2585-39.5.729.

Oliveira, S., Caleffe, R. and Conte, H. (2017) 'Chemical control of Aedes aegypti: a review on effects on the environment and human health', *Revista Eletrônica em Gestão, Educação e Tecnologia Ambiental - REGET*, 21, pp. 240–247. Available at: https://doi.org/10.5902/2236117027692.

Otieno-Ayayo, Z.N. *et al.* (2008) 'Variations in the mosquito larvicidal activities of toxins from Bacillus thuringiensis ssp. israelensis', *Environmental Microbiology*, 10(9), pp. 2191–2199. Available at: https://doi.org/10.1111/j.1462-2920.2008.01696.x.

Panevska, A. *et al.* (2019) 'Pore-forming protein complexes from Pleurotus mushrooms kill western corn rootworm and Colorado potato beetle through targeting membrane ceramide phosphoethanolamine', *Scientific Reports*, 9(1), p. 5073. Available at: https://doi.org/10.1038/s41598-019-41450-4.

'Pathophysiology of Severe Dengue' (no date), p. 1.

Payne, J.M. and Davidson, E.W. (1984) 'Insecticidal activity of the crystalline parasporal inclusions and other components of the Bacillus sphaericus 1593 spore complex', *Journal of Invertebrate Pathology*, 43(3), pp. 383–388. Available at: https://doi.org/10.1016/0022-2011(84)90084-3.

Pérez, C. *et al.* (2005) 'Bacillus thuringiensis subsp. israelensis Cyt1Aa synergizes Cry11Aa toxin by functioning as a membrane-bound receptor', *Proceedings of the*

National Academy of Sciences, 102(51), pp. 18303–18308. Available at: https://doi.org/10.1073/pnas.0505494102.

Qureshi, N. *et al.* (2014a) 'The Cry Toxin Operon of Clostridium bifermentans subsp. malaysia Is Highly Toxic to Aedes Larval Mosquitoes', *Applied and Environmental Microbiology*, 80(18), pp. 5689–5697. Available at: https://doi.org/10.1128/AEM.01139-14.

Qureshi, N. *et al.* (2014b) 'The Cry Toxin Operon of Clostridium bifermentans subsp. malaysia Is Highly Toxic to Aedes Larval Mosquitoes', *Applied and Environmental Microbiology*, 80(18), pp. 5689–5697. Available at: https://doi.org/10.1128/AEM.01139-14.

Ran, F.A. *et al.* (2013) 'Genome engineering using the CRISPR-Cas9 system', *Nature Protocols*, 8(11), pp. 2281–2308. Available at: https://doi.org/10.1038/nprot.2013.143.

Rao, D.R. *et al.* (1995) 'DEVELOPMENT OF A HIGH LEVEL OF RESISTANCE TO BACILLUS SPHAERICU,SIN A FIELD POPULATION OF CTJLEX QUINQUEFASCIATUS FROM KOCHI, INDIA', p. 5.

Reimer, L. *et al.* (2008) 'Relationship Between kdr Mutation and Resistance to Pyrethroid and DDT Insecticides in Natural Populations of Anopheles gambiae', *Journal of Medical Entomology*, 45(2), pp. 260–266. Available at: https://doi.org/10.1093/jmedent/45.2.260.

Rodcharoen, J. and Mulla, M.S. (1994) 'Resistance Development in Culex quinquefasciatus (Diptera: Culicidae) to Bacillus sphaericus', *Journal of Economic Entomology*, 87(5), pp. 1133–1140. Available at: https://doi.org/10.1093/jee/87.5.1133.

Rosso, M.L. and Delécluse, A. (1997) 'Contribution of the 65-kilodalton protein encoded by the cloned gene cry19A to the mosquitocidal activity of Bacillus thuringiensis subsp. jegathesan', *Applied and Environmental Microbiology*, 63(11), pp. 4449–4455. Available at: https://doi.org/10.1128/aem.63.11.4449-4455.1997.

Shah, S.A. *et al.* (2013) 'Protospacer recognition motifs', *RNA Biology*, 10(5), pp. 891–899. Available at: https://doi.org/10.4161/rna.23764.

Siegel, J.P. and Shadduck, J.A. (1990) 'Mammalian Safety of Bacillus sphaericus', in H. de Barjac and D.J. Sutherland (eds) *Bacterial Control of Mosquitoes & Black Flies: Biochemistry, Genetics & Applications of Bacillus thuringiensis israelensis and Bacillus sphaericus*. Dordrecht: Springer Netherlands, pp. 321–331. Available at: https://doi.org/10.1007/978-94-011-5967-8_21.

Silberman, J. and Taylor, A. (2021) ‘Carbamate Toxicity’, in *StatPearls*. Treasure Island (FL): StatPearls Publishing. Available at: http://www.ncbi.nlm.nih.gov/books/NBK482183/ (Accessed: 26 December 2021).

Silva Filha, M.H.N.L., Berry, C. and Regis, L. (2014) ‘Chapter Three - Lysinibacillus sphaericus: Toxins and Mode of Action, Applications for Mosquito Control and Resistance Management’, in T.S. Dhadialla and S.S. Gill (eds) *Advances in Insect Physiology*. Academic Press (Insect Midgut and Insecticidal Proteins), pp. 89–176. Available at: https://doi.org/10.1016/B978-0-12-800197-4.00003-8.

Silva-Filha, M.H. *et al.* (2001) ‘Impact of a 26-month Bacillus sphaericus trial on the preimaginal density of Culex quinquefasciatus in an urban area of Recife, Brazil’, *Journal of the American Mosquito Control Association*, 17(1), pp. 45–50.

Silva-Filha, M.H.N.L. *et al.* (2021) ‘Bacterial Toxins Active against Mosquitoes: Mode of Action and Resistance’, *Toxins*, 13(8), p. 523. Available at: https://doi.org/10.3390/toxins13080523.

Sinègre, G. *et al.* (1994) ‘First field occurrence of Culex pipiens resistance to Bacillus sphaericus in southern France’, *8th European Meeting of Society for Vector Ecology* [Preprint].

Soliman, F. and Mehana, E.-S. (2015) ‘Pesticides Toxicity in Fish with Particular Reference to Insecticides’, *Asian Jo urnal of Agriculture and Food Sciences (ISSN: 2321 – 1571)*, Volume 03, pp. 2321–1571.

Solomon, H.M. and Lilly Jr, T. (2001) ‘BAM Chapter 17: Clostridium botulinum’, *FDA* [Preprint]. Available at: https://www.fda.gov/food/laboratory-methods-food/bam-chapter-17-clostridium-botulinum (Accessed: 19 June 2022).

Souza-Neto, J.A., Powell, J.R. and Bonizzoni, M. (2019) ‘Aedes aegypti vector competence studies: A review’, *Infection, Genetics and Evolution*, 67, pp. 191–209. Available at: https://doi.org/10.1016/j.meegid.2018.11.009.

Sugii, S. and Sakaguchi, G. (1975) ‘Molecular construction of Clostridium botulinum type A toxins.’, *Infection and Immunity*, 12(6), pp. 1262–1270.

Sun, W. *et al.* (2022) ‘Strategies for Enhancing the Homology-Directed Repair Efficiency of CRISPR-Cas Systems’, *The CRISPR Journal*, 5(1), pp. 7–18. Available at: https://doi.org/10.1089/crispr.2021.0039.

Sun, Y. *et al.* (2013) ‘Identification and Characterization of Three Previously Undescribed Crystal Proteins from Bacillus thuringiensis subsp. jegathesan’, *Applied and Environmental Microbiology*, 79(11), pp. 3364–3370. Available at: https://doi.org/10.1128/AEM.00078-13.

Tabashnik, B.E. *et al.* (1996) 'Cross-resistance of the diamondback moth indicates altered interactions with domain II of Bacillus thuringiensis toxins', *Applied and Environmental Microbiology*, 62(8), pp. 2839–2844. Available at: https://doi.org/10.1128/aem.62.8.2839-2844.1996.

Tetreau, G. *et al.* (2013) 'Monitoring resistance to Bacillus thuringiensis subsp. israelensis in the field by performing bioassays with each Cry toxin separately', *Memórias do Instituto Oswaldo Cruz*, 108(7), pp. 894–900. Available at: https://doi.org/10.1590/0074-0276130155.

Tetsch, L. (2017) 'The adaptive bacterial immune system CRISPR-Cas and its therapeutic potential', *Medizinische Monatsschrift Fur Pharmazeuten*, 40(1), pp. 17–23.

Thiery, I. *et al.* (1992) 'Host range of Clostridium bifermentans serovar. malaysia, a mosquitocidal anaerobic bacterium', *Journal of the American Mosquito Control Association*, 8(3), pp. 272–277.

Thiery, Isabelle *et al.* (1992) 'Vertebrate Safety of Clostridium bifermentans Serovar malaysia, a New Larvicidal Agent for Vector Control', *Journal of Economic Entomology*, 85(5), pp. 1618–1623. Available at: https://doi.org/10.1093/jee/85.5.1618.

Tiwari, A. and Nagalli, S. (2022) 'Clostridium Botulinum', in *StatPearls*. Treasure Island (FL): StatPearls Publishing. Available at: http://www.ncbi.nlm.nih.gov/books/NBK553081/ (Accessed: 19 June 2022).

Toymentseva, A.A. and Altenbuchner, J. (2019) 'New CRISPR-Cas9 vectors for genetic modifications of Bacillus species', *FEMS Microbiology Letters*, 366(1). Available at: https://doi.org/10.1093/femsle/fny284.

Trevors, J.T. (1986) 'Plasmid curing in bacteria', *FEMS Microbiology Reviews*, 1(3–4), pp. 149–157. Available at: https://doi.org/10.1111/j.1574-6968.1986.tb01189.x.

Wells, C.L. and Wilkins, T.D. (1996) 'Clostridia: Sporeforming Anaerobic Bacilli', in S. Baron (ed.) *Medical Microbiology*. 4th edn. Galveston (TX): University of Texas Medical Branch at Galveston. Available at: http://www.ncbi.nlm.nih.gov/books/NBK8219/ (Accessed: 17 June 2022).

West Nile virus (no date). Available at: https://www.who.int/news-room/fact-sheets/detail/west-nile-virus (Accessed: 16 March 2021).

WHO | Fact sheet: WHO/UNICEF report "Achieving the malaria MDG target" (no date) *WHO*. World Health Organization. Available at: http://www.who.int/malaria/media/malaria-mdg-target/en/ (Accessed: 16 March 2021).

Wirth, M.C. *et al.* (1998) 'Variable Cross-Resistance to Cry11B from Bacillus thuringiensis subsp. jegathesan in Culex quinquefasciatus (Diptera: Culicidae) Resistant to Single or Multiple Toxins of Bacillus thuringienisis subsp. israelensis', *Applied and Environmental Microbiology*, 64(11), pp. 4174–4179.

Wirth, M.C. *et al.* (2000) 'Laboratory Selection for Resistance to Bacillus sphaericus in Culex quinquefasciatus (Diptera: Culicidae) from California, USA', *Journal of Medical Entomology*, 37(4), pp. 534–540. Available at: https://doi.org/10.1603/0022-2585-37.4.534.

Wirth, M.C. *et al.* (2004) 'Synergy between toxins of Bacillus thuringiensis subsp. israelensis and Bacillus sphaericus', *Journal of Medical Entomology*, 41(5), pp. 935–941. Available at: https://doi.org/10.1603/0022-2585-41.5.935.

Wirth, M.C. (2010) 'Mosquito Resistance to Bacterial Larvicidal Toxins', *The Open Toxinology Journal*, 3(1), pp. 126–140. Available at: https://doi.org/10.2174/1875414701003010126.

Wirth, M.C., Delécluse, A. and Walton, W.E. (2004) 'Laboratory Selection for Resistance to Bacillus thuringiensis subsp. jegathesan or a Component Toxin, Cry11B, in Culex quinquefasciatus (Diptera: Culicidae)', *Journal of Medical Entomology*, 41(3), pp. 435–441. Available at: https://doi.org/10.1603/0022-2585-41.3.435.

Wirth, M.C. and Georghiou, G.P. (1997) 'Cross-Resistance Among CryIV Toxins of Bacillus thuringiensis subsp. israelensis in Culex quinquefasciatus (Diptera: Culicidae)', *Journal of Economic Entomology*, 90(6), pp. 1471–1477. Available at: https://doi.org/10.1093/jee/90.6.1471.

Wolabu, T.W. *et al.* (2020) 'Improving the genome editing efficiency of CRISPR/Cas9 in Arabidopsis and Medicago truncatula', *Planta*, 252(2), p. 15. Available at: https://doi.org/10.1007/s00425-020-03415-0.

Wong, Y.M. *et al.* (2014) 'Draft Genome Sequence of Clostridium bifermentans Strain WYM, a Promising Biohydrogen Producer Isolated from Landfill Leachate Sludge', *Genome Announcements*, 2(2). Available at: https://doi.org/10.1128/genomeA.00077-14.

World Health Organization (2019) *World malaria report 2019*. Available at: https://www.who.int/publications/i/item/9789241565721 (Accessed: 15 March 2021).

Yasuno, M. and Tonn, R.J. (1970) 'A study of biting habits of Aedes aegypti in Bangkok, Thailand.', *Bulletin of the World Health Organization*, 43(2), pp. 319–325.

Yiallouros, M. *et al.* (1994) 'Efficacy of Clostridium bifermentans serovar Malaysia on target and nontarget organisms', *Journal of the American Mosquito Control Association*, 10(1), pp. 51–55.

Yung, C.-F. *et al.* (2015) ‘Dengue Serotype-Specific Differences in Clinical Manifestation, Laboratory Parameters and Risk of Severe Disease in Adults, Singapore’, *The American Journal of Tropical Medicine and Hygiene*, 92(5), pp. 999–1005. Available at: https://doi.org/10.4269/ajtmh.14-0628.

Zhang, X. *et al.* (2005) ‘Cytotoxicity of Bacillus thuringiensis Cry1Ab toxin depends on specific binding of the toxin to the cadherin receptor BT-R1 expressed in insect cells’, *Cell Death and Differentiation*, 12(11), pp. 1407–1416. Available at: https://doi.org/10.1038/sj.cdd.4401675.

Zhang, X. *et al.* (2006) ‘A mechanism of cell death involving an adenylyl cyclase/PKA signaling pathway is induced by the Cry1Ab toxin of Bacillus thuringiensis’, *Proceedings of the National Academy of Sciences of the United States of America*, 103(26), pp. 9897–9902. Available at: https://doi.org/10.1073/pnas.0604017103.